ABSTRACT

The purpose of this research was to investigate the performance of treatment with magnetic ion exchange (MIEX) resin followed by ozonation of waters from the San Francisco Bay Delta in achieving disinfection goals while controlling bromate and chlorinated disinfection by-product (DBP) formation. Three water samples were collected from raw water supplies impacted by the Delta to represent the varying levels of bromide and organic carbon that occur throughout the year. A fourth water was prepared by spiking bromide and chloride into a portion of one of the samples. Jar testing with alum and MIEX resin was conducted to determine optimal doses for total organic carbon (TOC) and (in the case of MIEX resin) bromide removal. Samples of each water were treated with alum or MIEX resin, and the raw and treated waters were subsequently ozonated under semi-batch conditions to assess the impact of treatment on ozone demand, ozone exposure for disinfection ("CT"), and bromate formation. Finally, aliquots of raw, coagulated, resin-treated, and ozonated waters were chlorinated in order to measure trihalomethane formation potential (THMFP). In the waters studied, MIEX resin removed 41-68% of raw water TOC, compared to 12-44% for alum. MIEX resin also reduced the bromide concentration by 20-50%. The removal of TOC by alum and MIEX resin significantly reduced the ozone demand of all waters studied, resulting in higher dissolved ozone concentrations and CT values for a given amount of ozone transferred into solution. For a given level of disinfection (CT), the amount of bromate produced by ozonation of MIEX-treated waters was similar to or slightly less than that of raw water. MIEX resin removed 39-85% of THMFP compared to 16-56% removal by alum. Ozonation reduced THMFP by 35-45% in all cases. This work indicates that in bromide-rich waters in which ozone disinfection is used, MIEX resin is a more appropriate treatment than alum for the removal of organic carbon, as it achieves superior TOC and THM precursor removal and decreases the production of bromate.

ACKNOWLEDGMENTS

I owe thanks to many people for their help and support in making my graduate studies successful. First and foremost, I would like to thank Dr. Singer for granting me the opportunity to work and study in such an excellent department, and for helping me to hone my research skills. Thanks are also due to Dr. Orlando Coronell and Dr. Rose Cory for serving on my committee. Ken Mercer and Stefani Harrison of MWH provided valuable information and logistical support. I am grateful for their assistance in coordinating sample collection and shipping from California. I would also like to thank CALFED for sponsoring this research.

My fellow students in the department made my time at UNC enjoyable and memorable. I am grateful to Riley Flowers and Ryan Gustafson for helping me learn my way around a chemistry lab, and for their assistance in numerous experiments. Mitch Dyrdahl deserves thanks for helping me troubleshoot the ozone apparatus, the XAD columns, and for assistance with other experiments. Bonnie Lyon and Jen Chu spent many hours teaching me to extract THMs and to use the GC and IC; I am thankful to them for enabling such a key part of my research. Glenn Walters of the ESE Design Center was also instrumental in helping me establish a working IC procedure; without his assistance I would probably still be wrestling to get good results out of the instrument. I also want to thank Rory Polera for his time and assistance in obtaining EEMs of my water samples. Many other students and faculty have enriched my thinking as a researcher and my growth as a person over the last two years; they are too numerous to name here.

Finally, I would like to thank my wife, Katherine, for her willingness to move across the country with me so that I could study at UNC, and for being so supportive and understanding throughout the ups, downs, and busy times of my graduate career.

CONTENTS

LIST OF TABLES

LIST OF FIGURES

CHAPTER 1: INTRODUCTION

Chlorine is the most widely-used disinfectant in public drinking water supplies, offering potent disinfection of viruses and bacteria at a low cost. However, ozone is increasingly being used as an alternative to chlorine because it is more effective against *Cryptosporidium*, and because it aids in controlling halogenated organic disinfection by-products (DBPs; Jacangelo et al., 1989; Najm and Krasner, 1995; Crittenden et al., 2005). Ozone cannot provide a residual disinfectant concentration in a distribution system, so it must be used in combination with chlorine or chloramines.

When water is treated with free chlorine, natural organic matter (NOM) acts as a precursor for the formation of halogenated by-products such as trihalomethanes (THMs), which are regulated under the Disinfectants and Disinfection Byproducts Rule (D/DBPR) with a maximum contaminant level (MCL) of 80 μg/L. NOM can also increase the ozone demand of a water, hampering the effectiveness of ozone for disinfection. Because higher amounts of ozone are needed to overcome the demand, the formation of oxidation by-products, such as aldehydes, is increased in waters with elevated NOM concentrations (Najm and Krasner, 1995; Johnson and Singer, 2004).

A second precursor substance is bromide, which occurs naturally in saline or brackish waters. Ozonation of bromide-containing waters can result in the production of bromate, which is classified as a possible human carcinogen and is regulated with an MCL of 10 μg/L. Furthermore, when bromide-containing waters are disinfected with free chlorine, the speciation of THMs and other halogenated by-products shifts toward the more brominated species, which are thought to have a more detrimental public health impact than their chlorinated analogs (Richardson et al., 1999; Singer and Bilyk, 2002).

The San Francisco Bay Delta provides a source of drinking water to communities throughout central and southern California. Because of its connectivity to the San Joaquin and Sacramento Rivers and to the Pacific Ocean, water quality in the Delta exhibits considerable seasonal variation. Runoff

from agricultural activity in the watersheds of the two rivers results in high levels of total organic carbon (TOC, a surrogate for NOM) in Delta water during rainy periods, while salinity from the Pacific Ocean and San Francisco Bay increases the bromide concentration in the Delta during dry periods. Because both substances act as precursors for DBPs, this situation presents a unique challenge for water treatment. In response, many utilities that draw water from the Delta employ ozone in order to control the formation of halogenated organic DBPs.

This research evaluates the combination of pre-treatment with a magnetic ion exchange (MIEX) resin followed by ozonation of Delta waters for achieving disinfection goals and controlling bromate and halogenated DBP formation. The MIEX resin has been shown to be more effective than enhanced coagulation for the removal of dissolved organic carbon (DOC; Singer and Bilyk, 2002; Fearing et al., 2004; Boyer and Singer, 2005; Humbert et al., 2005; Boyer and Singer, 2006) and is also able to remove bromide to some extent (Singer and Bilyk, 2002; Johnson and Singer, 2004; Hsu and Singer, 2010). Johnson and Singer (2004) demonstrated that when MIEX is used before ozonation, the resin reduces ozone demand and increases the ozone exposure for a given amount of ozone transferred. This research aims to confirm each of these findings in an integrated set of experiments using several raw waters from the Delta, which represent some of the seasonal variability in bromide and DOC concentration, and to explore the implications of these findings for disinfection practice under challenging water quality conditions.

CHAPTER 2: BACKGROUND AND LITERATURE REVIEW

2.1 WATER QUALITY IN THE SAN FRANCISCO BAY DELTA

The San Francisco Bay Delta is an estuary situated at the confluence of the Sacramento and San Joaquin Rivers and the San Francisco Bay that serves as a source of drinking water for much of central and southern California. While many utilities draw water directly from the Delta for use in the San Francisco Bay area, the Central Valley and State Water Projects convey large quantities of Delta water to communities throughout California via pipelines and aqueducts. Some 23 million people, inhabiting an area that extends nearly the full length of the state, receive at least some of their drinking water from the Delta (CALFED, 2007).

Figure 2.1: Map of the San Francisco Bay Delta, showing drinking water intakes (Source: CALFED, 2007)

Due to its connectivity to the Pacific Ocean and two major rivers, water quality in the Delta varies seasonally, and is characterized at various times of the year by high salinity (16-133 mg/L chloride) and, at other times of the year, by high TOC concentrations (2.5 – 10.5 mg/L). Runoff from areas of intensive agricultural activity in the watershed elevates TOC levels in the Delta during rainy periods,

while the increased freshwater flow lowers salinity. During drier periods, seawater from the San Francisco Bay intrudes more readily, increasing bromide and chloride levels while lowering TOC concentrations (CALFED, 2007).

This situation presents unique challenges for water treatment because both bromide and TOC serve as DBP precursors. Many of the treatment facilities in the region employ ozone for disinfection to avoid halogenated by-product formation. However, bromate formation is a concern during certain periods of the year because it is a by-product of bromide oxidation by ozone. Figures 2.2 and 2.3 show box and whisker plots representing the variability in TOC and bromide concentrations, respectively, at various pumping stations in the Delta (CALFED, 2007).

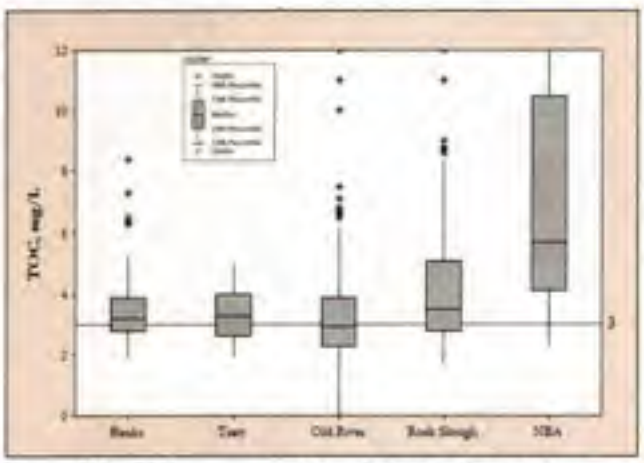

Figure 2.2: TOC concentration at five Delta intakes (Source: CALFED, 2007)

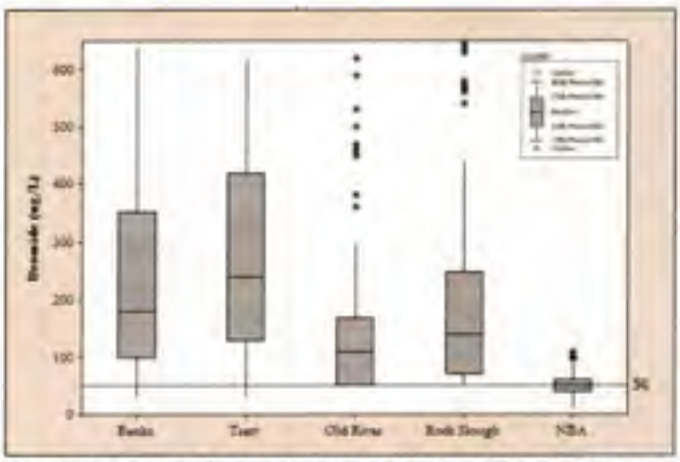

Figure 2.3: Bromide concentration at five Delta intakes (Source: CALFED, 2007)

Despite these challenges, regulations proposed by California's drinking water agency—CALFED—will make water quality standards even more stringent than those in the EPA Stage 2 D/DBPR. Maximum contaminant levels of 40 µg/L total THMs and 5 µg/L bromate have been proposed, in addition to requirements for 1-2 additional logs of *Giardia* inactivation and 1 additional log of *Cryptosporidium* inactivation (CALFED, 2007). The continuous horizontal lines in Figures 2.2 and 2.3 represent the estimated TOC and bromide concentrations (3 mg/L and 50 µg/L, respectively) that must be achieved prior to conventional treatment in order to meet CALFED's proposed DBP standards.

Clearly, innovative approaches to water treatment will be needed if disinfection targets are to be achieved without exceeding the new limits on DBP formation.

2.2 USE OF OZONE IN DRINKING WATER TREATMENT

2.2.1 History

Ozone was first discovered in 1839 by Belgian chemist Christian Schönbein, who noted that the distinctive odor produced during electrolysis of water was the same as that associated with arcs of electricity between electrodes. Early experiments with the new substance showed that ozone had the ability to oxidize many inorganic compounds to their highest oxidation states. The invention of an easy-to-use electrolytic ozone generator by Ernst Werner von Siemens in 1857 facilitated continued experiments with ozone gas during the latter half of the nineteenth century (Rubin, 2001).

In 1886, experiments by French scientist Auguste de Meritens indicated that ozone had bactericidal properties, a fact which was further investigated by German scientist O. Frölich. This led to the construction of the world's first drinking water treatment plant employing ozone in Oudshoorn, Netherlands in 1893 (Rice et al., 1981). In 1906, another ozonation plant began operation in Nice, France, and ozone has been used for disinfection at this site ever since. By the mid-twentieth century, ozone was being used at several hundred drinking water treatment plants throughout Europe (Rice et al., 1981).

In 1940, a 7 MGD plant employing ozonation for disinfection was opened in Whiting, Indiana, marking the first significant use of ozone for drinking water treatment in the United States. Ozone has continued to be used there ever since (Rice, 1999). Over the next few decades, ozone saw limited use, primarily for taste and odor control, and did not become widespread until passage of the Safe Drinking Water Act amendments in 1986. Recognition of the hazards of halogenated by-products of chlorine, new microbial inactivation requirements, and the introduction of the "CT" concept (see below) spurred

expansion of the use of ozone for municipal drinking water disinfection. As of 2008, approximately 10% of water utilities in the U.S. employed ozone for disinfection, and another 5% were considering switching to ozone (AWWA, 2008).

2.2.2 Chemistry of Ozone

Ozone is unstable under ambient conditions. Therefore, for most drinking water applications, it is generated electrolytically near the point of treatment from either air or oxygen. Ozone-containing gas is then bubbled through porous stone or ceramic diffusers in special purpose basins. The ozone diffuses into the aqueous phase as the bubbles rise through the water column. Venturi injectors or static mixers are also used to accomplish ozone transfer, but these are less common (Crittenden et al., 2005).

Once dissolved in water, ozone reacts with organic matter and other dissolved constituents via two parallel reaction pathways. In the first, ozone oxidizes the substrates directly. In the second, ozone decomposes to produce highly reactive hydroxyl radicals. Molecular ozone is a selective oxidant, while the hydroxyl radical is nonspecific and reacts very rapidly with many dissolved constituents, including ozone itself (von Gunten, 2003a). Activated aromatic compounds, chromophoric organic species, unsaturated carbon bonds, and deprotonated amines are most vulnerable to direct oxidation by ozone (Rice, 1999; von Gunten, 2003a). Molecular ozone is also responsible for disinfection of microbes, which is proportional to ozone exposure, or "CT." CT is defined as the product of the dissolved ozone residual and the contact time. Hydroxyl radicals do not participate in microbial inactivation (Gurol and Singer, 1982; von Gunten, 2003a), but oxidation by hydroxyl radicals plays an important role in the decomposition of ozone and in ozone reactivity with other dissolved species. If solution conditions are such that some ozone decomposition has taken place, the hydroxyl radical may become the primary oxidizing species (Hoigné and Bader, 1976). Table 2.1 compares the rate constants for oxidation of a variety of organic and inorganic substances by ozone and hydroxyl radicals (collected in von Gunten, 2003a).

Table 2.1 - Comparison of rate constants for oxidation of various compounds by ozone and hydroxyl radicals (Source: von Gunten, 2003a)

Compound	k_{O3} $M^{-1} s^{-1}$	half life[a]	k_{OH} $M^{-1} s^{-1}$
Ammonia (NH_3)	20	96 hr	9.7×10^7
Bromide	160	215 s	1.1×10^9
Manganese (Mn II)	1.5×10^3	23s	2.6×10^7
Iron (Fe II)	8.2×10^5	0.07 s	3.5×10^8
Atrazine	6	96 min	3.0×10^9
Geosmin	<10	>1 hr	8.2×10^9
Chloroform	<0.1	>100 hr	5.0×10^7

[a] Half-life due to reaction with 1 mg/L ozone at pH 7

In addition to the oxidation reactions outlined above, ozone undergoes spontaneous decomposition according to a first-order reaction with respect to ozone concentration (Staehelin and Hoigne, 1982; von Gunten, 2003a). Decomposition is initiated when ozone reacts with hydroxide ions to produce hydroxyl and superoxide (O_2^-) radicals. Because of the importance of hydroxide ion as an initiator, the rate of ozone decomposition increases rapidly with pH above pH 4 (Gurol and Singer, 1982; Staehelin and Hoigne, 1982; von Gunten, 2003a). Decomposition may also be initiated by other substances in addition to hydroxide, such as reduced iron, formate, or humic materials in natural systems and hydrogen peroxide in engineered advanced oxidation processes (Staehelin and Hoigne, 1982). As a result of this decomposition process, the half-life of ozone in water may range from seconds to hours (von Gunten, 2003a).

After the initiation reaction, the superoxide radicals are further oxidized to ozonide (O_3^-) by ozone. The ozonide ions combine with water and disproportionate to form molecular oxygen and more hydroxyl radicals. Finally, these radicals react with molecular ozone to form unstable HO_4, which evolves molecular oxygen and HO_2, beginning the cycle again (Staehelin, Buehler, and Hoigne, 1984). This reaction scheme is depicted in Figure 2.4.

As shown, hydroxyl radicals are key intermediates in ozone decomposition, and catalyze further decomposition (Buehler, Staehelin, and Hoigne, 1984). In natural systems, hydroxyl radical scavengers, such as phosphate and carbonate, have a retarding effect on ozone decomposition (Hoigné and Bader, 1976; Gurol and Singer, 1982; Johnson and Singer, 2004). By suppressing the formation of hydroxyl radicals, these species also reduce the degree of oxidation of some chemical contaminants (Hoigné and Bader, 1976). Carbonate ions further suppress ozone decay because carbonate radicals, formed when the hydroxyl radical is scavenged, react with ozonide (O_3^-) to produce ozone and carbonate ions, thus replenishing the dissolved ozone concentration (Nemes, Fabian, and van Eldik, 2000).

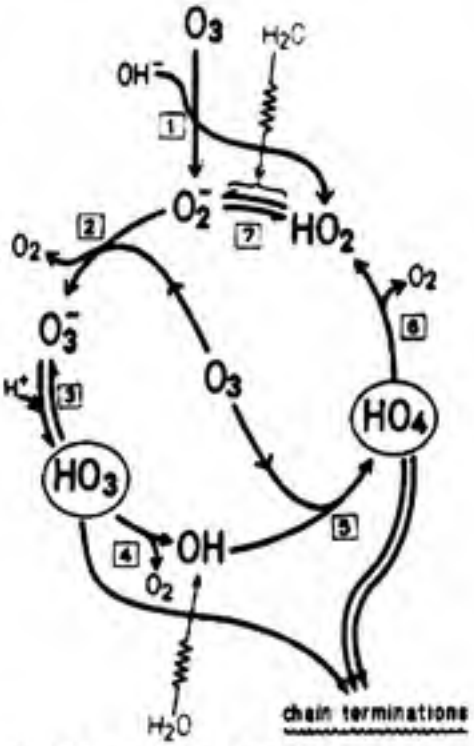

Figure 2.4: Schematic of ozone decay reactions in pure water. (Source: Staehlin, Bühler, and Hoigné, 1984)

2.2.3 Applications of Ozone in Drinking Water Treatment

Oxidation of Nuisance Compounds

Many nuisance tastes, odors, and colors in drinking water arise from the presence of organic molecules, as well as iron and manganese. Ozone is especially reactive with the types of unsaturated groups that cause organic molecules to impart color to water, and so is highly effective in removing color. It is also capable of oxidizing reduced iron and manganese to insoluble forms, even if the metals are present as organic complexes (Rice, 1999). Pesticides, microcystin LR, chlorinated solvents, and some pharmaceuticals are also susceptible to oxidation by ozone or hydroxyl radicals (von Gunten, 2003a).

In addition, ozone reduces the molecular weight and aromatic character of NOM molecules,

thereby increasing the fraction of DOC that is biodegradable (Urfer et al.,1997; Carlson and Gary, 1998; Crittenden et al., 2005; Hammes et al., 2006). A consequence of these transformations is the formation of lower molecular-weight organic by-products, including aldehydes, ketones, and carboxylic acids (Weinberg et al., 1993; Najm and Krasner, 1995; Richardson et al., 1999b). Many treatment plants utilize ozone in conjunction with biologically active filtration to remove these by-products and improve the biological stability of treated water to prevent excessive biofilm growth in the distribution system (Weinberg et al., 1993; Urfer et al., 1997).

Disinfection

Because of its powerful disinfecting properties, ozone can inactivate bacteria at relatively low doses and short contact times relative to other disinfectants (Rice, 1999). It is also highly effective against viruses and protozoan cysts, such as *Cryptosporidium*. However, the activation energy for inactivation of protozoa is significantly higher than for viruses, bacteria, or most chemical reactions (von Gunten, 2003a). This fact implies that a higher level of ozone exposure (CT) is required if inactivation of *Cryptosporidium* is a treatment objective. The higher exposure increases the possibility that undesirable by-products (e.g. bromate) may be formed. Table 2.2 lists the required ozone exposure values for various levels of *Cryptosporidium* inactivation by ozone (U.S. EPA, 2006a).

A second major attraction of ozone for disinfection is its impact on halogenated DBP formation. Jacangelo et al. (1989) reported that the use of ozone as a primary disinfectant in place of free chlorine

Table 2.2: Ozone exposure required for *Cryptosporidium* inactivation (excerpted from USEPA, Long-term 2 Enhanced Surface Water Treatment Rule, 2006)

CT VALUES (MG·MIN/L) FOR *Cryptosporidium* INACTIVATION BY OZONE [1]

Log credit	Water Temperature °C										
	<=0.5	1	2	3	5	7	10	15	20	25	30
(i) 0.25	6.0	5.8	5.2	4.8	4.0	3.3	2.5	1.6	1.0	0.6	0.39
(ii) 0.5	12	12	10	9.5	7.9	6.5	4.9	3.1	2.0	1.2	0.78
(iii) 1.0	24	23	21	19	16	13	9.9	6.2	3.9	2.5	1.6
(iv) 1.5	36	35	31	29	24	20	15	9.3	5.9	3.7	2.4
(v) 2.0	48	46	42	38	32	26	20	12	7.8	4.9	3.1
(vi) 2.5	60	58	52	48	40	33	25	16	9.8	6.2	3.9
(vii) 3.0	72	69	63	57	47	39	30	19	12	7.4	4.7

[1] Systems may use this equation to determine log credit between the indicated values: Log credit = (0.0397 × (1.09757)$^{(\text{Temp})}$) × CT

resulted in a decrease in most classes of halogenated DBPs, including the regulated THMs and HAAs, upon subsequent chlorination. The decrease in THMs are attributable to two factors. First, where ozone is the primary disinfectant, chlorine is only applied at low doses to provide a residual. This reduces the extent of its reaction with NOM and limits the formation of THMs. Secondly, oxidation of NOM by ozone can render it less reactive with chlorine, thus reducing the quantity of THM and other DBP precursors in the water (von Gunten, 2003b). Ozone itself does not form halogenated by-products to any significant degree unless high bromide concentrations are present (Richardson et al., 1999b). As noted above, however, several classes of oxidation by-products are formed by reaction of ozone with NOM (Weinberg et al., 1993; Najm and Krasner, 1995; Richardson et al., 1999b).

2.3 DISINFECTION BY-PRODUCT PRECURSORS IN DRINKING WATER

2.3.1 Bromide

Bromide occurs naturally in many surface drinking water supplies in coastal areas due to the intrusion of saltwater. Groundwaters may also contain bromide for the same reason. In addition, the use of brine to extract crude oil can introduce bromide into aquifers, as is the case in some areas of Texas (Richardson et al., 1999a). A 1993 study of 11 utilities in the U.S. found bromide concentrations ranging from 10 µg/L to 800 µg/L in the source waters, with a median of 60 µg/L (Krasner et al., 1993). 37% of U.S. water utilities surveyed as part of the Occurence Assessment for the Stage 2 D/DBPR reported bromide concentrations between 30 µg/L and 100 µg/L, while 19% reported higher concentrations (U.S. EPA, 2005). Bromide concentrations in the range of 2-4 mg/L have been reported at select locations in the United States (Richardson et al., 1999a), England, Australia, and Israel (Magazinovic et al., 2004).

Bromide represents a public health concern because of its multiple roles as a DBP precursor. If a bromide-containing water is treated with ozone, bromate may be produced. Chronic exposure to

bromate has been observed to cause cancer in rats, and the International Association for Research on Cancer (IARC) classified potassium bromate as a possible human carcinogen in 1986 (U.S. EPA, 2001). In addition, acute exposure to elevated levels of bromate is known to cause kidney damage and hearing loss (U.S. EPA, 2001). Bromate is currently regulated under the Stage 2 D/DBPR with an MCL of 10 μg/L (U.S. EPA, 2006b). The U.S. EPA has considered reducing the MCL to 5 μg/L, but has not done so for fear that this action may compromise the microbial quality of drinking water by making it difficult to achieve adequate disinfection without violating the standard (U.S. EPA, 2006b). Generally speaking, bromate production is likely to be a concern only in ozonated waters containing 50 μg/L bromide or more (von Gunten, 2003b).

Bromide is undesirable even if ozone is not used as the primary disinfectant. When bromide-containing waters are disinfected with chlorine, bromide is oxidized to hypobromous acid, which subsequently reacts with NOM to form brominated THMs, HAAs, and other brominated by-products (Rook et al., 1978). As the Br:DOC ratio increases, the speciation of THMs and HAAs tends to shift toward the more brominated species even though the absolute quantity of each class remains approximately the same (Krasner et al., 1989; Singer and Bilyk, 2002). This fact is significant because the brominated forms of halogenated by-products are thought to have a more detrimental public health impact than their chlorinated analogs (Richardson et al., 1999a; Plewa et al., 2002; Singer and Bilyk, 2002).

In addition to bromate and brominated THM and HAA species, a host of other by-products have been identified in high-bromide waters treated with a combination of ozone and chlorine or chloramines. These include bromopicrin, dibromoacetonitrile, bromoacetone, cyanogen bromide, and others. As with the THMs and HAAs, these compounds are thought to be more carcinogenic than their chlorinated counterparts (Richardson et al., 1999a).

Chemistry of Bromate Formation

As discussed above, ozone reacts with dissolved constituents in water via two parallel pathways – direct oxidation and through the formation of hydroxyl radicals. Both pathways are involved in the production of bromate during ozonation of a bromide-containing water. Figure 2.5 provides a schematic of the multiple reaction pathways.

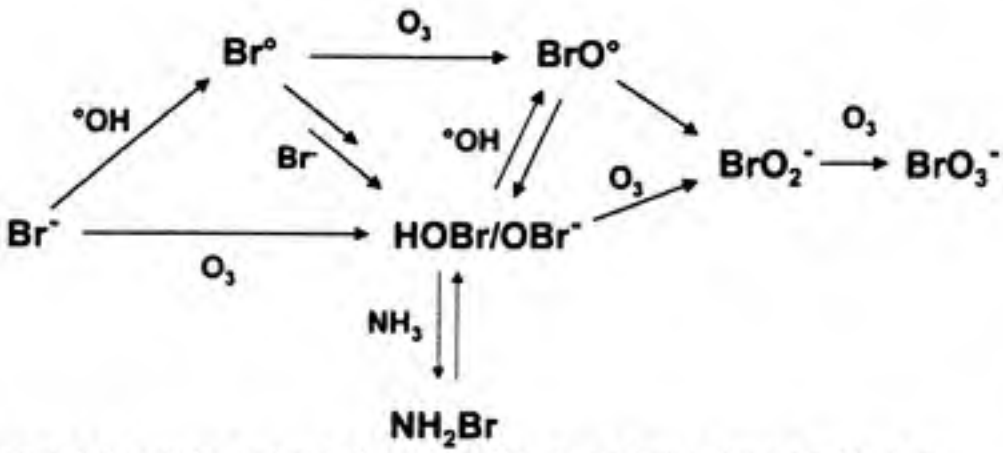

Figure 2.5: Reaction pathways for bromate formation during ozonation. (Source: Pinkernell and von Gunten, 2001)

Along the upper path, bromide is oxidized by hydroxyl radicals to form a bromide radical which is further oxidized by ozone to ultimately form bromate. In the lower path, molecular ozone oxidizes the bromide ion directly to form hypobromous acid and hypobromite ion. These species are oxidized again to bromite, and then to bromate. During the initial stages of ozonation, bromate formation through the upper (bromide radical) pathway is important, but after an initial period the molecular ozone pathway dominates (Pinkernell and von Gunten, 2001). There is no evidence that hydroxyl radicals will form bromate directly from bromide. Rather, direct oxidation by ozone is a necessary part of any bromate formation pathway (von Gunten and Hoigne, 1994). Because all direct ozone pathway reactions are first-order in ozone concentration, ozone exposure (CT) is correlated with the amount of bromate formed (von Gunten and Hoigne, 1994).

As shown in Figure 2.5, hypobromite / hypobromous acid play a central role in the reaction

pathways leading to bromate formation. While ozone reacts readily with hypobromite ion (OBr^-), it does so to only a limited extent with hypobromous acid (HOBr) (Haag and Hoigne, 1983). At low pH, bromate formation is slowed because most of the Br(I) is present as HOBr ($pK_a \approx 9$), which does not participate further in the direct ozonation pathway (von Gunten and Hoigne, 1994; Pinkernell and von Gunten, 2001). However, low pH conditions do favor the formation of bromoform from NOM in the water because the reaction of HOBr with NOM is faster than its reaction to form bromite (Haag and Hoigne, 1983).

Bromate formation increases with increasing ionic strength, but is nearly independent of hydroxyl radical scavenger concentrations, such as carbonate, because the scavengers become secondary oxidants themselves. Bromate production per unit of ozone exposure (CT) has also been shown to be independent of NOM concentration (von Gunten and Hoigne, 1994; Berne, Chasson, and Legube, 2004). During ozonation, the sum of bromine concentrations as Br^-, $HOBr/OBr^-$, and BrO_3^- remains nearly constant, indicating that no other species form to any significant degree (Haag and Hoigne, 1983; Pinkernell and von Gunten, 2001).

If ammonia is present in the water, it will delay bromate formation by forming monobromamine with HOBr. Over time, this species is oxidized by ozone to form nitrate and release bromide, which then continues to produce bromate as in Figure 2.5 (von Gunten and Hoigne, 1994). For this reason, ammonia is sometimes added to water as a means to control bromate (Pinkernell and von Gunten, 2001). A study by the Swiss Federal Institute for Environmental Science and Technology (EAWAG) found that the addition of chlorine and ammonia prior to ozonation significantly reduced the formation of bromate in a water containing over 500 µg/L bromide (Buffle, Galli, and von Gunten, 2004).

2.3.2 Natural Organic Material

NOM is ubiquitious in natural waters. It refers to a complex mixture of dissolved, colloidal, and particulate substances arising from the photosynthetic activity of plants, decay of vegetative material,

bacterial metabolism, and human activities such as agriculture (Hudson, Baker, and Reynolds, 2007; Leenheer, 2009). Amino acids, fatty acids, phenols, hydrocarbons, sugars, and polymers are all constituents of NOM (Bolto et al., 2002a). Its exact composition in a given water varies widely, and is influenced by the source of carbon (plant material vs. bacterial activity), temperature, pH, ionic composition of the water, and properties of sediments that may acts as sorbents (Leenheer and Croué, 2003). NOM molecules consist primarily of aromatic and aliphatic hydrocarbon structures with various functional groups, the most common being carboxyl, hydroxyl, amide, and ketone groups (Leenheer and Croué, 2003). NOM is somewhat more refractory to rapid biodegradation than other substances, but (slow) degradation of NOM in aerobic environments, such as most surface waters, results in the addition of carboxyl and hyrdoxyl functional groups that tend to make NOM molecules more soluble (Leenheer, 2009). The more hydrophobic components of NOM are referred to as humic substances and comprise operationally-defined humic and fulvic acids. These materials result from the decomposition of plant material leached from soil and water (White et al., 1997). While humic substances are dominated by aromatic compounds, the hydrophilic portions of NOM comprise mostly aliphatic structures. Because most natural waters contain only trace levels of anthropogenic organic pollutants, total and dissolved organic carbon (TOC / DOC) are frequently accepted as surrogate measures for NOM (Leenheer and Croué, 2003).

Impact of NOM on Finished Drinking Water Quality

NOM is widely known to act as a precursor material for the formation of various halogenated organic DBPs when exposed to chlorine (Rook et al., 1978; Krasner et al., 1989). Humic and fulvic acids, which comprise a substantial fraction of most NOM (White et al., 1997), as well as hydrophilic fractions of DOC, can react with chlorine to form a host of halogenated by-products. Among these, chloroform, dichloro- and trichloroacetic acids are among the most abundant (Christman et al., 1983). The hydrophobic fraction of NOM has been shown to be more reactive with chlorine, while the

hydrophobic fraction is more reactive with bromine (Liang and Singer, 2003). With respect to the formation of regulated THMs and HAAs from chlorine, Liang and Singer (2003) showed that the hydrophobic fraction of NOM has a higher formation potential than the hydrophilic fraction. NOM can also react with ozone to produce several classes of organic DBPs, including aldehydes and ketoacids (Najm and Krasner, 1995).

In addition to DBP formation, the presence of NOM in water that undergoes treatment can result in nuisance tastes, odors, and colors. NOM also increases coagulant and oxidant doses, shortens filter run times, contributes to membrane fouling, interferes with the adsorption of micropollutants by activated carbon, and can promote biological regrowth in the distribution system (White et al., 1997; Bolto et al., 2002a; Crittenden et al., 2005). As such, removing NOM from source waters is a major objective of water treatment.

NOM has a significant and complex impact on ozone decomposition as well. When NOM reacts with hydroxyl radicals, one fraction gives rise to superoxide radicals which accelerate the formation of additional hydroxyl radicals and ozone decomposition, while another fraction of the NOM scavenges these radicals and thereby inhibits the decomposition of ozone (von Gunten, 2003a). NOM can also react directly with ozone to produce ozonide ions that accelerate the formation of hydroxyl radicals and the decomposition of ozone (von Gunten, 2003a). Thus, NOM can act both as a source and a scavenger of hydroxyl radicals depending on the specific characteristics of the water and the NOM itself. As yet, it is not possible to deduce the net effect on ozone decomposition from the character of the NOM (von Gunten, 2003a).

These direct oxidation reactions between ozone and NOM are responsible for ozone demand, i.e. the amount of ozone that must be applied to the water before any dissolved ozone residual appears. By increasing ozone demand, NOM can also be expected to slow the formation of bromate (Johnson and Singer, 2004), and to reduce the effectiveness of microbial inactivation. It has been reported that ozone

demand is not affected by bromide concentration (Najm and Krasner, 1995), but high ionic strength solutions do increase the mass transfer coefficient of ozone gas into solution and reduce the solubility of ozone slightly (Gurol and Singer, 1982).

2.4 DBP PRECURSOR REMOVAL STRATEGIES

It is well-established that the removal of NOM from water is an effective strategy for reducing DBP formation (White et al., 1997). As such, numerous water treatment technologies have been developed for this purpose, including coagulation/flocculation, nanofiltration and reverse osmosis membranes, granular activated carbon (GAC) adsorption, rapid media filtration, and ion exchange. Coagulation an anion exchange are the two processes of most relevance to this study.

2.4.1 Coagulation

Coagulation with alum or ferric iron salts is one of the most widely used water treatment processes for NOM removal. Under the Stage 1 D/DBPR, water utilities are required to achieve a certain percentage removal of TOC by "enhanced coagulation," depending on the TOC concentration and alkalinity of the source water (U.S. EPA, 1998). For utilities whose source water NOM is not "amenable" to removal by coagulation, the alum (or ferric iron) dose may be chosen based on the "point of diminishing returns," defined as the alum dose at which 0.3 mg/L TOC is removed for each additional 10 mg/L alum (U.S. EPA, 1998).

Alum or ferric iron salts remove NOM by one of two primary mechanisms. First, metal-hydroxide floc particles may adsorb organic material. Second, humic and fulvic acids that constitute NOM may complex with the metal ions to form insoluble species (Krasner and Amy, 1995). Downstream separation processes then remove the suspended floc material by gravity or other means. Coagulation for NOM removal is most effective in the pH range of 5-6, where many of the functional groups on NOM molecules become protonated (White et al., 1997). This reduces the effective surface charge of

the molecules and renders them more hydrophobic (Krasner and Amy, 1995).

The specific ultraviolet absorbance (SUVA) of a water is an indicator of the hydrophobicity of the NOM in the water, and is defined as 100 times the UV absorbance at 254 nm divided by DOC concentration. Waters with high SUVA are more amenable to treatment by coagulation than those with low SUVA, because alum coagulation preferentially removes the hydrophobic component of DOC (White et al., 1997; Liang and Singer, 2003).

Because removal of flocculated NOM occurs through a physical separation process, coagulation does not remove bromide or most other dissolved ions. As a result, treatment of bromide-containing waters with alum increases the Br:DOC ratio. As noted above, higher Br:DOC ratios result in a greater fraction of bromine-substituted THM and HAA species when the water is chlorinated (Krasner et al., 1989; Singer and Bilyk, 2002). The bromine incorporation fraction (BIF) is a value between 0 and 1 representing the molar fraction of brominated THM species relative to total THMs, and is defined as follows (after Obolensky and Singer, 2005):

$$BIF = \frac{BrCl_2CH + 2*Br_2ClCH + 3*Br_3CH}{3*(Cl_3CH + BrCl_2CH + Br_2ClCH + Br_3CH)} \qquad [2.1]$$

Chlorination of bromide-containing water treated with alum is expected to result in a higher BIF than chlorination of the same raw water, even though the total DBP formation will be lower

2.4.2 Ion Exchange for NOM Removal

In waters dominated by hydrophilic NOM, conventional coagulation may be inadequate for removing organic material and controlling the formation of DBPs. Anion exchange resins provide an alternative treatment option, and have been shown to be effective for removing NOM and reducing the THM formation potential of a water(Bolto et al., 2002b; Singer and Bilyk, 2002; Humbert et al., 2005). As noted above, both hydrophobic and hydrophilic components of NOM consist largely of carboxylic acid groups, making the NOM molecules polyanionic (Leenher, 2009). As a result, ion exchange is able to remove a fraction of DOC that is inaccessible to treatment by coagulation, which targets only

high molecular-weight, hydrophobic DOC (Bolto et al., 2002b; Drikas, Chow, and Cook, 2003; Morran et al., 2004; Humbert et al., 2005).

Resins used for NOM removal typically have quaternary amine functional groups charged with chloride ions, which are exchanged for negatively-charged NOM molecules during treatment (Bolto et al., 2002b). A macroporous structure was found to be more advantageous for removal of large NOM molecules than a gel structure (Bolto et al., 2002b).

Magnetic Ion Exchange (MIEX) Resin

MIEX is a strong base anion exchange resin specifically designed to remove DOC. Like many resins of this type, it has a polyacrylic, macroporous structure and uses Type I quaternary ammonium functional groups. The resin beads are 20-50% smaller (about 180 μm) than those of more traditional resins, giving the MIEX resin a high surface area that is well suited to the removal of NOM. In addition, an iron oxide is incorporated into the resin structure that gives the beads magnetic properties. This feature causes the resin beads to agglomerate rapidly, allowing the resin to be applied as a slurry in a completely mixed reactor rather than in a fixed bed (Boyer and Singer, 2005). This continuous-flow treatment scheme provides increased turbulence around the resin beads and less resistance to liquid-phase mass transfer than fixed beds (Boyer and Singer, 2005).

Typically, the MIEX process is installed at the head of a treatment plant to complement conventional treatment. Figure 2.6 illustrates a typical MIEX process. In brief, raw water flows into a resin contactor, where it is mixed with resin for approximately 20 minutes. Flow

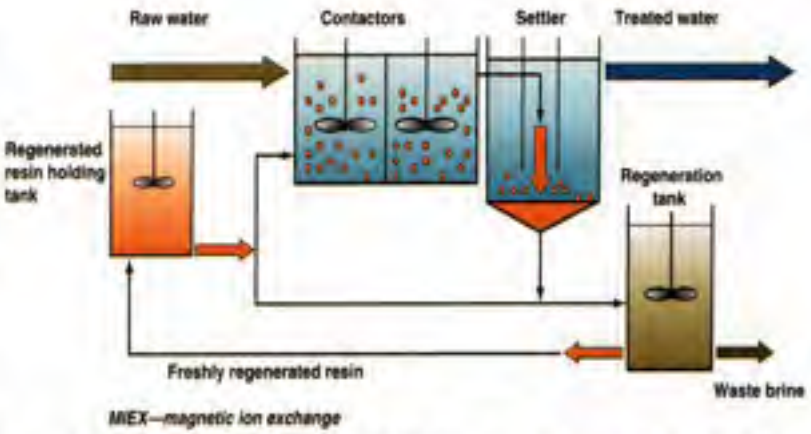

Figure 2.6: Schematic of a typical MIEX process (Source: Boyer et al., 2009)

then passes into a clarifier, where the resin beads quickly settle and clarified water continues on for further treatment. Most of the settled resin is recycled to the contactor, while a small percentage (3-10%) is sent to a regeneration tank, where it is most often regenerated with sodium chloride (Boyer et al., 2009). MIEX resin doses in the contactor are typically 20-30 mL resin per liter of water (Wert et al., 2005; Boyer et al., 2009). If one defines the effective resin dose (ERD) as the product of the steady-state MIEX resin concentration in the contactor and the regeneration ratio (Boyer and Singer, 2006), then the 20-30 mL/L range given above, operating at a 5% regeneration ratio, is equivalent to an ERD of 1-1.5 mL/L. The ERD represents the loading rate of freshly-regenerated resin in the contactor at any given time. Boyer et al. (2009) showed that batch studies conducted using virgin resin yield comparable results to pilot-scale continuous-flow processes at the same ERD. To reflect operating conditions at pilot- and full-scale, continuous-flow MIEX plants, batch studies to evaluate the effectiveness of the resin should be conducted at ERDs of 0.5-1.5 mL/L (Boyer et al., 2009).

Removal of NOM by MIEX Resin

Several bench, pilot, and full-scale tests have documented substantial removal of DOC and UV-absorbing substances by MIEX resin at ERDs on the order of 1.0 mL/L (Fearing et al., 2004; Johnson and Singer, 2004; Humbert et al., 2005; Boyer and Singer, 2006; Boyer et al., 2009). MIEX resin has been shown to be more effective than enhanced coagulation for the removal of DOC and UV-absorbing substances (Singer and Bilyk, 2002; Boyer and Singer, 2005; Humbert et al., 2005; Boyer and Singer, 2006). One study also showed that MIEX resin lowered bacterial regrowth potential more than enhanced coagulation (Drikas, Chow, and Cook, 2003).

Unlike coagulation, MIEX resin does not appear to preferentially remove hydrophobic or hydrophilic carbon (Singer and Bilyk, 2002). Studies by Johnson and Singer (2004) found that the SUVA value of waters treated with various doses of MIEX resin did not change significantly during treatment, indicating that both hydrophobic and hydrophilic acids were being removed by the resin to

similar degrees. The resin is also capable of removing low molecular-weight UV-absorbing organic acids, which are refractory to removal by coagulation (Drikas, Chow, and Cook, 2003; Fearing et al., 2004; Morran et al., 2004; Humbert et al., 2005). Removal of DOC by MIEX resin is most effective in waters with high SUVA and low anionic strength (Boyer and Singer, 2005). In low SUVA waters, NOM molecules contain relatively more carboxylic acid groups than their hydrophobic counterparts, and thus each molecule of NOM occupies more exchange sites on the resin beads, limiting the removal capacity of the resin (Boyer et al., 2009).

If used in combination with conventional coagulation, pre-treatment with the MIEX resin significantly lowers the optimal coagulant dosage required for DOC and turbidity removal (Singer and Bilyk, 2002; Fearing et al., 2004; Mercer et al., 2004; Morran et al., 2004). The use of enhanced coagulation in addition to MIEX resin treatment generally does not improve DOC removal compared to MIEX resin alone (Drikas, Chow, and Cook, 2003; Boyer and Singer, 2005). This indicates that the MIEX resin removes nearly all fractions of NOM that are removed by coagulation.

When used prior to ozonation, MIEX resin treatment has been shown to reduce the ozone demand and increase the level of CT achieved for a given amount of ozone transferred (Johnson and Singer, 2004; Wert et al., 2005). A 45%-60% increase in CT for the same ozone contact time was observed at pilot-scale by Wert et al. (2005).

Removal of Bromide by MIEX Resin

In addition to removing DOC, MIEX resin treatment has been shown to remove bromide and other inorganic anions to a limited extent (Singer and Bilyk, 2002; Johnson and Singer, 2004; Humbert et al., 2005; Boyer and Singer, 2006; Hsu and Singer, 2010). In South Bay Aqueduct (CA) water, batch treatment with 2 ml/L MIEX resin reduced bromide by 45% (Boyer and Singer, 2005). A batch study of two Australian waters achieved bromide removal of 50-60% at resin doses of 6-8 ml/L (Drikas, Chow, and Cook, 2003). Results from several other studies indicate that significant bromide removal

is only achieved at higher MIEX resin doses than are normally used for DOC removal (Johnson and Singer, 2004; Hsu and Singer, 2010). Although polystyrene ion exchange resins are more selective for bromide than polyacrylic resins like the MIEX resin, polystyrene resins are not as effective for NOM removal (Hsu and Singer, 2010). Therefore, MIEX resin treatment is a viable choice where removal of both DOC and bromide is desired.

In general, bromide removal by MIEX resin increases with increasing initial bromide concentration, which leads to more effective competition for ion exchange sites (Johnson and Singer, 2004). However, waters with high bromide concentration also tend to have high concentrations of other dissolved salts. For example, chloride has been shown to occur in a 333:1 mass ratio with bromide in most natural waters (Hsu and Singer, 2010). Anionic species, such as chloride and bicarbonate (alkalinity), compete with bromide for exchange sites and therefore interfere with bromide removal (Singer and Bilyk, 2002; Johnson and Singer, 2004; Hsu and Singer, 2010). Competition by other anions could be expected to interfere with DOC removal as well (Boyer and Singer, 2005; Hsu and Singer, 2010), but because of its design, the MIEX resin has a much stronger affinity for DOC than for bromide or other salts (Hsu and Singer, 2010). As such, bromide removal is greatest in the absence of DOC. However, DOC concentration has a relatively small impact on bromide removal, with higher DOC concentrations decreasing bromide removal by 7-10% (Hsu and Singer, 2010).

Electroneutrality arguments can be used to gain insight into the degree of exchange of different anionic species. MIEX resin has an exchange capacity of approximately 440 meq/L (Boyer et al., 2009), which places an upper limit on the quantity of anionic molecules that can be exchanged. The charge density of natural hydrophobic organic acids is 9-12 meq/g at pH 8, and is relatively insensitive to pH in the neutral pH range (Boyer et al., 2009). This information can be used to compare the removal of DOC to that of various anionic species on an equivalent basis. For example, Singer and Boyer (2008) demonstrated a stoichiometric relationship between chloride release and DOC uptake

onto the MIEX resin.

Effect on Disinfection By-Product Formation

Because of its effectiveness for removal of DOC, treatment with MIEX resin has been shown to reduce the THM formation potential of many waters by 25% - 70% (Drikas, Chow, and Cook, 2003; Morran et al., 2004; Boyer and Singer, 2005). For North Bay Aqueduct (CA) water, MIEX treatment prior to conventional coagulation and sedimentation reduced THM and HAA formation from subsequent chlorination below regulated limits, while water without pre-treatment exceeded the standards (Mercer et al., 2004). In general, the percentage removal of THMFP is similar to the removal of DOC for a given water matrix and resin dose (Boyer and Singer, 2005). Although MIEX resin removes bromide, DOC is removed to a much greater extent, so that the Br:DOC ratio increases following MIEX treatment. As a result, MIEX treatment results in a shift toward the more brominated THM species and a higher BIF relative to the raw water (Boyer and Singer, 2005). Because MIEX removes both DOC and bromide, however, the BIF of a MIEX-treated water is expected to be somewhat lower than that of a coagulated water (for the same degree of DOC removal).

For ozonated waters, MIEX resin pre-treatment removes ozone-demanding material from the water, leading to a higher dissolved ozone concentration for a given transferred ozone dose. Bromate formation is expected to be reduced by MIEX pre-treatment because of both decreased bromide ion concentration and a lower transferred ozone dose to achieve a given dissolved ozone concentration (Johnson and Singer, 2004).

CHAPTER 3: MATERIALS AND METHODS

3.1 GENERAL APPROACH

Three waters from the San Francisco Bay Delta in California, representing moderate TOC / low bromide, low TOC / high bromide, and high TOC / low bromide were used in this analysis. A fourth water, representing high TOC / high bromide, was prepared by spiking bromide into the high TOC / low bromide water. These waters are identified according to their characteristics in Table 3.1. Upon receipt, the raw waters were analyzed for TOC, DOC, and UV absorbance at 254 nm. Portions of the raw water were used to conduct jar tests with MIEX resin and alum, and the performance of each in removing NOM was compared. Jar testing was also used to compare the performance of the chloride and bicarbonate forms of MIEX resin in removing bromide. Based on these jar tests, 16 L of the raw water was treated with MIEX resin or alum and subsequently ozonated in a semi-batch reactor to achieve a target dose of 1 mg O_3 / mg TOC. The impact of each pre-treatment on ozone demand, ozone exposure (CT), and bromate formation was evaluated. Finally, the raw, alum-treated, MIEX resin-treated, and ozonated waters were chlorinated under Uniform Formation Conditions (after Summers et al., 1996) to determine their THM formation potential. The performance of MIEX resin in reducing ozone demand and DBP formation was compared to conventional alum coagulation and direct ozonation of the raw waters. Excitation-emission fluorescence spectroscopy and XAD8 fractionation were used to further characterize the NOM present in the raw, bulk-treated, and ozonated waters. Figure 3.1 illustrates the overall experimental approach.

Table 3.1: Classification of water samples by TOC and bromide concentration

		TOC Concentration	
		Low/Moderate	High
Bromide Concentration	Low	North Bay Aqueduct	Lake Campbell
	High	South Bay Aqueduct	Spiked Lake Campbell

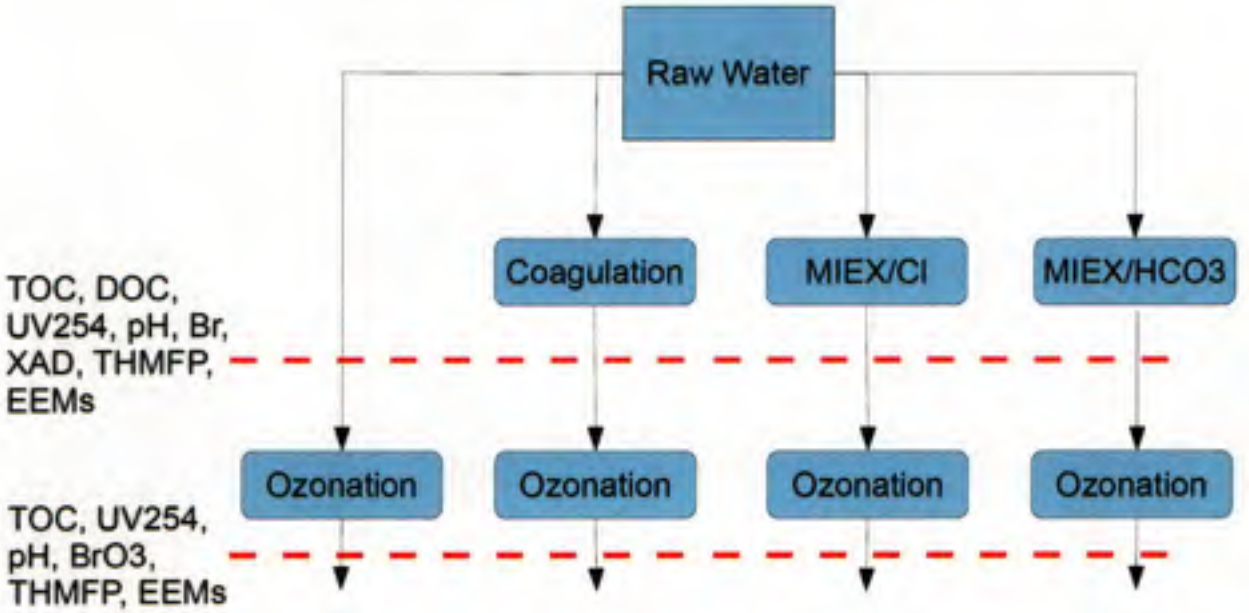

Figure 3.1: General experimental approach

3.1.1 Glassware

Glassware used in these experiments was initially cleaned by soaking in detergent (Alconox Inc., White Plains, NY) overnight. The glassware was rinsed thoroughly with tap water and then placed in a bath of 10% nitric acid overnight. Following the acid bath, the glassware was rinsed a minimum of three times with deionized organic-free water (DOFW). DOFW was produced by passing tap water through a Dracor (Durham, NC) water treatment system, consisting of a 1.0 µm pre-filter, 0.5 ft^3 of activated carbon, and two mixed-bed deionizer resins. In between experiments, glassware was rinsed thoroughly with DOFW, then rinsed with 10% nitric acid, and rinsed a minimum of three times with DOFW and allowed to air-dry before being returned to service. Volumetric glassware was not subjected to the overnight acid bath, but was instead rinsed with 10% nitric acid followed immediately by rinsing with DOFW.

3.1.2 Sample Collection and Handling

All water samples were collected by water treatment plant staff in California and shipped via freight carrier to the University of North Carolina. Samples were collected in a 55-gallon HDPE barrel, which staff were instructed to rinse three times with sample before filling. The North Bay Aqueduct water sample was collected at the North Bay Regional Water Treatment Plant (WTP) in Fairfield, CA on 5/28/09 and was received on 6/3/09. South Bay Aqueduct water was collected at the Santa Clara Valley Water District's Penitencia Plant in San Jose, CA on 9/10/09. It was received 9/18/09. The Lake Campbell water sample was collected from Lake Campbell, CA (near North Bay Regional WTP) on 12/15/09 and received 1/4/09.

Upon receipt, the barrels were immediately placed in a refrigerator at 4 °C. Aliquots of sample were periodically withdrawn from the barrel for analysis and experimentation. Prior to withdrawal, the barrel was opened and stirred for approximately 1 minute with a 1.5 m length of PVC conduit, which had been washed with detergent (Alconox, Inc., White Plains, NY) and thoroughly rinsed with deionized water prior to use. Before the water in the barrel became quiescent, a 2 m length of polyurethane tubing was used to siphon sample into pre-rinsed 2.5-gallon collapsible plastic containers. These containers were placed on the lab bench to warm to room temperature before use. In some cases, sample containers were placed in a shallow bath of warm water to accelerate their return to room temperature. The containers were removed from the bath before the water temperature increased above ambient room temperature (20° C).

3.1.3 Magnetic Ion Exchange Resin

Orica Watercare (Denver, CO) provided samples of MIEX resin in 500-mL plastic containers. The resin was received in slurry form containing approximately 10% water by volume. Resin charged with chloride as the counterion was stored in a 10-L Nalgene carboy; resin charged with bicarbonate as the counterion was kept in the original container. Resin was stored at room temperature (20° C), and

DOFW was added to each container to ensure that the resin remained in a wet slurry form during storage.

3.2 EXPERIMENTAL PROCEDURES

3.2.1 Preliminary Jar Testing

MIEX Resin

500 mL of raw water was measured into each of six glass beakers fitted with sampling ports approximately 1 inch from the bottom. To prepare MIEX resin doses, the resin storage containers were shaken vigorously, and then resin slurry was poured into a 10-mL graduated cylinder. The cylinder was gently tapped by hand for 30 seconds and the resin was allowed to settle for approximately 1 minute. A specific dose was extracted by using a disposable glass Pasteur pipette to transfer the desired volume of settled resin to a glass beaker. DOFW was added to the beaker to keep the resin in slurry form. After all six doses had been prepared, the jars containing the raw water were placed under a six-paddle stirrer (Phipps and Bird, Richmond, VA) fitted with 1-inch by 2-inch rectangular paddles. The contents of each beaker containing MIEX resin were transferred to their respective water samples and the beaker was rinsed with DOFW to ensure all resin beads were transferred. For bulk-treatment experiments involving large volumes of resin, sample water was used to wash resin from the beaker to avoid diluting the sample. The paddle stirrer was then set to 100 rpm for 30 minutes. Following the resin contact period, samples were allowed to settle for 30 minutes. Approximately 200 mL of supernatant was decanted and stored in 250-mL amber bottles at 4 °C. These samples were subsequently analyzed for UV absorbance at 254 nm, TOC, and bromide (see below). The results were plotted as a function of resin dose and used to select an appropriate dose for bulk treatment.

Alum Coagulation

A 2.5 g/L alum stock solution was prepared on the day of jar testing by dissolving 1.25 g technical grade aluminum sulfate (Fisher Scientific, Fair Lawn, NJ) into 500 mL DOFW. 500 mL of raw water was measured into each of six glass beakers and placed under a six-paddle stirrer (Phipps and Bird, Richmond, VA) fitted with 1-inch by 2-inch rectangular paddles. Doses of alum were added to each jar in succession using an adjustable pipette, and the paddle stirrer was set to 100 rpm for 1 minute to provide dispersion of the coagulant. After the rapid mixing period, the stirrer was slowed to 35 rpm and mixed for 30 minutes, after which the samples were allowed to settle for 30 minutes. Approximately 200 mL of supernatant was decanted and stored in 250-mL amber bottles at 4 °C. These samples were later analyzed for UV absorbance at 254 nm, TOC, and turbidity (see below). The results were plotted as a function of alum dose and used to select an appropriate dose for bulk treatment.

3.2.2 Bulk Treatment Experiments

Bulk coagulation and bulk MIEX treatment were performed in a 16-L glass carboy fitted with a variable-speed motor and an 8-inch by 1.25-inch rectangular paddle (Dayton Electric Mfg. Co., Niles, IL). 16 L of raw water was measured into the carboy, and the initial pH and temperature were measured. The desired dose of alum or MIEX resin was added to the water, and the sample was rapidly mixed for 1 minute at 80 revolutions per minute. The stirrer was then slowed to either 22 rpm (coagulation treatment) or 62 rpm (MIEX resin treatment). These speeds were calculated to replicate the velocity gradient in the containers used for jar testing. However, the calculations were based on 3-inch paddles in the jar tester, where were inadvertently replaced with smaller (2-inch) paddles before experiments began. This change went unnoticed until after experiments were complete, and as a result the mixing intensity associated with bulk treatment was significantly higher than that for jar testing. Details of the mixing intensity calculations appear in Appendix A.

After mixing for 30 minutes, the electric motor and paddle were removed from the carboy, the top was covered with foil, and the sample was allowed to settle for 30 minutes. At the end of the settling period, a plastic tube was inserted through the top of the carboy and used to siphon 12 L of supernatant into pre-rinsed 2.5-gal collapsible plastic containers. Care was taken not to disturb the settled alum floc or MIEX resin accumulated at the bottom of the carboy. Bulk-treated samples were immediately analyzed for temperature and pH, and later analyzed for TOC, UV absorbance at 254 nm, and bromide.

3.2.3 Ozonation Experiments

Ozonation experiments were conducted at bench-scale in a semi-batch reactor. Ozone gas was generated from oxygen and bubbled through the sample continuously while the influent and effluent gas-phase concentrations were monitored.

Ozonation Apparatus

The ozonation apparatus (schematically depicted in Figure 3.2) consisted of an ultra-high purity oxygen tank (National Welders Supply Co., Durham, NC), a moisture trap (Alltech Associates, Deerfield IL), a rotameter (Dwyer Instruments, Michigan City, IN), an ozone generator (Sander Model Certizon 200, Uetze-Eltze, Germany), and an 11.5-L cylindrical plexiglass reactor measuring 5.5 inches in diameter and 29.5 inches in height. The reactor was fitted with a sintered glass diffuser with a nominal pore size of 25-50 μm (Ace Glass Inc., Vineland, NJ). The reactor had a removable top affixed with eight stainless steel bolts and a PTFE gasket to prevent loss of ozone. Two liquid sampling ports were located 5.5 inches and 13 inches from the bottom. Connections between components were made using PTFE tubing and stainless steel fittings. The moisture trap was used to control the humidity of the oxygen gas and ensure a steady output concentration from the ozone generator. A stainless steel needle valve located on the oxygen tank enabled control of the gas flow. Several stainless steel valves allowed ozone from the generator to be directed either to the reactor, to a set of "traps," or to sampling ports immediately upstream and downstream of the reactor.

The ozone traps consisted of two gas washing bottles in series, both equipped with fine bubble diffusers. These were used to destroy any ozone gas exiting the reactor, and to provide a way to warm up the ozone generator while bypassing the reactor. The first bottle contained dilute sodium hydroxide (NaOH), prepared by dissolving approximately 10 g of food-grade NaOH pellets (Mallinckrodt Baker, Paris, KY) into DOFW. The off-gas from this trap entered a second gas washing bottle filled with potassium iodide (KI), prepared by dissolving approximately 18 g of ACS-grade KI (Mallinckrodt Baker, Paris, KY) into DOFW. The KI trap served as a visual indicator of the efficiency of ozone capture: ozone that was not destroyed by the NaOH oxidized the iodide to iodine, changing the solution from clear to brown. Traps were prepared fresh when this color change was observed. The entire

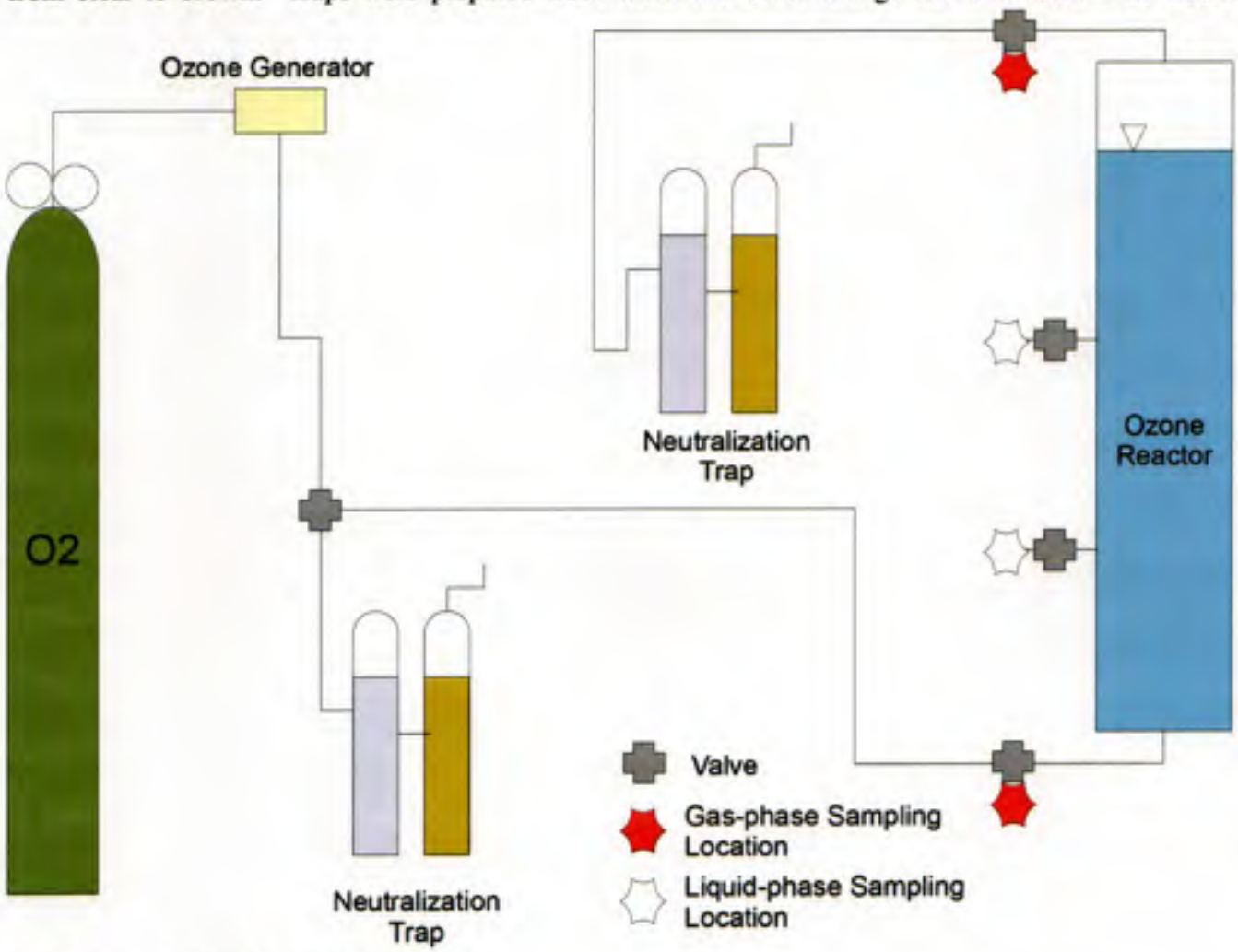

Figure 3.2: Schematic of ozonation apparatus

apparatus (except for the oxygen tank) was placed in a fume hood as a safety precaution against exposure to ozone.

Ozonation Procedure

Prior to each set of ozonation experiments (each new water sample), the ozone reactor was cleaned by filling with approximately 10 L of DOFW and ozonating for a minimum of 30 minutes. The DOFW was left in the column for several hours to ensure any ozone-demanding materials on the walls of the column were destroyed, and the column was drained. 9 L of the target water sample was brought to room temperature and poured into the reactor, and the top was sealed. Valves on the apparatus were set to direct gas flow to the ozone traps, bypassing the reactor, and the gas supply was turned on. After setting the desired flow rate, the power to the ozone generator was turned on, and the system was allowed to warm up for 30 minutes. During this time, the pH and temperature of a water sample from the sampling port on the reactor were measured.

After 30 minutes, the gas-phase ozone concentration exiting the generator was measured (see below) to verify that it was operating as expected. If the value was within the expected range, the valves were adjusted to direct the ozone gas into the reactor, beginning the experiment. Liquid- and gas-phase samples were withdrawn from the reactor and the gas lines, respectively, at various time intervals to track the dissolved ozone concentration and the amount of ozone transferred. These procedures are described below. Additional liquid-phase samples were collected periodically for subsequent bromate analysis. Approximately 20 mL of sample was collected into a 40-mL glass vial and quenched with 1 drop of 100 mg/mL ethylenediamine (EDA) preservative solution, as specified in EPA Method 300.1 (U.S. EPA, 1997).

The amount of ozone transferred into solution was calculated in real-time based on influent and effluent UV absorbance readings (see below), according to the equation:

$$[O_3]_{trans} = \frac{\Delta O_3 Q t}{V} \qquad [3.1]$$

Where:
$[O_3]_{trans}$ = ozone transferred into solution, mg/L
ΔO_3 = difference between influent and effluent ozone gas-phase concentrations, mg/L_{gas}
Q = gas flow rate, L/min
t = time interval, min
V = volume of water in the reactor, L

Ozonation was continued until a quantity of ozone corresponding to 1 mg O_3 per mg TOC had been transferred to the sample. Once this condition was achieved, valves were switched to direct ozone away from the reactor and into the traps, and the power to the generator was turned off. The ozonated sample was allowed to sit in the column for approximately one hour while liquid-phase ozone measurements were taken (see below), after which the sample was drained into two collapsible plastic containers for storage and subsequent analysis.

Gas-Phase Ozone Concentration

During ozonation experiments, the gas-phase ozone concentration entering and leaving the semi-batch reactor was measured using a spectrophotometer (Hitachi U-2000, Hitachi Instruments, Inc., Danbury, CT). The instrument was allowed to warm up for approximately 30 minutes prior to any measurements, and was zeroed using a 5-cm quartz cell containing ambient air.

Gas samples were collected in a 5-cm quartz cell fitted with two PTFE caps. A sampling tube from the inlet or outlet from the ozonation apparatus was inserted into one of the openings, and the gas was flushed through the cell for 10 seconds. The opposite opening was capped, then the sampling tube was removed and the other opening was capped. The sample was immediately analyzed for absorbance at 253.7 nm. Absorbance measurements were converted into gas-phase ozone concentrations using Beer's

Law:

$$[O_3]_{gas} = \frac{(MW)(\text{Abs})}{b\epsilon} \qquad [3.2]$$

where:
$[O_3]_{gas}$ = ozone gas concentration, mg/L
MW = molecular weight of ozone, 48,000 mg/mol
Abs = absorbance value at 253.7 nm
b = path length of cell, 5 cm
ϵ = molar absorptivity of ozone, 3,000 $\frac{L}{cm-mol}$ (IOA, 1998)

Prior to beginning ozone experiments, a stainless steel needle valve was installed on the influent gas sampling line. This valve was adjusted so that the gas flow rate through the system during influent sampling, which bypasses the ozone reactor, was the same as the gas flow rate during ozonation. Without the valve in place, opening the influent sampling port removed the back-pressure created by the water column and the traps, leading to an unrealistically high gas flow rate and dilution of the influent ozone gas concentration. By inducing artificial head loss, the needle valve kept the gas flow rate constant between sampling and ozonation, allowing reliable influent gas-phase ozone concentration measurements during sampling.

Liquid-Phase Ozone Concentration

Dissolved ozone was measured according to the Indigo Method (Bader and Hoigne, 1981; Standard Method 4500-O3 B, APHA et al., 1998). Indigo stock solution was prepared by adding 0.5 mL concentrated, ACS-grade phosphoric acid (Mallinckrodt Baker, Paris, KY) and 335 mg potassium indigo trisulfonate (Aldrich Chemical, Milwaukee, WI) to a 500-mL volumetric flask and filling to the mark with DOFW. A working indigo solution was prepared by adding 25 mL of the stock solution, 1.75 mL concentrated phosphoric acid, and 2.5 g sodium dihydrogen phosphate (Fisher Scientific, Fair Lawn, NJ) to a 250-mL volumetric flask and filling to the mark with DOFW. Both solutions were stored in the dark in amber glass bottles. The stock solution was prepared fresh every 4 months, and the working solution was prepared fresh before each set of ozonation experiments.

Prior to each ozonation experiment, 1 mL of the indigo working solution was transferred to 10-mL ozone-demand free volumetric flasks. One flask was filled to the mark with DOFW and another with the sample to be ozonated to serve as blanks. All flasks were placed in a dark cabinet near the ozonation apparatus. At pre-determined time intervals, dissolved ozone samples were taken from a sampling port on the ozone reactor, which was fitted with a Pasteur pipette. The sampling port was opened and water from the column was wasted for a few seconds, then the port was closed. The Pasteur pipette was then placed below the surface of the indigo solution in one of the 10-mL flasks, and the sampling port was opened to fill the flask to the mark. The flask was immediately capped and placed back in the dark cabinet.

The indigo-containing flasks were analyzed immediately following each ozonation experiment (within one hour of sample collection). Beginning with the most recent sample (highest ozone concentration, lowest absorbance), the reacted indigo solutions were filtered through a 0.45 μm PVDF or PTFE syringe filter (Whatman, Inc., Piscataway, NJ and Fisher Scientific, Fair Lawn, NJ, respectively) to minimize the effect of turbidity on absorbance readings. 13-mm syringe filters were pre-rinsed with 40 mL DOFW, which provides an equivalent volume of water per unit of filter area as 500 mL for a standard 47-mm disc filter. The first 1-2 mL of sample was used to rinse a 5-cm quartz cell which was then filled with the remaining sample. The absorbance of the sample was measured at 600 nm on a Hitachi U-2000 spectrophotometer (Hitachi Instruments, Inc., Danbury, CT). Dissolved ozone concentration was calculated based on the difference in absorbance between the sample and the blank using the following equation (from Standard Method 4500-O3 B, APHA et al., 1998):

$$[O_3]_{aq} = \frac{10(\Delta \text{Abs})}{f\,b\,V} \qquad [3.3]$$

where:
$[O_3]_{aq}$ = dissolved ozone concentration, mg/L
Δ Abs = difference between blank and sample absorbance at 600 nm, cm^{-1}
f = conversion factor, 0.42 (APHA et al., 1998)
b = path length of cell, 5 cm
V = Volume of sample, 9 mL
10 = indigo dilution factor

The absorbance of the sample blank (prepared from sample before ozonation) and the DOFW blank were compared to assure that turbidity or other interferences were not significantly altering the measured absorbances. Dissolved ozone concentrations were calculated based on the absorbance of the sample blank. Examples of transferred ozone calculations appear in Appendix B.

3.2.4 Chlorination Procedure and THM Formation Potential

4-6% sodium hypochlorite stock solution (Fisher Scientific, Fair Lawn, NJ) was used to prepare chlorine dosing solutions for both chlorine demand and THM formation potential experiments. The stock solution was diluted 2:100 with DOFW in a 100-mL chlorine-demand free volumetric flask, and the resulting working solution was titrated with standard sodium thiosulfate (Fisher Scientific, Fair Lawn, NJ) according to Standard Method 4500-Cl-B (APHA et al., 1998) to determine its strength. Based on the results, a dosing solution was prepared by diluting an appropriate quantity of working solution with DOFW in a 100-mL chlorine-demand free volumetric flask. pH 6.7 borate buffer, prepared in accordance with the procedure given by Summers et al. (1996), was added in a 4-5:1 volume ratio with the chlorine working solution to form a pH 8 combined buffer and chlorine dosing solution. Volumes were selected to prepare a solution at 100 mg/L as Cl_2 for chlorine demand experiments and 300 mg/L as Cl_2 for THM formation potential tests. When not in use, the sodium hypochlorite stock solution was stored at 4 °C to slow degradation.

After the dosing solution was prepared, a blank test was run to verify its strength. For the 100 mg/L Cl_2 dosing solution, a 100-mL volumetric flask was filled roughly halfway with DOFW, 1 mL of

chlorine solution and 0.2 mL of pH 8 borate buffer were added as per Summers et al. (1996), and the flask was filled to the line with DOFW. An identical procedure was followed for the 300 mg/L Cl_2 solution, except that a 300-mL biological oxygen demand (BOD) bottle was used and 0.6 mL of buffer was added. In either case, the chlorine residual expected in the bottle was 1.0 mg/L. The residual was immediately measured by the DPD titrimetric method (Standard Method 4500-Cl-F; APHA et al., 1998). If the residual was not within 20% of the expected concentration, the blank test was repeated. If the result was confirmed, the dosing solution was discarded and re-prepared.

THM formation potential experiments were performed in accordance with the Uniform Formation Conditions (UFC) procedure outlined by Summers et al. (1996). The UFC are those conditions that produce a free chlorine residual of 1 mg/L at pH 8 after incubation in the dark for 24 hours at 20 °C. To determine the required chlorine dose, chlorine demand experiments employing three or four doses of chlorine per water were conducted. 100-mL volumetric flasks were filled to approximately 90% capacity with water sample, and 0.2 mL of pH 8 borate buffer was added. The desired chlorine dosage was transferred using an adjustable volumetric pipette. The flasks were then filled to the line with DOFW and placed in a dark cabinet inside a constant-temperature room at 20 °C for 24 hours. At the end of the incubation period, the chlorine residual was measured using the DPD titrimetric procedure (Standard Method 4500-Cl-F; APHA et al., 1998).

The results of the chlorine demand experiments were used to select an appropriate UFC dose for each water sample. 300-mL BOD bottles were filled about 90% full with water sample and 0.6 mL of pH 8 borate buffer. If necessary, 0.1 N sodium hydroxide or hydrochloric acid was used to adjust the pH of the buffered water samples to 8 +/- 0.2. The appropriate dose of chlorine was added to each sample, and the bottles were filled headspace-free and incubated in the dark at 20 °C for 24 hours. After 24 hours, the chlorine residual was measured as above.

After the 24-hr incubation period, THM samples were collected from the 300-mL BOD bottles in

40-mL glass vials with PTFE-lined caps. Each vial contained approximately 0.25 g of ACS-grade ammonium sulfate (Mallinckrodt Baker, Paris, KY) to quench the free chlorine residual and prevent further formation of THMs. For North Bay Aqueduct water, sodium sulfite was used to quench the chlorine residual. The water sample was poured carefully down the side of the vials to minimize volatilization and the vials were filled headspace-free and capped. Each chlorinated sample was collected in duplicate vials and stored at 4 °C until extraction, which was performed within 2 weeks of chlorination.

3.2.5 XAD Fractionation

The TOC was separated into hydrophilic and hydrophobic organic acid fractions using XAD-8 resin (Rohm and Haas, Philadelphia, PA) following procedures similar to those in Thurman and Malcolm (1981) as modified by Boyer (2005). The fractionation apparatus consisted of a glass column containing 12 mL of resin. Prior to use, the resin was cleaned by pumping 1 N sodium hydroxide through the column for 10 minutes at a flow rate of 4 mL/min, followed by 1 N hydrochloric acid for 10 minutes at the same flow rate. This process was repeated three times. Approximately 1 L of the water sample to be fractionated was vacuum-filtered through a 0.45 μm membrane filter (Pall Corporation, Ann Arbor, MI), pre-rinsed with 500 mL DOFW, to remove particulate matter. The sample was acidified with concentrated hydrochloric acid until the pH fell below 2. The entire sample was then pumped through the column at 4 mL/min. The first bed volume (12 mL, 3 minutes) of effluent was discarded, and the remainder was collected in an Erlenmeyer flask. Approximately 150 mL of XAD-8 effluent was collected in an amber glass bottle and stored at 4°C for subsequent DOC and UV254 analysis. The hydrophobic acid content of the sample was calculated by subtracting the DOC of the XAD-8 effluent from the DOC of the whole water.

3.3 ANALYTICAL METHODS

3.3.1 Ultraviolet Absorbance at 254 nm

Ultraviolet absorbance measurements were made on a Hitachi U-2000 spectrophotometer (Hitachi Instruments Inc., Danbury CT) using a 1-cm quartz cell. Before making measurements, the instrument was allowed to warm up for approximately 30 minutes, then was set to 254 nm and zeroed using DOFW. Prior to analysis, all samples were filtered through a pre-rinsed 0.45 μm membrane filter (Pall Corporation, Ann Arbor, MI) or PVDF or PTFE syringe filters (Whatman, Inc., Piscataway, NJ and Fisher Scientific, Fair Lawn, NJ, respectively) as outlined above. The cell was rinsed several times with DOFW between samples to prevent cross-contamination.

3.3.2 Total and Dissolved Organic Carbon

TOC and DOC were measured on a Shimadzu TOC 5000 Analyzer fitted with an ASI 5000 autosampler (Shimadzu Corporation, Atlanta, GA). The instrument measures non-purgeable organic carbon according to the High Temperature Combustion Method (Standard Methods 5310 B, APHA et al., 1998).

A standard solution of organic carbon was prepared by dissolving 2.125 g of ACS-grade potassium hydrogen phthalate (Fisher Scientific, Fair Lawn, NJ) into 1 L of DOFW; this solution was made fresh every two months. A working solution was prepared weekly by diluting the stock solution 1:10 in DOFW. Calibration standards were prepared on the day of analysis by diluting appropriate quantities of working solution with DOFW in 100-mL volumetric flasks. All solutions were stored at 4 °C.

Samples and calibration standards were placed in 20-mL glass vials and acidified with 2N hydrochloric acid to pH 2-3. During the run, each sample was sparged for five minutes with zero-grade air (National Welders Supply Co., Durham, NC) to remove inorganic carbon before being analyzed for total carbon. Measured values for each sample represent the average of three injections made by the instrument. As an additional quality control measure, check standards and DOFW blanks were placed

between every six samples to verify the consistency of the instrument response. For DOC measurements, samples were filtered through pre-rinsed 0.45 μm membrane filters (Pall Corporation, Ann Arbor, MI) or PVDF or PTFE syringe filters (Whatman, Inc., Piscataway, NJ and Fisher Scientific, Fair Lawn, NJ, respectively) prior to analysis.

3.3.3 pH

pH was measured using an Accumet AB-15 electronic pH meter with an Accumet electrode (Fisher Scientific, Fair Lawn, NJ). The meter was calibrated before each use using pH 4, 7, and 10 buffer solutions (Fisher Scientific, Fair Lawn, NJ). The electrode was refilled with saturated potassium chloride solution (Fisher Scientific, Fair Lawn, NJ) whenever the fluid level fell below half full. All buffers and samples were stirred either with a magnetic stir bar or by manually moving the electrode through the sample to ensure more stable and accurate pH measurements.

3.3.4 Bromide and Bromate

Bromide and bromate were analyzed by ion chromatography according to a method derived from EPA Method 300.1 (U.S. EPA, 1997). A Dionex (Sunnyvale, CA) ion chromatography (IC) system consisting of a GPM-2 gradient pump, CDM-II conductivity detector, and eluent degas module was used. Dionex analytical and guard columns (IonPac AS-19 and AG-19, respectively) were installed for the detection of bromate and bromide. A Dionex ASRS chemical suppressor was used to mask the background conductivity of the eluent.

15.0 mM NaOH was used as eluent. This was prepared by diluting 1.2 g of certified 50% NaOH stock solution (Fisher Scientific, Fair Lawn, NJ) in a 1-L volumetric flask with DOFW. The headspace in the bottle was flushed with nitrogen whenever the cap was open in order to prevent absorption of carbon dioxide into the solution from the air, and the bottle was stored at room temperature. Eluent was immediately vacuum-filtered through a pre-rinsed 0.45 μm membrane filter (Pall Corporation, Ann Arbor, MI) and placed in a plastic eluent bottle which was sparged with nitrogen. Eluent was prepared

no more than one day before analysis, and was sparged with helium for 30 minutes after being installed in the eluent degas module. Regenerant (50 mN H_2SO_4) was prepared by adding 5.6 mL concentrated H_2SO_4 (Fisher Scientific, Fair Lawn, NJ) to 4 L DOFW.

A calibration mixture containing bromide, bromate, and chloride was prepared from granular ACS-grade reagents. Chloride and bromide were added in a 333:1 ratio to reflect their occurrence in natural water (Stumm and Morgan, 1996; Magazinovic et al., 2004; Hsu and Singer, 2010). 1,000 mg/L stock solutions of each ion were prepared by dissolving 1.336 g potassium bromate (Mallinckrodt Baker, Paris, KY), 1.2875 g sodium bromide (Fisher Scientific, Fair Lawn, MJ), and 1.657 g sodium chloride (Mallinkcrodt Baker, Paris, KY) into 100-mL volumetric flasks filled with DOFW. 50 mL of the chloride stock solution plus 15 mL of a 1:100 dilution of the bromide stock solution were combined in a 100-mL volumetric flask to achieve the desired Cl:Br ratio. Two serial 1:100 dilutions of the bromate stock solution were performed in separate 100-mL volumetric flasks to make a 100 µg/L working solution. Individual calibration standards were prepared by adding appropriate volumes of the 100 µg/L bromate solution and the working mixture containing 500 mg/L chloride and 1.5 mg/L bromide. A typical set of calibration points is illustrated in Table 3.2:

Table 3.2: Typical ion chromatograph calibration standards

Calibration Level	Bromate (µg/L)	Bromide (µg/L)	Chloride (mg/L)
0	0	0	0
1	1	20	6.7
2	3	50	16.5
3	5	100	33.3
4	10	150	50
5	20	200	66.7
6	50	300	100

After sparging the eluent for 30 minutes with helium and priming the gradient pump, the IC system

was allowed to equilibrate for 30 minutes before any samples were run. If the system back pressure and background conductivity were within expected limits, samples were loaded onto the column and analyzed according to the conditions given in Table 3.3. All samples were filtered using pre-rinsed 0.45 μm PVDF or PTFE syringe filters (Whatman, Inc., Piscataway, NJ and Fisher Scientific, Fair Lawn, NJ, respectively) prior to analysis. Typical retention times for bromate, bromide, and chloride were 6.5, 12, and 7.9 minutes, respectively. Check standards were injected after every group of 5 samples to monitor for changes in instrument response. The resulting chromatograms were analyzed by manually integrating the peak areas and converting these to concentrations using the calibration curve. A typical chromatogram and an illustrative set of calibration curves are shown in Appendix C.

Table 3.3: Ion chromatograph conditions for bromate and bromide analysis

Eluent and Flow Rate	15 mM NaOH at 1.0 mL/min
Regenerant and Flow Rate	50 mN H_2SO_4 at 4.0±1 mL/min
Analytical Column	Dionex IonPac AS-19
Guard Column	Dionex IonPac AG-19
Sample Loop Size	500 μL
Suppressor	Chemical, Dionex ASRS

3.3.5 Total Trihalomethanes

THM analysis was performed according to the liquid-liquid extraction procedure similar to that described in Standard Method 6232 (APHA et al., 1998). The four THMs analyzed were chloroform ($CHCl_3$), bromodichloromethane ($CHBrCl_2$), dibromochloromethane ($CHBr_2Cl$) and bromoform ($CHBr_3$). Samples were analyzed on a Hewlett Packard Model 5890A Series II gas chromatograph (GC) with electron capture detection (Hewlett Packard Co., Cary, NC).

Working standard solutions were prepared from a stock solution containing 2,000 μg/mL of each THM species (EPA THM Calibration Standard Mixture, Supelco, Inc., Bellefonte, PA). Working standards were prepared by diluting 100 μL and 20 μL of stock solution into 2-mL volumetric flasks

using ACS-grade methyl tert-butyl ether (MtBE; Sigma Aldrich, St. Louis, MO). Both the stock and working solutions were stored in amber vials in a freezer when not in use.

Calibration standards were prepared from these two working solutions by adding appropriate volumes to a 100-mL volumetric flask to which at least 90 mL of DOFW had been added. The flasks were placed in a fume hood, and the working solution was injected below the water surface using an adjustable pipette. The flasks were then filled to the mark and capped. A typical calibration curve consisted of 0, 1, 5, 25, 50, 100, 200, and 300 µg/L concentrations of each THM species.

1,2 dibromopropane (Sigma Aldrich, St. Louis, MO) was used as the internal standard (IS). The extracting solvent was prepared by adding 1,2 dibromopropane to ACS-grade MtBE. A stock solution of the internal standard was prepared by adding 10 µL of the concentrated standard with MtBE in a 5 mL volumetric flask. A primary dilution of the stock solution was made by diluting 125 µL in a 5-mL volumetric flask. Finally, the extracting solvent was prepared by diluting 250 µL of the primary dilution into a 500-mL volumetric flask with MtBE. Extracting solvent was prepared fresh on the day of extraction and was placed in a 1-L amber glass jar fitted with a repipetter to facilitate dispensing of the solution. All internal standard solutions were stored in amber glass vials in the freezer when not in use.

20 mL of each sample and calibration standard was measured using a graduated cylinder, which was rinsed with DOFW between samples and placed in a 40-mL glass vial. 3 drops of concentrated sulfuric acid (Fisher Scientific, Fair Lawn, NJ) were added to each vial to lower the pH to 2-3, then 2 mL of extracting solvent was added using the repipetter. Approximately 4 g of sodium sulfate (Mallinckrodt Baker, Paris, KY), which had been baked at 400 °C for 24 hours to remove moisture, was added to each vial to remove any remaining moisture from the solvent. Immediately after the addition of sodium sulfate, each vial was vortexed for 1 minute to provide intense mixing of the sample and solvent.

After the samples had separated for at least 5 minutes and a distinct organic layer was visible, a Pasteur pipette was used to withdraw solvent and place it in duplicate GC autosampler vials. Each vial was capped with a PTFE-faced cap and sealed with a crimping tool. All samples were extracted into duplicate GC vials and placed in the freezer until analysis. Table 3.4 shows the characteristics of the instrument and the temperature program used for THM analysis.

Blanks of MtBE and the extracting solvent (MtBE+IS) were placed at the beginning of each sample sequence, followed by the complete set of calibration standards and the unknown samples. For each water of interest, duplicate extracts were analyzed to provide quality assurance. Calibration check standards were placed periodically between groups of the unknown samples to monitor the instrument for drift. Chromatograms were analyzed by integrating the peak areas of each of the four THM species as well as the internal standard. The resulting THM peak areas were normalized by the area of the internal standard, and converted to concentrations using the calibration curves. For the SBA and Lake Campbell waters, co-eluting peaks near the internal standard made quantification of the internal standard peak area difficult, so calibration was performed based on relative peak height instead. Calibration curves were developed for each of the four THM species; illustrative chromatograms and calibration curves are shown in Appendix D.

Typical retention times for $CHCl_3$, $CHBrCl_2$, $CHBr_2Cl$, and $CHBr_3$ were 7.9, 12.9, 16.2, and 18.7 minutes, respectively.

3.3.6 Excitation-Emission Fluorescence Spectroscopy

Water samples were filtered through pre-rinsed 0.45 μm PVDF or PTFE syringe filters (Whatman, Inc., Piscataway, NJ and Fisher Scientific, Fair Lawn, NJ, respectively) prior to analysis, and placed in a 1-cm quartz cuvette. The absorbance spectrum of each sample over wavelengths from 200 nm to 700 nm (in increments of 2 nm) was measured using a Hewlett Packard Model 8452A diode array spectrophotometer (Hewlett Packard Co., Cary, NC). A Fluoromax-4 fluorometer (Horiba Jobin Yvon,

Table 3.4: Gas chromatograph conditions for THM analysis

Injector:	
Syringe Size	10 µL
Injection Volume	2 µL
Injector Temperature	150 °C
Solvents:	
Wash Solvent	MtBE
Pre-Injection Washes	3
Post-Injection Washes	2
Pumps	3
Oven / Column:	
Equilibration Time	3 min
Oven Maximum Temperature	300°C
Carrier Gas	Helium
Carrier Gas Flow Rate	1 mL/min
Carrier Gas Pressure	11.3 psi
Column	Agilent DB1
Column Dimensions	30.0 m, 0.25µm diameter, 0.25µm film thickness
Split Flow	1 mL/min
Temperature Program:	
35 °C for 10 minutes, increase at 10 °C / min to 150 °C (11.5 minutes), increase at 25 °C/min to 250 °C (4 minutes), hold at 250 °C for 11 minutes.	
Total run time	36.5 minutes
Detector:	
Type	ECD (electron capture detector)
Temperature	300 °C

Inc., Edison, NJ) equipped with a xenon lamp was used to generate excitation-emission fluorescence spectra (EEMs) using the parameters described in Cory et al. (2010): water samples were excited across wavelengths of 240 to 450 nm in increments of 5 nm, and fluorescent emissions were measured at 320 to 500 nm in increments of 2 nm. The slit width for both excitation and emission was 5 nm. All post-processing of EEM data was done in Matlab (v 7.7) following the procedures of Cory et al. (2010). Briefly, the absorbance spectrum of each sample was used to remove potential interference in the EEMs due to the inner-filter effect caused by strongly absorbing carbon in the sample (Mobed et al. 1996). Blank EEMs of laboratory grade water collected daily in the same manner as sample EEMs were then subtracted from the sample EEMs to minimize Rayleigh and Raman scattering peaks, after checking to verify that there was no detectable fluorescence in laboratory water EEMs. Next, all EEMs were corrected for instrument-specific response using excitation correction factors generated with rhodamine (DeRose et al. 2007) and manufacturer-generated emissions correction factors. Finally, EEMs were normalized to the area of the Raman peak in the blank EEM at an excitation wavelength 350 nm and thus EEM intensities are reported as Raman Units (Stedmon & Bro, 2008).

The fluorescence index (FI; McKnight et al. 2001), was calculated from each EEM as the ratio of the emission intensity at 470 nm to that at 520 nm at an excitation wavelength of 370 nm (Cory et al., 2010). Because of the different characteristics of fluorophores found in terrestrially- and microbially-derived fulvic acids, the FI offers insight into the nature and origin of the DOC in the water. Fluorescence index values less than 1.30 indicate terrestrial carbon, while values greater than 1.45 reflect microbially-derived carbon (Cory et al., 2010; McKnight et al., 2001).

CHAPTER 4: RESULTS AND DISCUSSION

4.1 RAW WATER CHARACTERISTICS

The characteristics of the four waters studied are summarized in Table 4.1. Water samples were collected in May, September, and December 2009 at three different locations in order to capture some of the temporal and spatial variability in TOC and salinity experienced in the Delta. The North Bay Aqueduct (NBA) water had a moderate TOC concentration and a low bromide concentration. Water from the South Bay Aqueduct was chosen for its high bromide concentration; this water contained low levels of TOC relative to the other samples, but had a SUVA and hydrophobic carbon content similar to that of the North Bay water. Finally, water from Lake Campbell was collected to represent the challenging water quality associated with the first rainfall events at the North Bay Regional WTP. This water had a very high TOC concentration but low bromide. The hydrophobic carbon content of this water was lower than that of the North and South Bay samples, possibly reflecting the fact that this water came from an inland lake rather than the Delta itself. In order to investigate the performance of MIEX resin on a high-TOC, high-bromide water, a sample of Lake Campbell water was spiked with bromide and chloride to achieve a bromide concentration of 380 µg/L, which corresponds to the 75th percentile concentration at the Banks pumping station in the Delta (CALFED, 2007).

Table 4.1: Summary of raw water characteristics

	North Bay Aqueduct	South Bay Aqueduct	Lake Campbell	Lake Campbell (spiked)
Sample Date	05/28/09	09/10/09	12/15/09	12/15/09
TOC, mg/L	3.7	2.3	8.7	8.7
DOC, mg/L	3.5	2.4	8.5	8.5
UV254, 1/cm	0.113	0.071	0.256	0.256
SUVA, L/mg-m	3.08	3.03	2.94	2.94
Hydrophobic Carbon	58%	51%	37%	37%
Fluorescence Index	1.39	1.43	1.43	1.43
pH	7.9	8.2	7.8	7.8
Ammonia, mg/L as N	BDL	0.11	0.04	0.04
Bromide, µg/L	40	360	33	380

4.2 NORTH BAY AQUEDUCT

4.2.1 Effect of MIEX Resin and Alum Treatment

Figures 4.1 and 4.2 illustrate the effect of alum coagulation and MIEX resin treatment, respectively, on North Bay Aqueduct water. Figure 4.1 shows that the removal of TOC and UV-absorbing substances increases with alum dose. At a dose of 35 mg/L, the TOC concentration was reduced by 27% and the UV absorbance was reduced by 50%. The greater removal of UV-absorbing substances indicates that alum coagulation preferentially removed the hydrophobic fraction of the TOC, consistent with observations by others (White et al., 1997; Liang and Singer, 2003).

Jar testing with MIEX resin also showed increasing removal of TOC and UV absorbance with increasing dose (see Figure 4.2). 2.0 mL/L of MIEX resin reduced the TOC concentration by 46% and the UV absorbance by 58%. No significant differences in performance between the chloride and bicarbonate forms of MIEX resin were apparent.

Based on these jar test results, 16-L aliquots of water were treated with either 35 mg/L alum or 1.0 mL/L MIEX, in both the chloride and bicarbonate forms. This alum dose was chosen to approximate

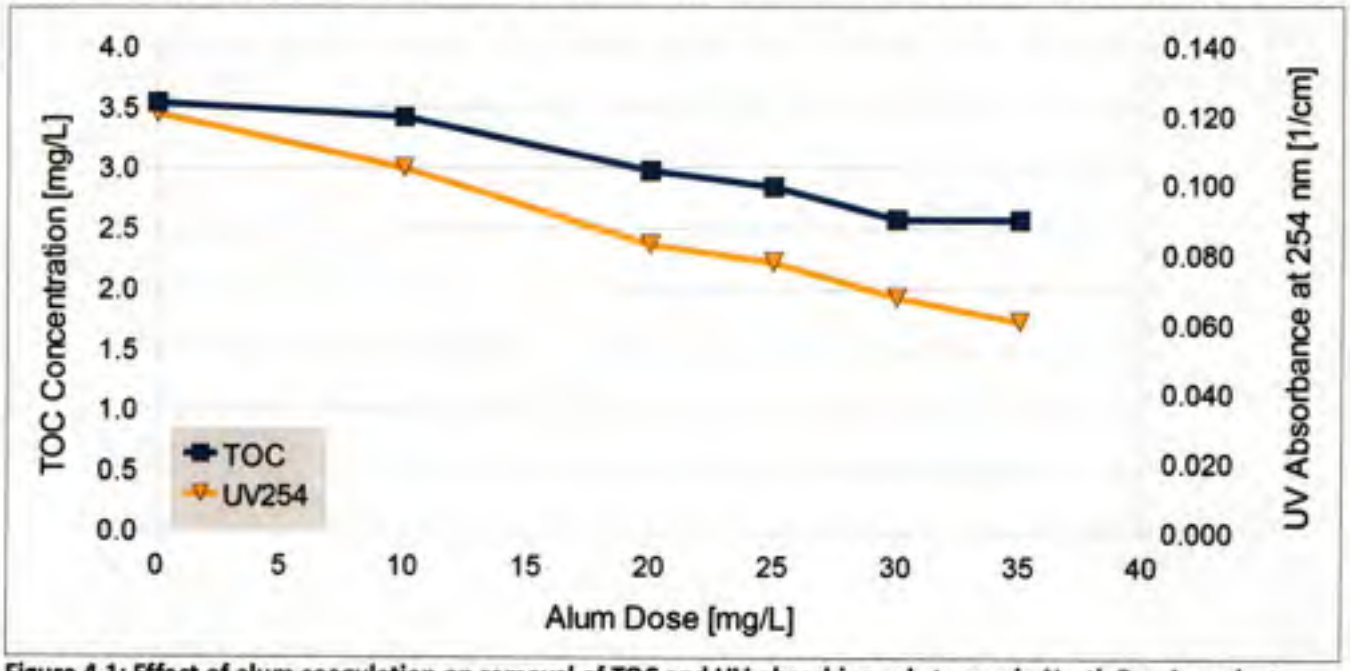

Figure 4.1: Effect of alum coagulation on removal of TOC and UV-absorbing substances in North Bay Aqueduct water.

the "point of diminishing returns" for TOC removal, while the MIEX dose was selected to achieve a reasonable degree of TOC removal at a dose likely to be used in practice. The water quality of these bulk-treated waters is summarized in Table 4.2. Because of the higher velocity gradient in the bulk treatment apparatus (see Section 3.2.2), removal of TOC and UV-absorbing substances was higher in the bulk MIEX resin-treated waters than in jar testing at the same dose. Removal of the same substances by alum was lower than in jar testing, which may have been due to some of the floc being disturbed and mixed with the sample when the settled water was decanted. As expected, the SUVA of the alum-coagulated water was lowest, reflecting the preferential removal of hydrophobic organic carbon by alum. MIEX resin treatment also reduced the SUVA, but to a lesser extent than alum. The hydrophobic acid content of the raw, alum, and resin-treated waters was similar, while treatment with either alum or MIEX resin increased the FI somewhat. The increase in FI indicates that more of the organic carbon remaining after treatment was microbial in origin, implying that both treatments

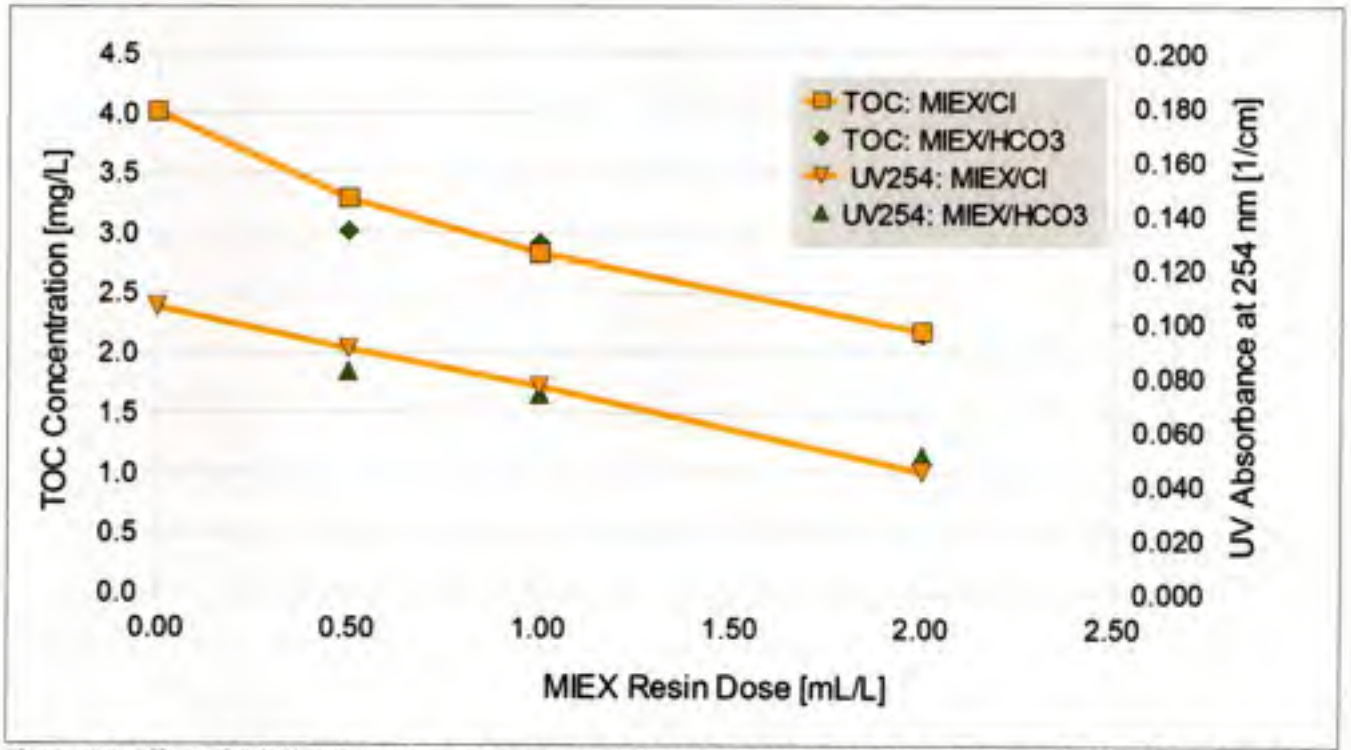

Figure 4.2: Effect of MIEX resin treatment on removal of TOC and UV-absorbing substances in North Bay Aqueduct water.

removed primarily terrestrial (humic) substances. Alum and MIEX/Cl treatment did not reduce the bromide concentration, while treatment with the MIEX/HCO_3 resin decreased it by a small amount.

Table 4.2: Summary of removal by bulk-treatment with alum and MIEX resin for North Bay Aqueduct water

Parameter	Type of Treatment			
	Raw	Alum	MIEX/Cl	MIEX/HCO_3
Dose	-	35 mg/L	1.0 mL/L	1.0 mL/L
TOC, mg/L	3.7	3.2	2.2	2.2
UV254, 1/cm	0.113	0.073	0.058	0.053
SUVA, L/mg-m	3.08	2.26	2.69	2.43
Hydrophobic Carbon	58%	58%	55%	-
Fluorescence Index	1.39	1.47	1.47	1.46
Bromide, µg/L	40	44	45	37
pH	7.9	7.7	8.2	8.2

4.2.2 Effect of Ozone

Each of the bulk-treated waters and the raw NBA water was ozonated to achieve a transferred ozone dose of 1.0 mg O_3/mg TOC. Ozone dose, or ozone transferred, refers to the mass of ozone transferred into the sample, which occurs in accordance with Henry's Law. The rate of mass transfer from the gaseous to aqueous phases is directly proportional to the degree of under-saturation of ozone in the aqueous phase relative to the equilibrium concentration. For these experimental conditions, the equilibrium dissolved ozone concentration was approximately 0.5 mg/L (see Appendix E). Figure 4.3 shows the impact of treatment with alum or MIEX resin on the kinetics of ozone transfer into solution. Treatment did not significantly alter the rate at which ozone was absorbed.

Figure 4.4 shows the relationship between dissolved ozone concentration and ozone transferred. Dissolved ozone concentration is a function both of the ozone absorbed by the solution (ozone transferred) and reactions with ozone-demanding substances in the water, including NOM. Treatment with MIEX resin or alum resulted in a significantly higher dissolved ozone concentration for a given amount of ozone transferred. At a transferred ozone dose of 2.0 mg/L, the dissolved ozone concentration in the MIEX resin- and alum-treated waters was 0.10-0.12 mg/L, while that in the raw

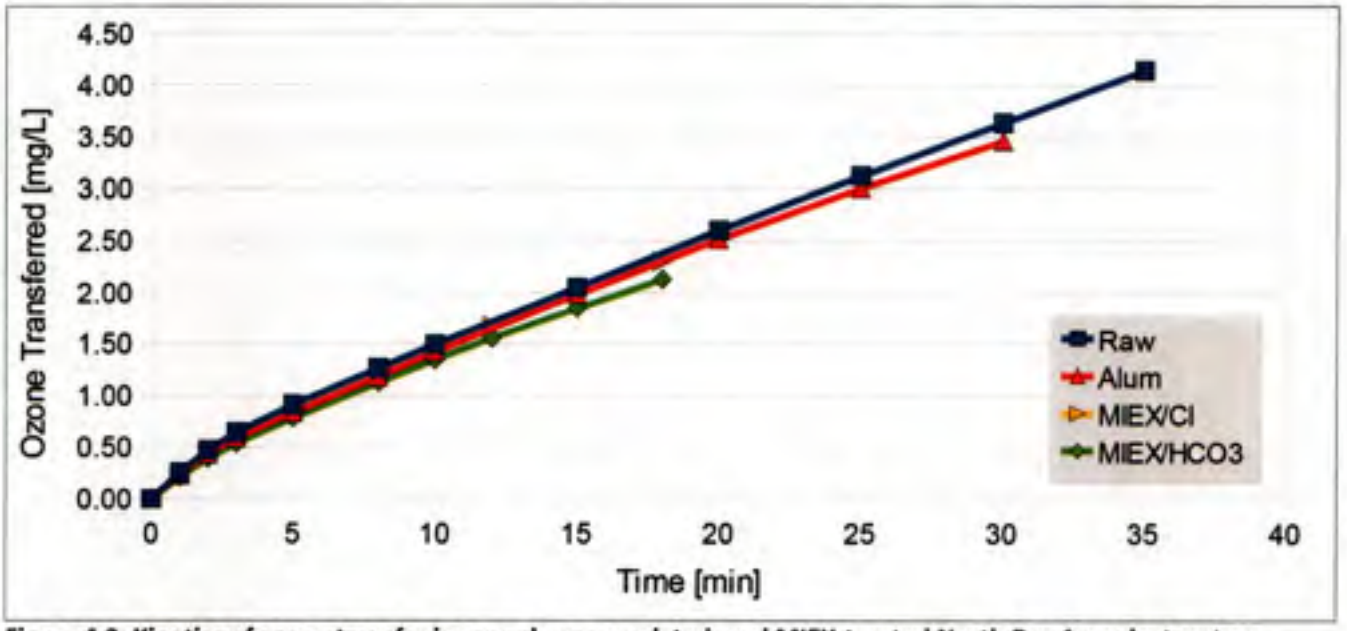

Figure 4.3: Kinetics of ozone transfer in raw, alum-coagulated, and MIEX-treated North Bay Aqueduct waters

water was only 0.03 mg/L. This fact was primarily a result of TOC removal; with fewer ozone-demanding substances in solution, alum-treated and MIEX resin-treated waters consumed less of the ozone transferred.

Figure 4.5 relates the amount of ozone transferred to the cumulative ozone exposure (CT). CT refers to the product of dissolved ozone concentration and contact time, and is the primary metric by which the efficacy of chemical disinfection is measured in water treatment. Treatment with either alum or MIEX substantially increased the CT for disinfection at a given ozone dose due to the higher dissolved ozone concentration shown in Figure 4.4. 4.2 mg/L of transferred ozone was required to achieve a CT value of 1.0 mg-min/L in the raw water, compared to 2.5 mg/L of ozone for alum-coagulated water and 2.25 mg/L of ozone in the MIEX resin-treated waters. Note that a CT value of 1.0 mg-min/L corresponds to 0.5-log inactivation credit of *Cryptosporidium* at 20 °C, as shown in Table 2.2 (U.S. EPA, 2006).

Due to the low initial bromide concentration in the North Bay Aqueduct water, no significant bromate formation took place during ozonation.

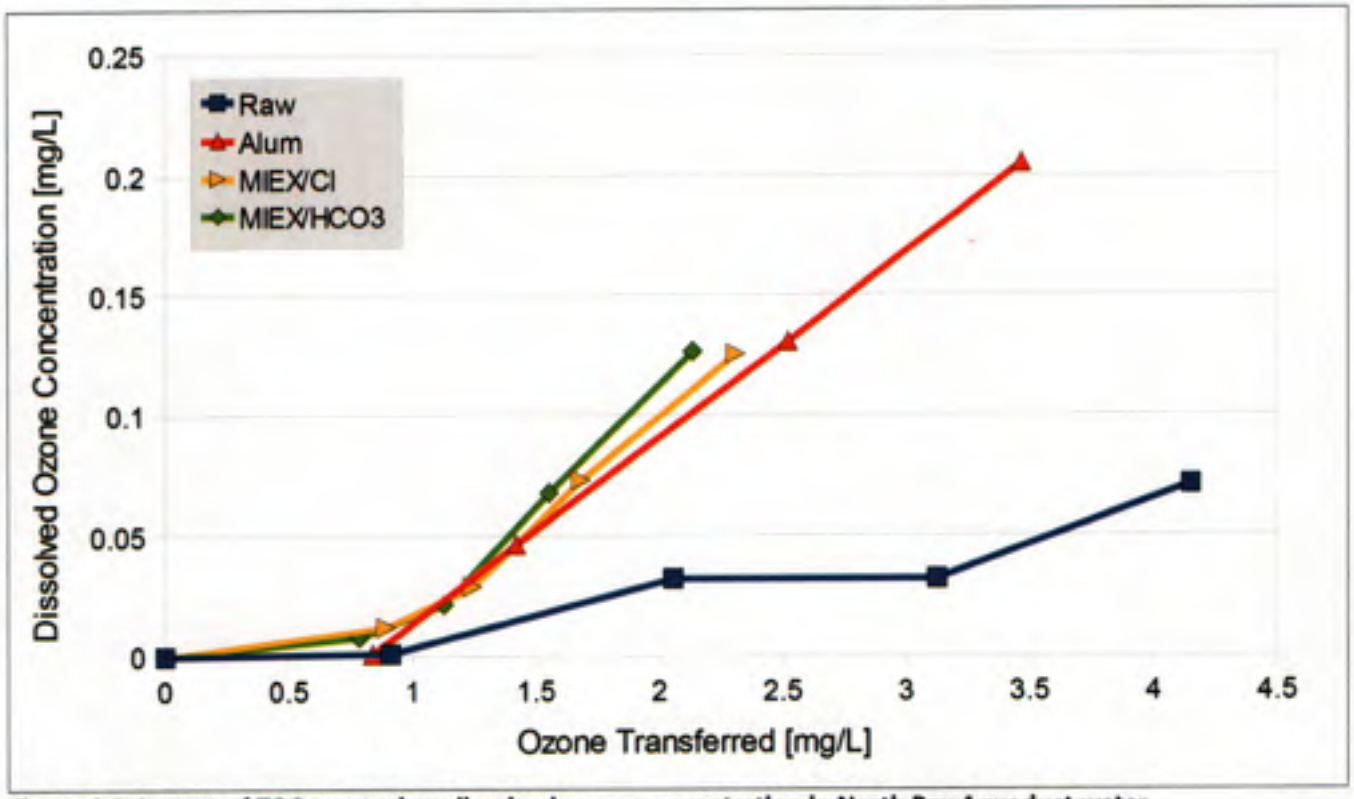

Figure 4.4: Impact of TOC removal on dissolved ozone concentration in North Bay Aqueduct water

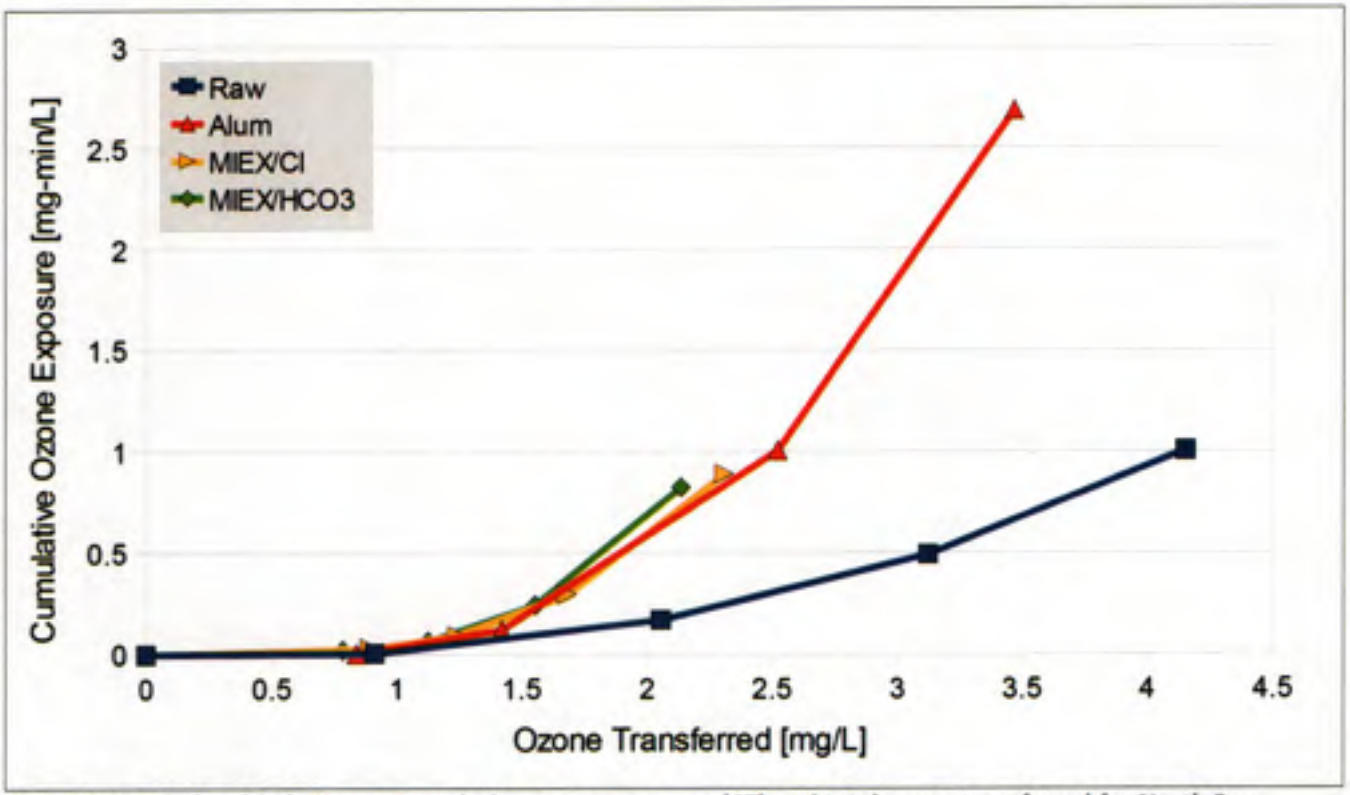

Figure 4.5: Relationship between cumulative ozone exposure (CT) and total ozone transferred for North Bay Aqueduct water

4.2.3 THM Formation Potential

Table 4.3 summarizes the impact of bulk treatment with alum or MIEX resin and subsequent ozonation on chlorine demand and THM formation potential. As expected, bulk treatment lowered the chlorine demand by removing organic carbon. Further, ozonation of each water reduced the UV absorbance and SUVA substantially. This is likely a consequence of the destruction of aromatic structures, which are known to be highly reactive with ozone (von Gunten, 2003a). Alum coagulation reduced the THM formation potential by 21%, while MIEX resin reduced THMFP by 42%. Ozonation of the alum-treated and MIEX resin-treated waters reduced the THMFP by an additional 41% and 53%, respectively, while ozonation of the raw water reduced the THMFP by 39%. The bromine incorporation factor (BIF) of all bulk-treated waters was similar, while ozonation increased the BIF of all waters slightly. This may be a consequence of transformations of the organic carbon by ozone, which rendered the resultant NOM more hydrophilic by destroying aromatic structures. Aliphatic carbon structures have been shown to be more reactive with respect to bromine (Liang and Singer, 2003). Figure 4.6 shows the speciation and formation of THMs for each water, before and after ozonation. Due to the low bromide concentration of North Bay Aqueduct water, chloroform was the dominant THM species formed.

Table 4.3: Impact of bulk treatment and ozonation on THM formation in North Bay Aqueduct water

Parameter	Type of Treatment					
	Raw	Alum	MIEX[1]	Raw+O_3	Alum+O_3	MIEX+O_3[1]
THM Formation Potential, µg/L	247	196	144	151	117	68
Bromine Incorporation Factor	0.06	0.07	0.07	0.12	0.12	0.17
Cl_2 demand, mg/L	6.0	3.6	3.5	3.5	3.1	2.8
UV254, 1/cm	0.113	0.073	0.056	0.046	0.033	0.027
SUVA, L/mg-m	3.08	2.26	2.56	1.30	1.07	1.16

[1] Reported value is an average MIEX/Cl and MIEX/HCO_3 treatments

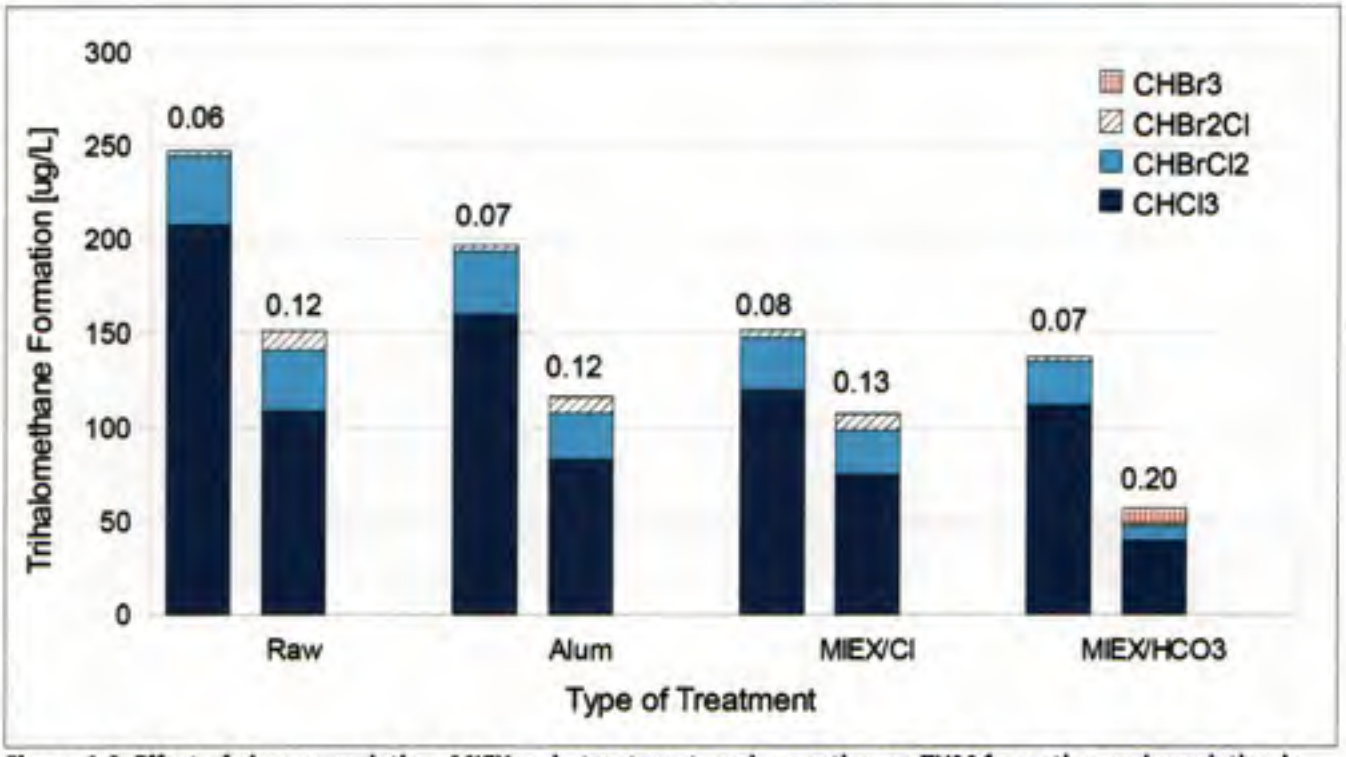

Figure 4.6: Effect of alum coagulation, MIEX resin treatment, and ozonation on THM formation and speciation in North Bay Aqueduct water. For each type of treatment, the left bar represents water before ozonation, while the right bar represents the same water after ozonation. Numbers above each bar represent the bromine incorporation factor of the total THMs.

4.3 SOUTH BAY AQUEDUCT

4.3.1 Effect of MIEX Resin and Alum

As with NBA water, removal of TOC and UV-absorbing substances during jar-testing increased with dose for both alum and MIEX resin. In jar testing, an alum dose of 25 mg/L reduced the TOC concentration by 31% and the UV absorbance by 48%. 2.0 mL/L MIEX/Cl and MIEX/HCO_3 reduced the TOC concentration by 36% and 25% and the UV absorbance by 44% and 42%, respectively. Jar-testing results for this water are shown in Appendix F.

Figure 4.7 illustrates the removal of bromide as a function of MIEX resin dose for both chloride and bicarbonate forms of the resin. Bromide removal increased with increasing MIEX dose, and no significant differences between MIEX/Cl and MIEX/HCO_3 were observed. 2.0 mL/L of MIEX/Cl and MIEX/HCO_3 reduced the bromide concentration by 29% and 33%, respectively. Alum coagulation did

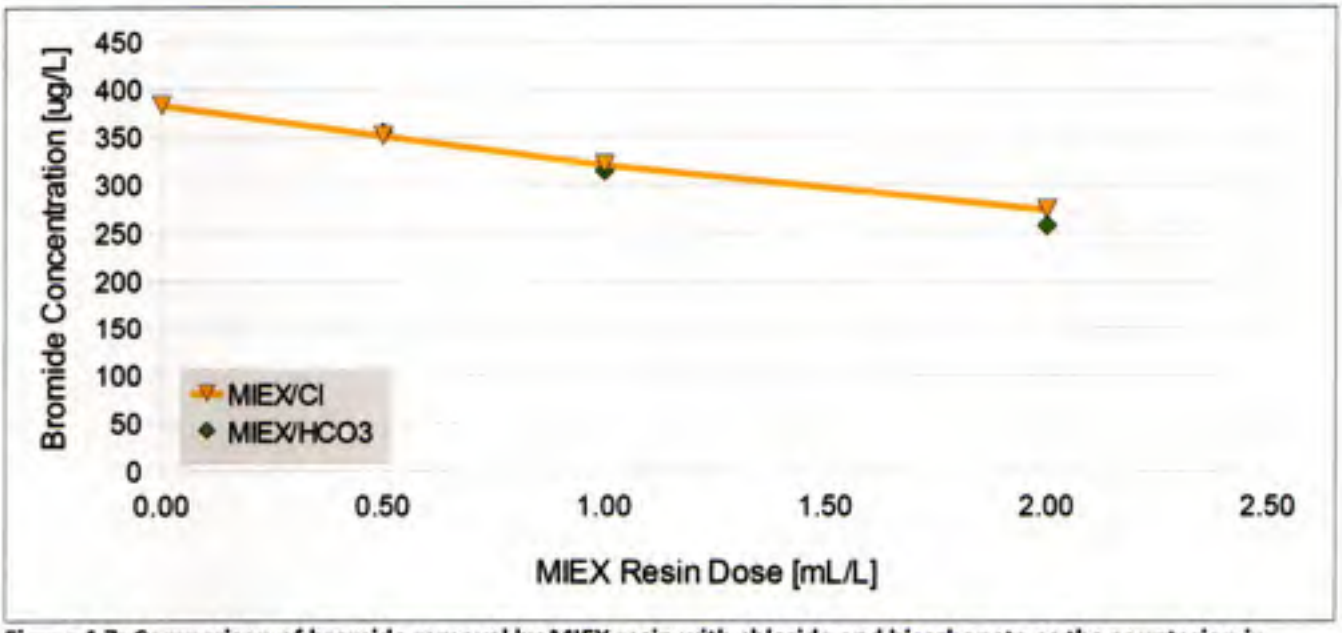

Figure 4.7: Comparison of bromide removal by MIEX resin with chloride and bicarbonate as the counterion in South Bay Aqueduct Water

not remove any bromide.

The removal of TOC, UV absorbance, and bromide as a result of bulk treatment of 16 L of raw water with alum and MIEX resin is shown is Table 4.4. Because bromide removal was of primary interest in this water, a higher MIEX dose was chosen than would have been selected on the basis of TOC removal alone. As before, the removal of TOC and UV-absorbing substances by MIEX was significantly higher after bulk treatment than in jar testing. This is attributable to the higher velocity gradient. In this water, MIEX resin reduced the SUVA of the water to a greater extent than alum, but

Table 4.4: Summary of removal by alum and MIEX resin for South Bay Aqueduct water

Parameter	Type of Treatment			
	Raw	Alum	MIEX/Cl	MIEX/HCO_3
Dose	-	25 mg/L	2.0 mL/L	2.0 mL/L
TOC, mg/L	2.3	1.7	1.1[1]	1.2
UV254, 1/cm	0.071	0.040	0.024[1]	0.021
SUVA, L/mg-m	3.03	2.3	2.08[1]	1.69
Hydrophobic Carbon	51%	54%	51%	58%
Fluorescence Index	1.43	1.56	1.61	1.64
Bromide, µg/L	360	361	289[1]	267
pH	8.2	7.6	8.1	8.2

[1] Values reported are the average of two duplicate experiments. Duplicate values for all parameters except SUVA fell within 15% of one another. SUVA values differed by 25%

the hydrophobic acid content of the waters did not change significantly after treatment. The FI increased as a result of both alum coagulation and MIEX resin treatment, indicating that both treatments preferentially removed terrestrial or humic substances.

4.3.2 Effect of Ozone

Figures 4.8 through 4.10 illustrate the results of ozonating each of the bulk-treated waters to a dose of 1 mg O_3/mg TOC. The relationship between ozone exposure (CT) and ozone transferred is depicted in Figure 4.8. As was the case with the North Bay Aqueduct water, substantially greater ozone exposure was achieved in the MIEX resin-treated waters than in the raw water. In this case, however, the MIEX resin treatment also produced a higher CT value than the alum-treated water, most likely due to the greater TOC removal. Ozone doses of 1.2-1.25 mg/L were required to achieve a CT value of 2.0 mg-min/L for the MIEX-treated waters, respectively, compared to 1.7 mg/L for alum-coagulated water and 2.2 mg/L for the raw water.

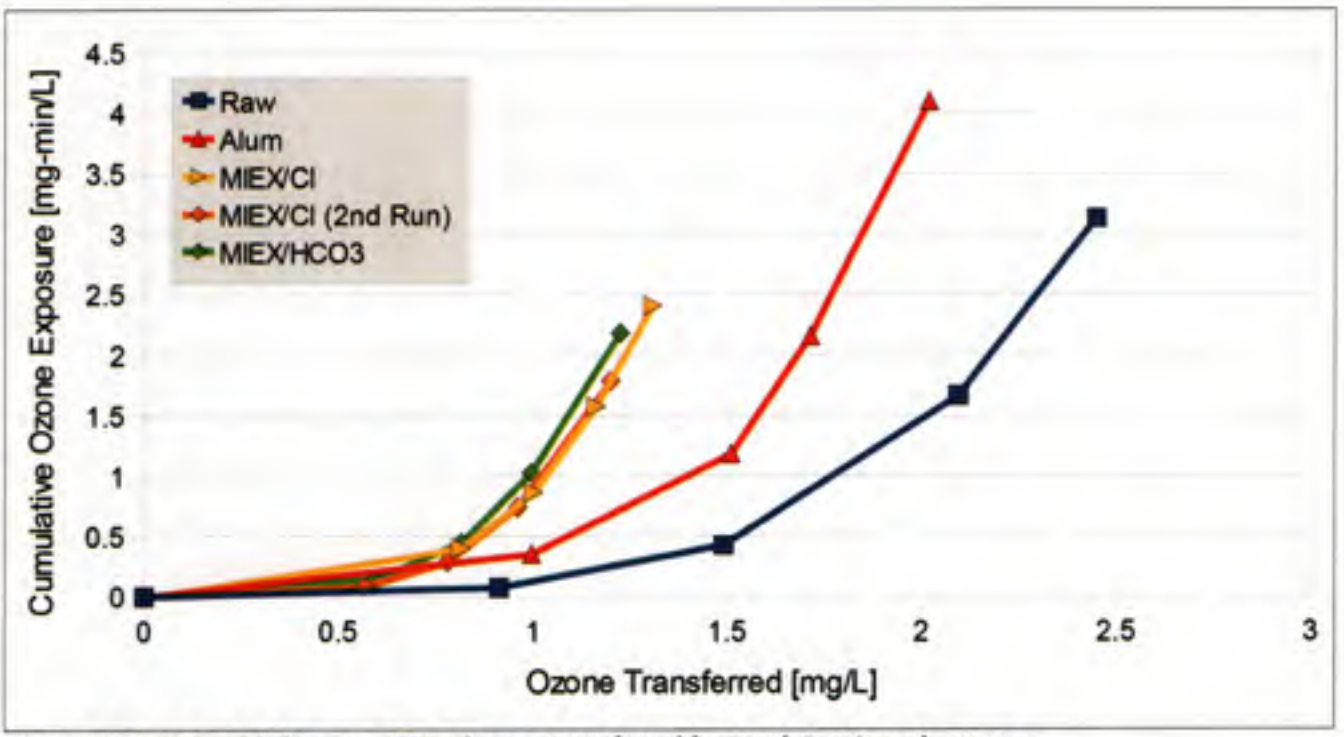

Figure 4.8: Relationship between CT and ozone transferred for South Bay Aqueduct water

The relationship between bromate formation and dissolved ozone concentration is illustrated in Figure 4.9. Error bars on this plot represent 10% of the measured bromate concentration, which reflects the observed variation in instrument response when measuring standards. It is clear that for a given dissolved ozone concentration, less bromate is produced in MIEX resin-treated waters than in either the raw or alum-coagulated waters. This result is most likely a consequence of bromide removal by the resin. Both forms of MIEX resin showed similar performance in controlling bromate, while alum coagulation increased the formation of bromate relative to the raw water to some degree. The reason for this finding is not clear, but it could be a consequence of the elevated Br:DOC ratio following alum treatment, which may make bromide relatively more accessible to oxidation by ozone.

Figure 4.10 illustrates the relationship between bromate formation and ozone exposure achieved during ozonation. Error bars on this plot represent 10% of the measured bromate concentration. There were no significant differences between the raw and MIEX/Cl-treated waters, while the MIEX/HCO_3-treated water produced slightly less bromate for a given CT, and the alum-coagulated water formed

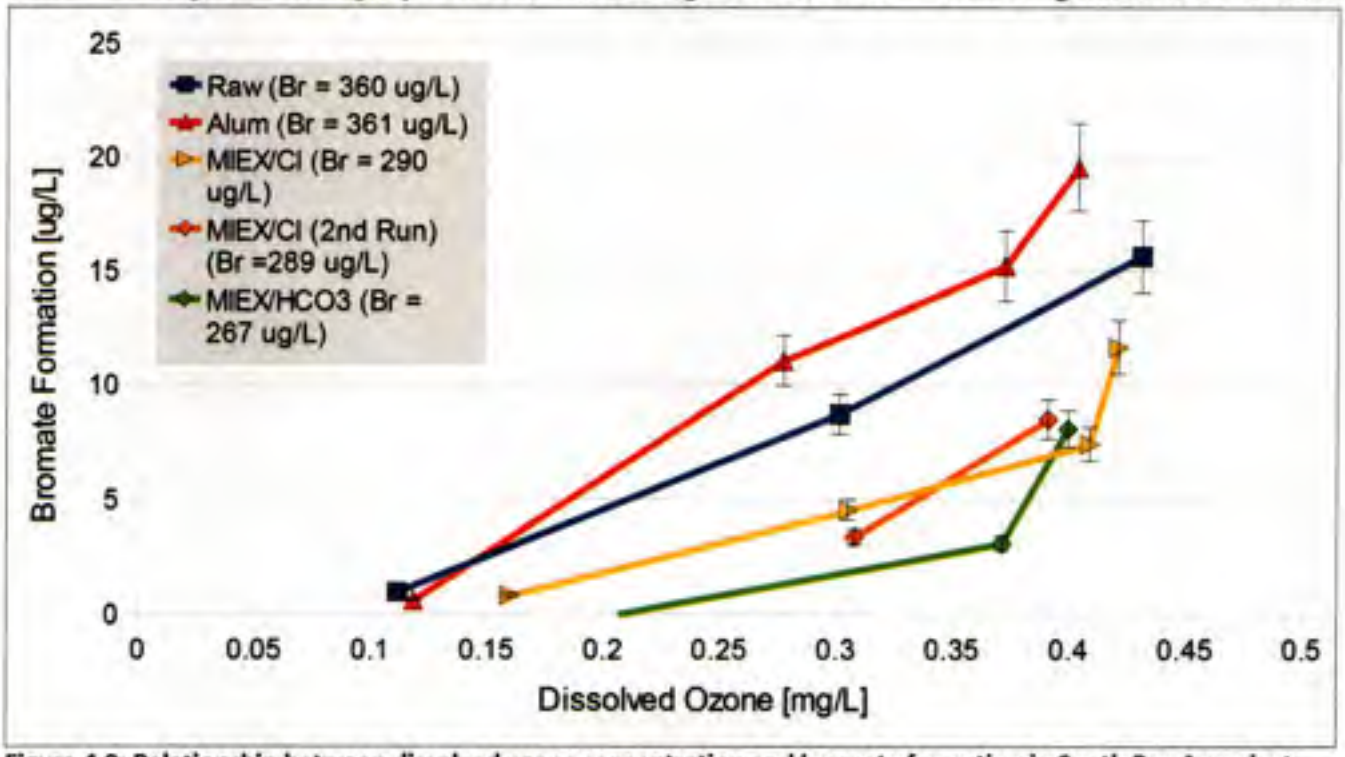

Figure 4.9: Relationship between dissolved ozone concentration and bromate formation in South Bay Aqueduct water

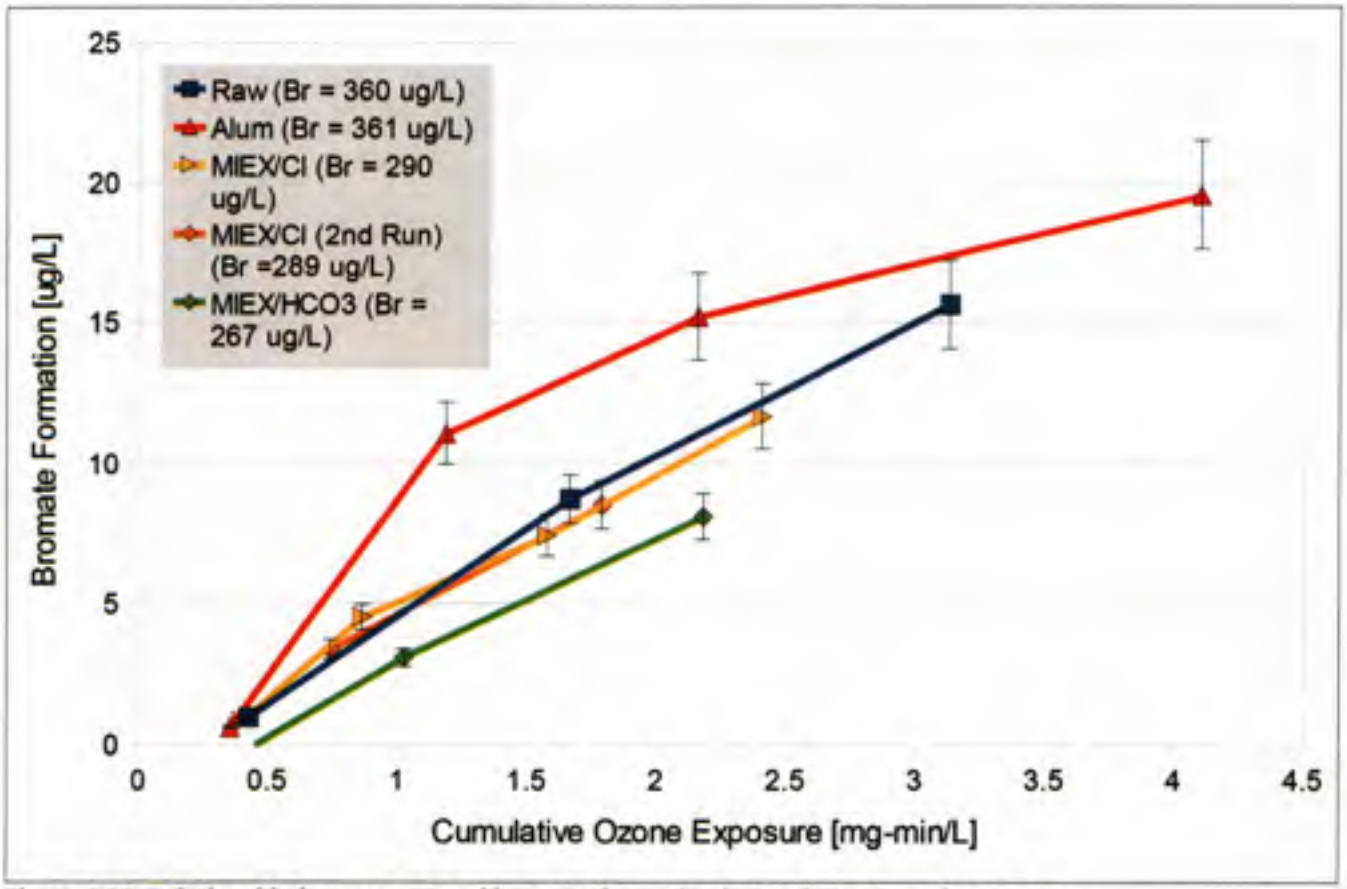

Figure 4.10: Relationship between CT and bromate formation in South Bay Aqueduct water

significantly higher levels of bromate than the other waters. At a CT value of 2.0 mg-min/L, 14.5 µg/L bromate were formed in the alum-coagulated water, compared to 10 µg/L in the raw water, 9.5 µg/L in the MIEX/Cl-treated water, and 7 µg/L in the MIEX/HCO_3-treated water. The MCL for bromate is 10 µg/L. The reasons for the similar degree of bromate formation in the raw and MIEX/Cl-treated waters are not entirely clear. As noted above, the Br:DOC ratio increases following resin treatment, but to a lesser degree than following treatment with alum. The elevated Br:DOC ratios in all the treated waters could make bromide more accessible to oxidation by ozone, despite lower overall bromide concentrations. The apparent trend in bromate formation (alum > MIEX/Cl > MIEX/HCO_3) is consistent with the trend in Br:DOC ratio.

4.3.3 THM Formation Potential

The impact of ozonation and bulk treatment with alum and MIEX resin on THM formation

potential is summarized in Table 4.5. Treatment with MIEX resin reduced the THMFP by a greater extent than treatment with alum, and ozonation reduced the THMFP further for all waters. Alum coagulation reduced the THMFP by 16%, compared to 51% for the MIEX resin. Ozonation of the alum-coagulated, and MIEX resin-treated waters reduced the THMFP by an additional 43%, and 38%, respectively, while ozonation of the raw water reduced THMFP by 31%. Once again, the reduction in THMFP by ozone reflects the large reductions in UV absorbance and SUVA which may have rendered the NOM less reactive with chlorine.

Because of the high bromide concentration in this water, the BIF is quite high. Alum and MIEX treatment both increased the BIF relative to that of the raw water. This can be explained by the elevated Br:DOC ratio that resulted from both treatments, i.e. greater removal of DOC than bromide. Finally, MIEX resin decreased the chlorine demand to a greater extent than alum.

Table 4.5: Impact of bulk treatment and ozonation on THM formation in South Bay Aqueduct water

South Bay Aqueduct	Type of Treatment					
	Raw	Alum	MIEX[1]	Raw+O_3	Alum+O_3	MIEX+O_3[1]
THM Formation Potential, µg/L	199	167	98	138	96	61
Bromine Incorporation Factor	0.56	0.66	0.74	0.71	0.75	0.75
Cl_2 demand, mg/L	3.9	3.3	2.4	3.4	2.5	2.0
UV254, 1/cm	0.071	0.040	0.023	0.028	0.021	0.010
SUVA, L/mg-m	3.03	2.30	1.95	1.19	1.07	0.75

[1] Reported value is an average of MIEX/Cl and MIEX/HCO_3 treatments

The amount and speciation of THMs produced in each of the four waters before and after ozonation is shown in Figure 4.11. As shown, the THMs are dominated by the more brominated species.

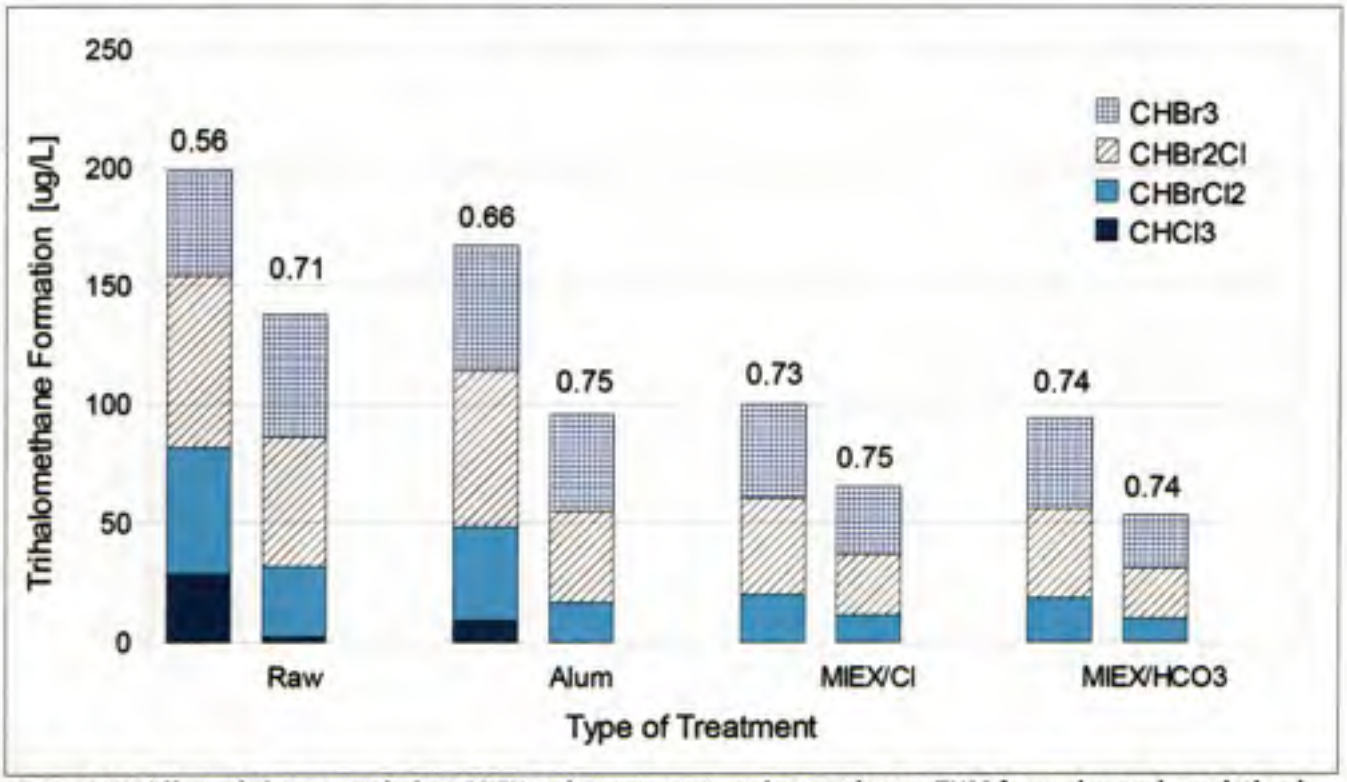

Figure 4.11: Effect of alum coagulation, MIEX resin treatment, and ozonation on THM formation and speciation in South Bay Aqueduct water. For each type of treatment, the left bar represents water before ozonation, while the right bar represents the same water after ozonation. Numbers above each bar represent the bromine incorporation factor of the total THMs.

4.4 LAKE CAMPBELL

4.4.1 Effect of MIEX Resin and Alum Treatment

During jar-testing, both alum and MIEX resin displayed increasing levels of TOC and UV absorbance removal with increasing dose. Due to the high TOC of this water sample, MIEX resin doses of up to 5 mL/L were tested. Figure 4.12 shows the removal of TOC and UV absorbance resulting from MIEX resin treatment; complete jar-testing results are shown in Appendix F. Error bars represent the difference between values in two duplicate experiments. 80 mg/L alum reduced the TOC concentration by 40% and the UV absorbance by 56% (see Appendix F), while 5.0 mL/L MIEX resin reduced TOC by 43% and UV absorbance by 80%. Because no significant differences in performance between the chloride and bicarbonate forms of the resin were observed in treating the previous waters,

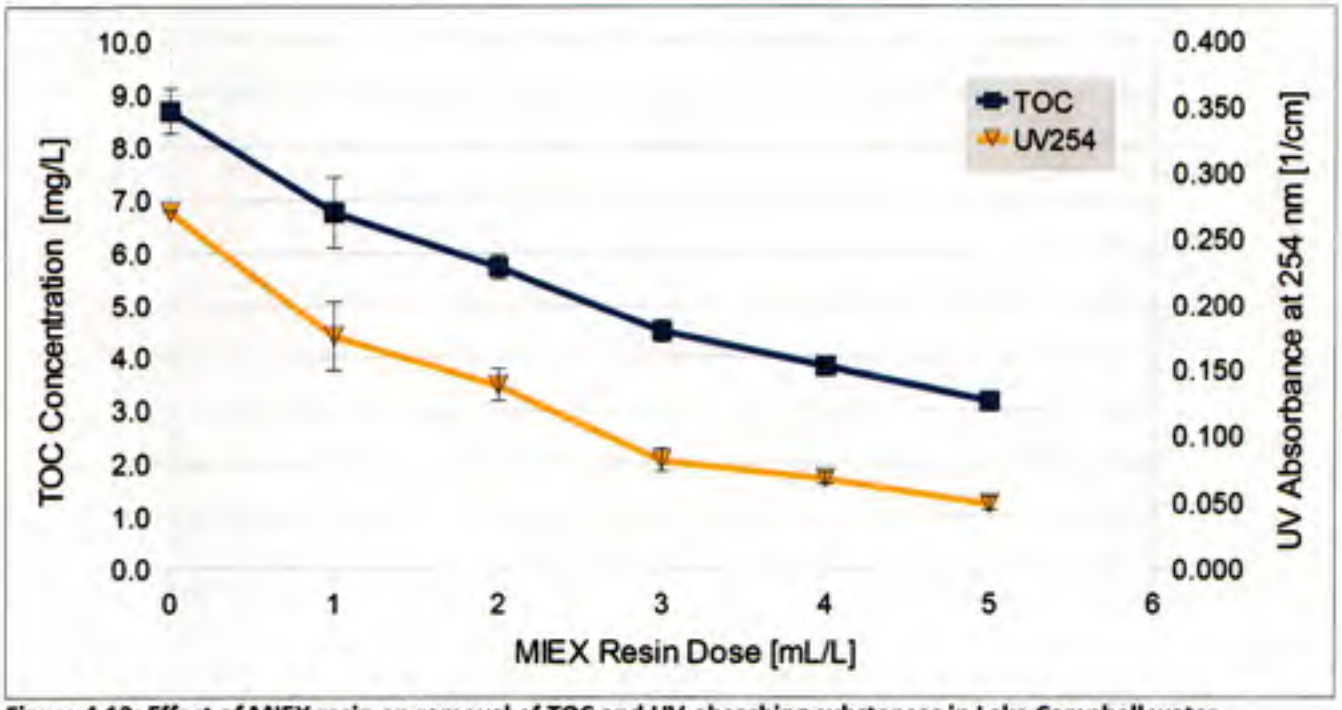

Figure 4.12: Effect of MIEX resin on removal of TOC and UV-absorbing substances in Lake Campbell water

only MIEX/HCO_3 was used for bulk treatment of this water. Table 4.6 summarizes the characteristics of the raw water and the alum-coagulated and MIEX-treated waters after bulk treatment. As with other waters, removal of TOC and UV-absorbing substances by MIEX was significantly greater following bulk treatment than in jar testing. In this case, TOC removal by alum was also greater after bulk treatment. Both results could be a consequence of the higher velocity gradient in the bulk treatment vessel. MIEX resin treatment reduced the SUVA of Lake Campbell water to a greater extent than alum

Table 4.6: Summary of removal by alum and MIEX resin for Lake Campbell water

Parameter	Type of Treatment		
	Raw	Alum	MIEX/HCO_3
Dose	-	80 mg/L	4.0 mL/L
TOC, mg/L	8.7	4.9	2.8
UV254, 1/cm	0.256	0.117	0.033
SUVA, L/mg-m	2.94	2.40	1.18
Hydrophobic Carbon	37%	-	-
Fluorescence Index	1.43	1.6	1.78
Bromide, µg/L	33	-	16
pH	8.2	7.7[1]	8.0

[1] estimated from the alum-coagulated spiked water results, discussed below

coagulation. Alum and MIEX resin both increased the FI of the water, while MIEX resin increased it to a greater degree than alum.

In order to investigate the performance of MIEX resin in a challenging water matrix containing both high TOC and high bromide concentrations, a portion of the Lake Campbell water was spiked with sodium bromide to achieve a final concentration of 380 μg/L bromide. This bromide level was chosen to correspond to the 75th percentile bromide concentration at Banks pumping station in the Delta (CALFED, 2007). Sodium chloride was also added to achieve a 126.5 mg/L chloride concentration and maintain a 333:1 mass ratio of Cl:Br, which is the ratio at which these anions occur in natural seawater (Stumm and Morgan, 1996; Magazinovic et al., 2004; Hsu and Singer, 2010).

Bromide removal by MIEX resin was of major interest for the spiked Lake Campbell water, so two additional sets of jar tests were conducted to measure the effectiveness of MIEX/Cl and MIEX/HCO_3 in removing bromide simultaneously with TOC and UV-absorbing substances. The results of these jar tests are shown in Figures 4.13 and 4.14. 4.0 mL/L of MIEX resin reduced the TOC concentration by approximately 53% and the UV absorbance by approximately 75%. While both forms of resin performed similarly with respect to UV removal, the MIEX/Cl resin removed slightly more TOC. This effect becomes more pronounced as the MIEX resin dose increases.

With respect to bromide removal, shown in Figure 4.14, the MIEX/HCO_3 resin performed slightly better than the MIEX/Cl resin, particularly at higher doses. 6.0 mL/L MIEX/HCO_3 reduced the bromide concentration by 57%, compared to 47% for MIEX/Cl. Although the affinity of MIEX for NOM is known to be greater than that for inorganic ions (Singer and Boyer, 2008; Hsu and Singer, 2010), competition by inorganic anions has been shown to decrease the degree of bromide removal (Singer and Bilyk, 2002; Johnson and Singer, 2004; Boyer and Singer, 2005). Because the naturally-occurring high chloride concentrations associated with bromide-containing waters were simulated in this spiked water, it is expected that the MIEX/HCO_3 resin would allow bromide to compete more

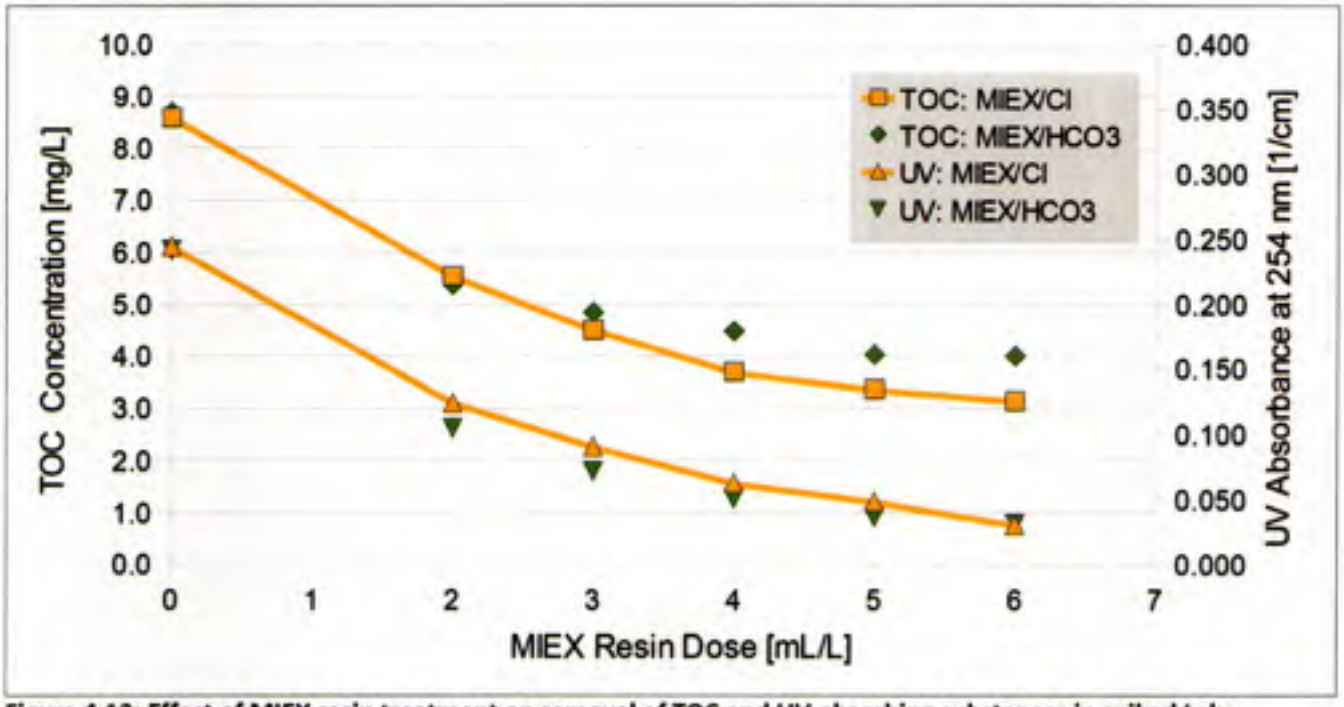

Figure 4.13: Effect of MIEX resin treatment on removal of TOC and UV-absorbing substances in spiked Lake Campbell water (380 µg/L bromide and 126.5 mg/L chloride).

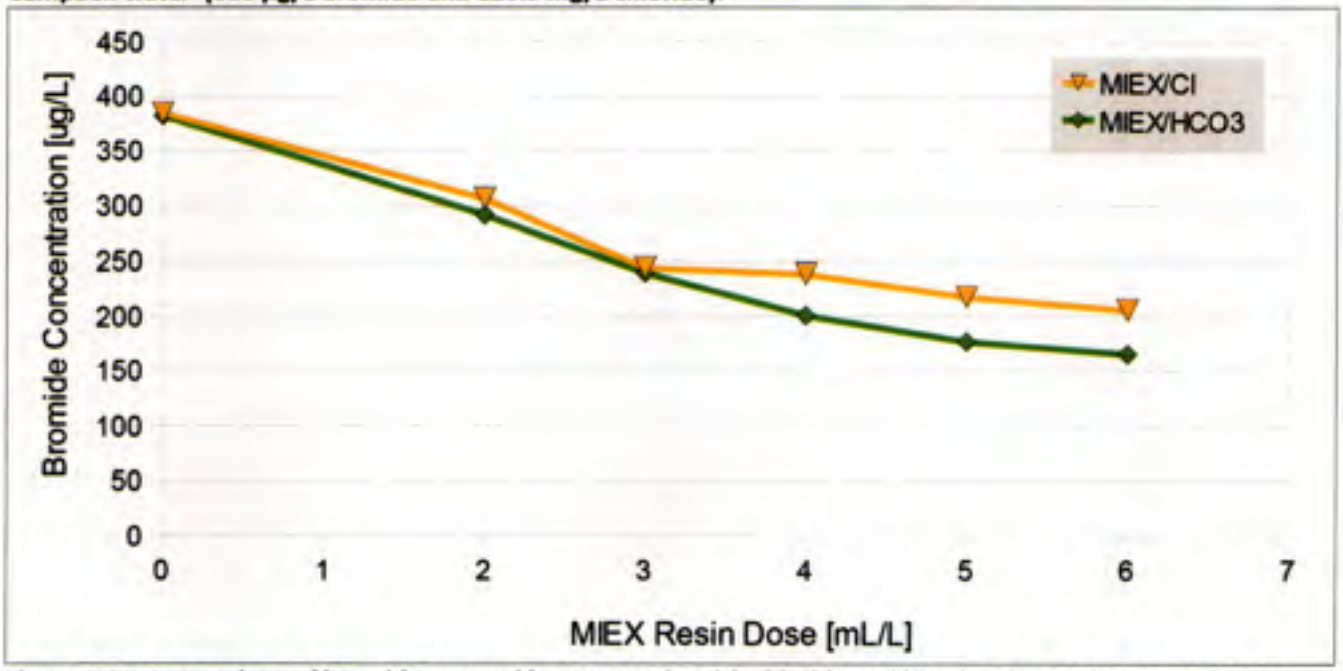

Figure 4.14: Comparison of bromide removal by MIEX resin with chloride and bicarbonate as the counterion in spiked Lake Campbell water (380 µg/L bromide and 126.5 mg/L chloride).

effectively for exchange sites because the resin has a lower selectivity for bicarbonate than chloride.

To achieve a high degree of bromide removal, spiked Lake Campbell water was bulk-treated using only the MIEX/HCO_3 resin at a dose of 4.0 mL/L, and alum. Table 4.7 summarizes the water quality

characteristics of the bulk-treated batches of spiked Lake Campbell water used for subsequent ozonation and chlorination experiments. As expected, alum coagulation did not remove any bromide. MIEX resin achieved approximately 50% bromide removal.

Table 4.7: Summary of organic carbon and bromide removal by alum and MIEX resin for spiked Lake Campbell water

Parameter	Type of Treatment		
	Raw	Alum	MIEX/HCO_3
Dose	-	80 mg/L	4.0 mL/L
TOC, mg/L	8.7	5.7	3.0
UV254, 1/cm	0.256	0.126	0.034
SUVA, L/mg-m	2.94	2.23	1.15
Hydrophobic Carbon	37%	22%	6%
Fluorescence Index	-	1.58	1.74
Bromide, µg/L	380	374	195
pH	8.2	7.7	8.3

4.4.2 Effect of Ozone

Figures 4.15 and 4.16 summarize the ozonation experiments conducted on Lake Campbell waters. Due to the high TOC concentration, raw water was not ozonated at the 1:1 O_3:DOC ratio, as this was deemed unrealistic in practice. As shown in Figure 4.15, both MIEX resin-treated waters (with and without added bromide) achieved significantly greater degrees of ozone exposure for a given amount of ozone transferred than the alum-coagulated water. Again, this is attributable to the greater TOC removal achieved by MIEX compared to that by alum. In addition, the unspiked MIEX resin-treated water achieved greater CT values than the spiked water. In the unspiked resin-treated water, 1.9 mg/L ozone was required to achieve a CT of 1.0 mg-min/L, compared to 2.2 mg/L for the spiked resin-treated water and 5.3 mg/L for the alum-coagulated water. The difference in performance between the spiked and unspiked MIEX-treated waters might be attributed to consumption of ozone by the bromide present in the spiked water.

The formation of bromate as it relates to ozone exposure (CT) is shown in Figure 4.16. Overall, bromate formation in the bromide-spiked Lake Campbell water was very low (<5 µg/L) compared to

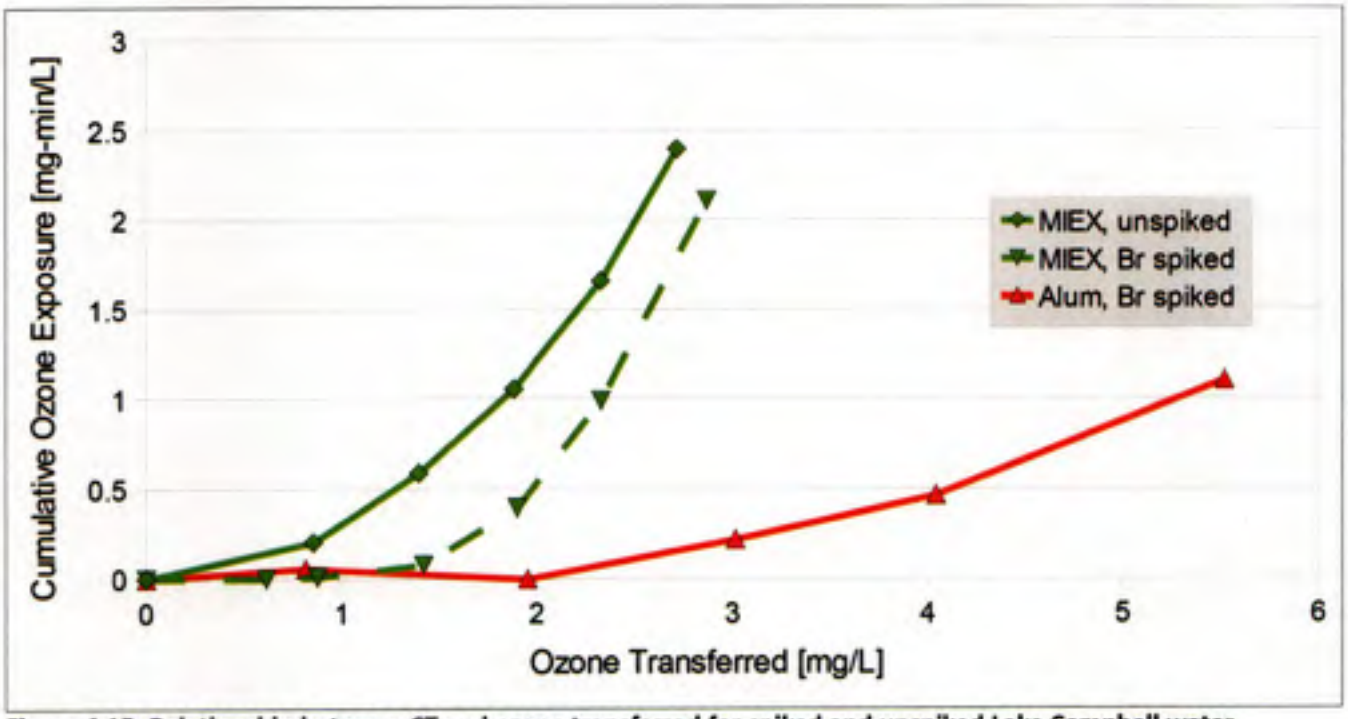

Figure 4.15: Relationship between CT and ozone transferred for spiked and unspiked Lake Campbell water.

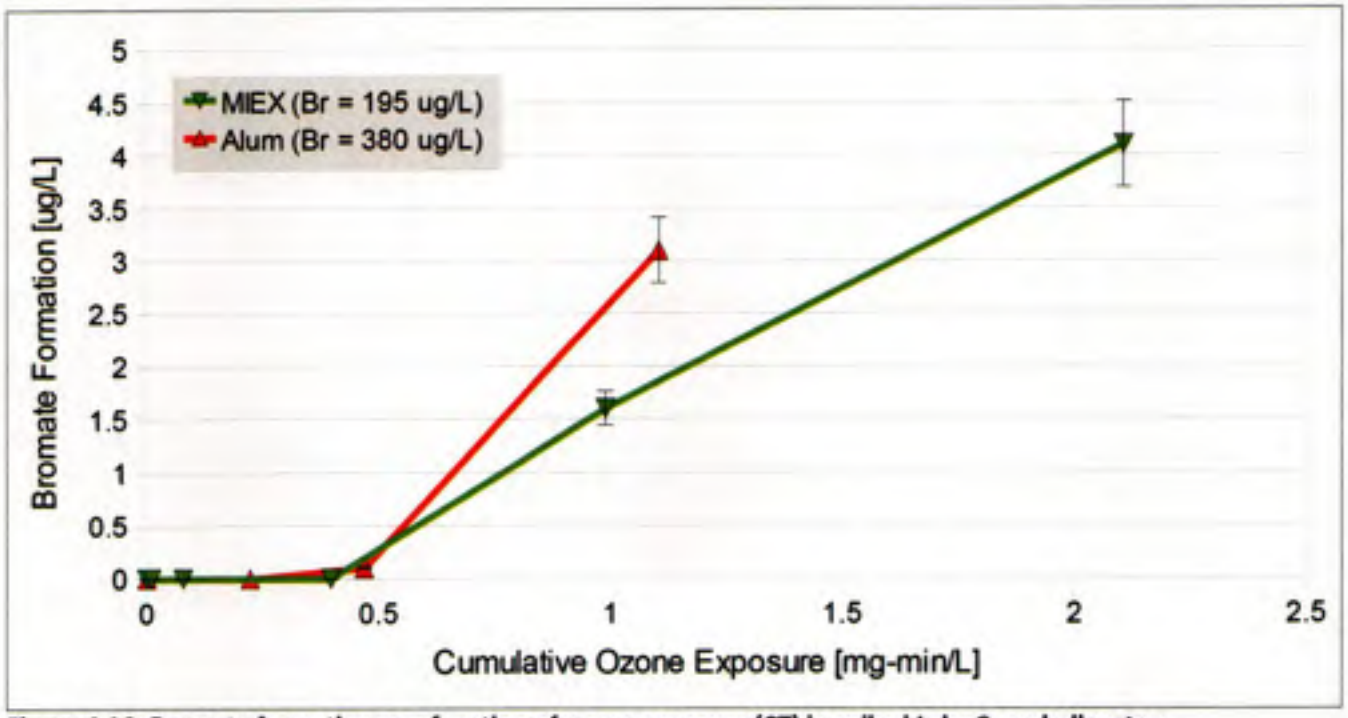

Figure 4.16: Bromate formation as a function of ozone exposure (CT) in spiked Lake Campbell water.

SBA water. This fact is most likely a consequence of the high TOC (and correspondingly high ozone demand) in this water. At these low concentrations, it is difficult to draw meaningful conclusions about

the relative rates of bromate formation in the two waters, but it does appear that less bromate was formed in the MIEX/HCO_3-treated water than in the alum-coagulated water. No significant bromate production took place in the unspiked MIEXresin-treated water because of the low bromide concentration (33 µg/L). At a CT value of 1.0 mg-min/L, 1.5 µg/L bromate was measured in the MIEX resin-treated water, compared to 2.5 µg/L in the alum-coagulated water. Both concentrations are well below the MCL of 10 µg/L.

4.4.3 THM Formation Potential

The impact of bulk alum and MIEX resin treatment before and after ozonation on the THM formation potential of unspiked and spiked Lake Campbell waters is summarized in Tables 4.8 and 4.9, respectively. A small aliquot of unspiked water was treated with 80 mg/L alum so that the THMFP of alum-coagulated water without elevated bromide could be measured for purposes of comparison. This aliquot was not ozonated.

In the unspiked water, alum coagulation reduced the THMFP by 56%, while MIEX resin treatment reduced THMFP by 85%. Ozonation of the MIEX resin-treated water reduced THMFP by an additional 47%. Due to the low bromide concentration, the bromine incorporation factor of all waters

Table 4.8: Impact of bulk treatment and ozonation on THM formation in Lake Campbell water

Lake Campbell	Type of Treatment					
	Raw	Alum	MIEX	Raw+O3	Alum+O3	MIEX+O3
THM Formation Potential, µg/L	520	227	76	-	-	40
Bromine Incorporation Factor	0.02	0.03	0.04	-	-	0.04
Cl_2 demand, mg/L	11.0	5.6	2.9	-	-	2.5
UV254, 1/cm	0.256	0.117	0.033	-	-	0.016
SUVA, L/mg-m	2.94	2.40	1.18	-	-	0.67

Table 4.9: Impact of bulk treatment and ozonation on THM formation in spiked Lake Campbell water

Lake Campbell (Spiked)	Type of Treatment					
	Raw	Alum	MIEX	Raw+O3	Alum+O3	MIEX+O3
THM Formation Potential, µg/L	-	375	156	-	239	83
Bromine Incorporation Factor	-	0.37	0.45	-	0.66	0.58
Cl_2 demand, mg/L	-	6.4	3.3	-	4.5	2.8
UV254, 1/cm	-	0.126	0.034	-	0.043	0.017
SUVA, L/mg-m	-	2.23	1.15	-	1.80	0.70

was very low (<0.06). THMFP results for the unspiked MIEX-treated water are somewhat questionable, as one set of duplicate pre- and post-ozone samples may have been reversed during analysis. The data presented here assume that was the case and are corrected accordingly.

Similar results were observed in the spiked water, except that the bromine incorporation factor was considerably higher due to the elevated bromide levels. The THMFP of spiked raw water was not measured, but it is clear that bromide played a major role as a THM precursor in this water. Alum coagulation (80 mg/L) reduced THMFP to 375 µg/L, compared to 227 µg/L in the unspiked water for the same alum dose. Similarly, MIEX resin (4.0 mL/L) reduced THMFP to 156 µg/L, compared to 62 µg/L in the unspiked water for the same resin dose. In both cases, the higher THMFP in the spiked water is a result of the formation of more brominated species, which have higher molecular weights than their chlorinated analogs. The BIF of the spiked alum- and resin-treated waters was 0.37 and 0.45, respectively, compared to 0.03 for the unspiked alum- and resin-treated waters. Ozonation of the alum-coagulated water reduced its THMFP by an additional 36%, while ozone reduced the THMFP of the MIEX resin-treated water by an additional 47%.

Figure 4.17 illustrates the removal of THMFP by bulk treatment with and without ozone, as well as the speciation of THMs before and after treatment. The large fraction of brominated THM species is notable in all bromide-spiked water samples. THMFPs for all treatments are higher in the spiked waters due to the higher molecular weight of the brominated THMs.

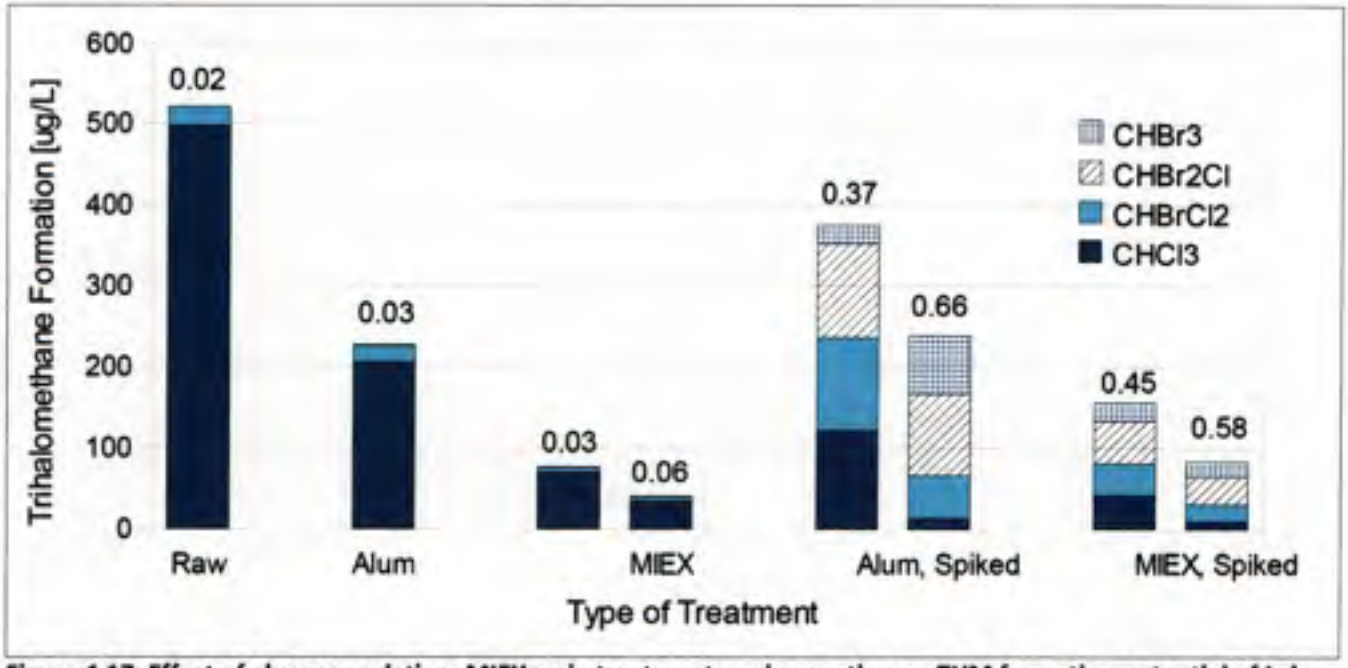

Figure 4.17: Effect of alum coagulation, MIEX resin treatment, and ozonation on THM formation potential of Lake Campbell water, showing speciation. For each type of treatment, the left bar represents water before ozonation, while the right bar (where shown) represents the same water after ozonation. Numbers above each bar indicate the bromine incorporation factor of the total THMs.

4.5 INTEGRATION AND DISCUSSION OF RESULTS

4.5.1 Organic Carbon and Bromide Removal

In all cases, MIEX resin applied at reasonable doses reflective of those used in practice achieved significantly greater removal of TOC and UV-absorbing substances than alum. This is consistent with previous research (Singer and Bilyk, 2002; Boyer and Singer, 2005; Humbert et al., 2005; Boyer and Singer, 2006). Water quality characteristics of all raw and bulk-treated waters are summarized in Table 4.10. Figure 4.18 displays a summary of the TOC removal achieved through alum coagulation and MIEX resin treatment for the waters studied.

In two of the three water examined, MIEX resin reduced SUVA to a greater extent than alum, indicating that MIEX preferentially removed UV-absorbing substances to a greater degree than alum. This finding is in conflict with Johnson and Singer (2004), who found that the SUVA remained

Table 4.10: Removal of DBP Precursors by alum and MIEX resin treatment

North Bay Aqueduct	Type of Treatment			
	Raw	Alum	MIEX/Cl	MIEX/HCO_3
Dose	-	35 mg/L	1.0 mL/L	1.0 mL/L
TOC, mg/L	3.7	3.2	2.2	2.2
UV254, 1/cm	0.113	0.073	0.058	0.053
SUVA, L/mg-m	3.08	2.26	2.69	2.43
Hydrophobic Carbon	58%	58%	55%	-
Fluorescence Index	1.39	1.47	1.47	1.46
Bromide, µg/L	40	44	45	37
pH	7.9	7.7	8.2	8.2
South Bay Aqueduct	**Type of Treatment**			
	Raw	Alum	MIEX/Cl	MIEX/HCO_3
Dose	-	25 mg/L	2.0 mL/L	2.0 mL/L
TOC, mg/L	2.3	1.7	1.1	1.2
UV254, 1/cm	0.071	0.040	0.024	0.021
SUVA, L/mg-m	3.03	2.3	2.08	1.69
Hydrophobic Carbon	51%	54%	51%	58%
Fluorescence Index	1.43	1.56	1.61	1.64
Bromide, µg/L	360	361	289	267
pH	8.2	7.6	8.1	8.2
Lake Campbell	**Type of Treatment**			
	Raw	Alum	MIEX/Cl	MIEX/HCO_3
Dose	-	80 mg/L	-	4.0 mL/L
TOC, mg/L	8.7	4.9	-	2.8
UV254, 1/cm	0.256	0.117	-	0.033
SUVA, L/mg-m	2.94	2.40	-	1.18
Hydrophobic Carbon	37%	-	-	-
Fluorescence Index	1.43	1.6	-	1.78
Bromide, µg/L	33	-	-	16
pH	8.2	7.7	-	8.0
Lake Campbell (Spiked)	**Type of Treatment**			
	Raw	Alum	MIEX/Cl	MIEX/HCO_3
Dose	-	80 mg/L	-	4.0 mL/L
TOC, mg/L	8.7	5.7	-	3.0
UV254, 1/cm	0.256	0.126	-	0.034
SUVA, L/mg-m	2.94	2.23	-	1.15
Hydrophobic Carbon	37%	22%	-	6%
Fluorescence Index	-	1.58	-	1.74
Bromide, µg/L	380	374	-	195
pH	8.2	7.7	-	8.3

relatively constant before and after MIEX resin treatment. This discrepancy could be related to the differences in characteristics of the waters in the two studies. Despite the decreases in SUVA, the hydrophobic acid fraction of the organic carbon did not change significantly as a result of treatment. Finally, both alum coagulation and MIEX resin treatment reduced the FI in all waters studied.

The relationship between FI and SUVA before and after ozonation is shown in Figure 4.19. There

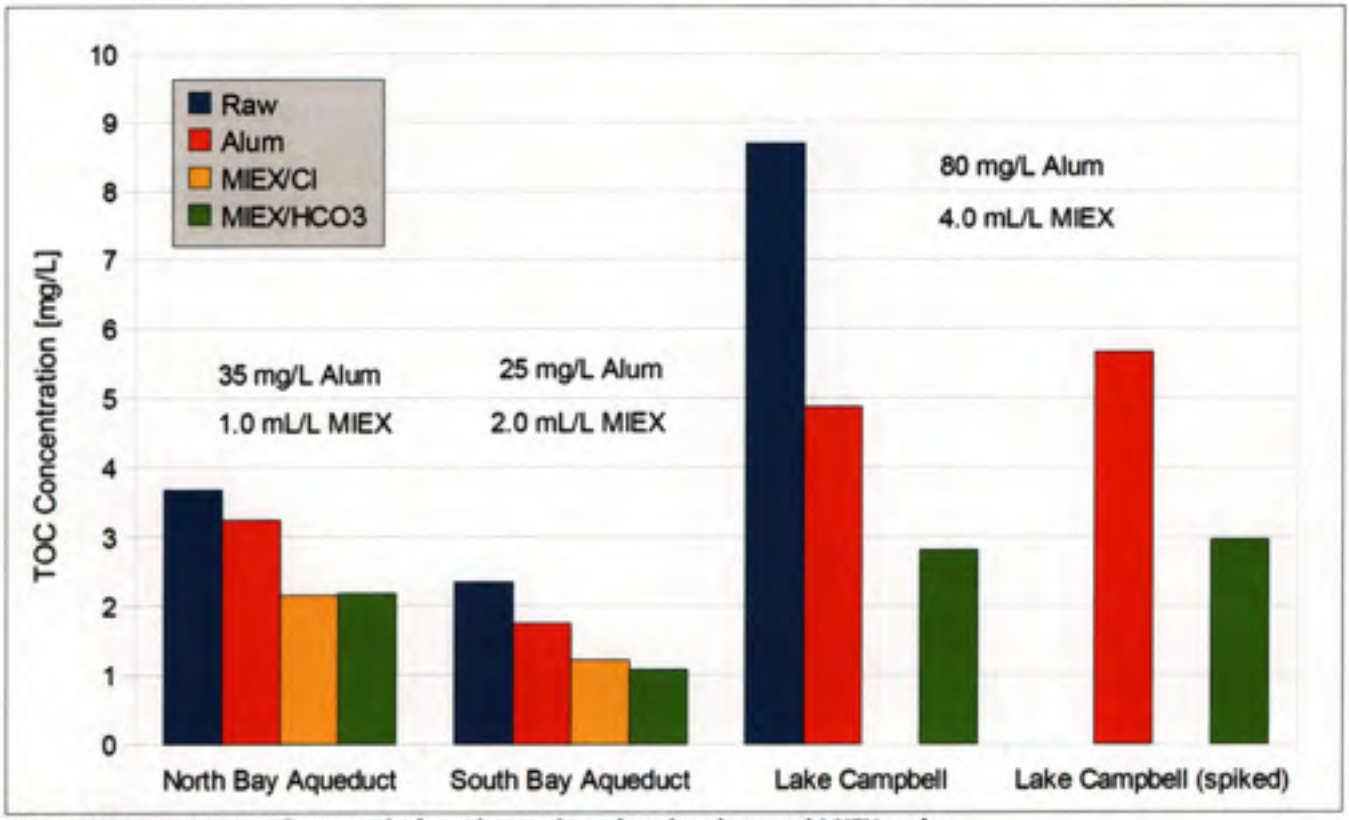

Figure 4.18: Summary of removal of total organic carbon by alum and MIEX resin

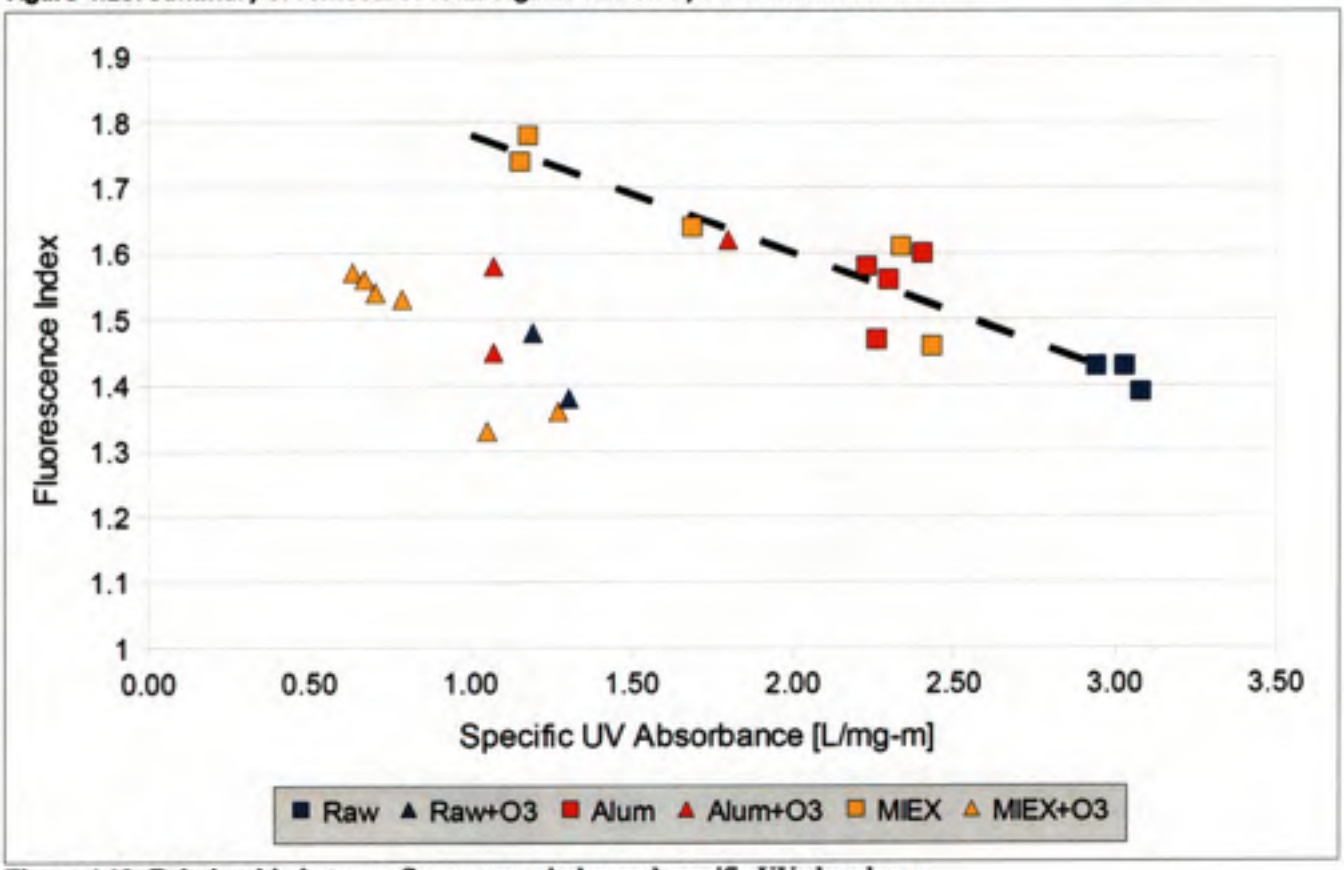

Figure 4.19: Relationship between fluorescence index and specific UV absorbance

is a clear correlation between lower SUVA values and a higher FI, indicating that the more hydrophilic components of DOC are microbially-derived. Moreover, the figure shows that water after MIEX resin treatment generally has a higher FI and lower SUVA than alum-coagulated or raw water. Ozone reduced the SUVA of all waters, indicating that it preferentially destroyed the UV-absorbing aromatic structures of the organic carbon. It is noteworthy that the reduction in SUVA by ozonation was proportionally larger than the reductions in FI. This indicates that ozone does not preferentially destroy microbially- or terrestrially-derived aromatic carbon. Raw EEMs data are available in Appendix G.

With respect to bromide, MIEX resin removed 20 - 50% of the bromide in the two high bromide waters studied. This is shown in Figure 4.20. Bromide removal was primarily dependent on the MIEX dose and the initial bromide concentration. Previous studies (Johnson and Singer, 2004; Hsu and Singer, 2010) have shown similar results. MIEX/HCO_3 showed slightly better bromide removal than MIEX/Cl in jar testing and bulk treatment, which can be explained by the lower selectivity of the resin

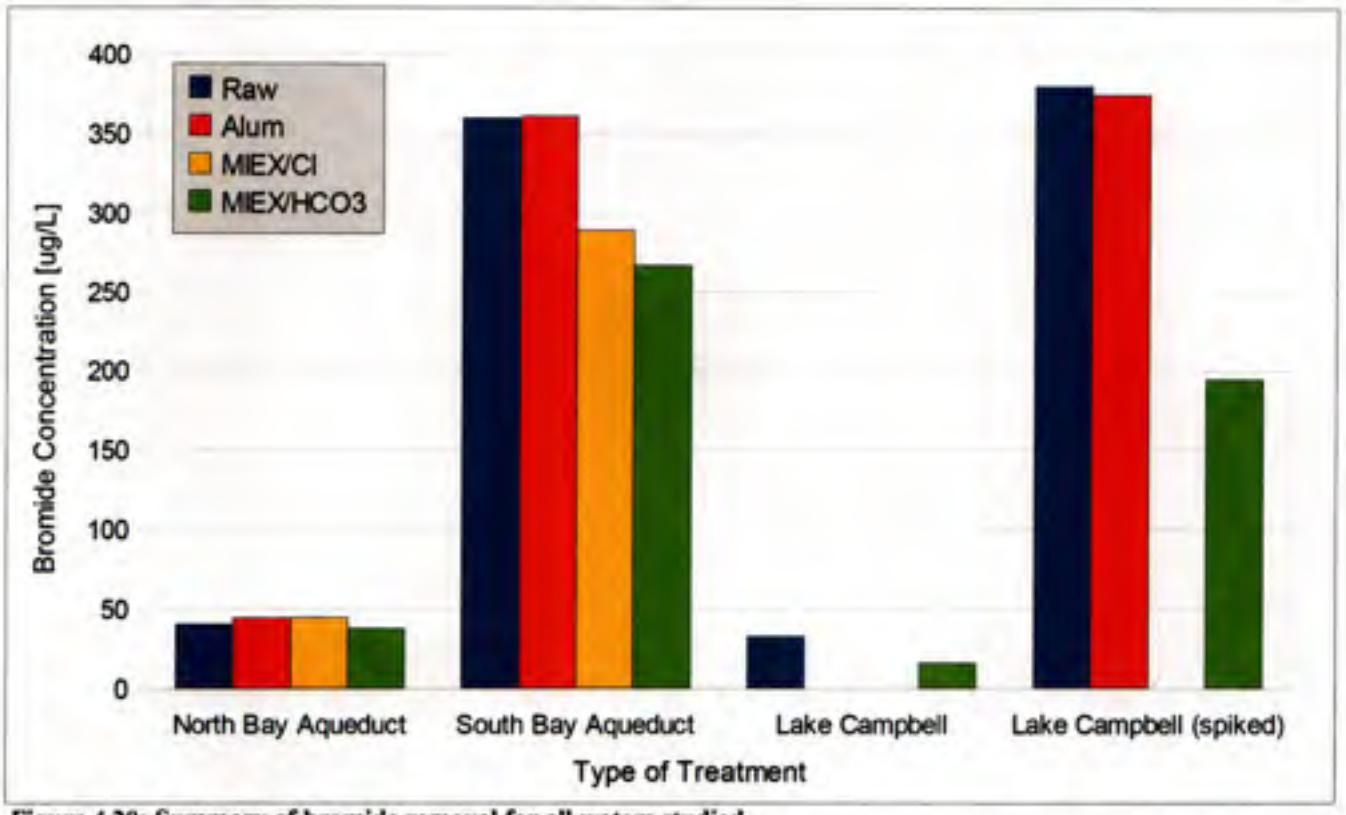

Figure 4.20: Summary of bromide removal for all waters studied

for bicarbonate compared to chloride.

4.5.2 THM Formation Potential

The reduction in THM formation potential and removal of DBP precursors by alum and MIEX resin treatment before and after ozonation for all waters studied is summarized in Table 4.11. Figure 4.21 shows that MIEX resin lowered the THM formation potential of all waters by a greater amount than treatment with alum. This result is in agreement with the organic carbon removal noted above (see Figure 4.18). The difference in performance between MIEX resin charged with chloride or with bicarbonate as the counterion was minimal with respect to THM formation. The figure also illustrates

Table 4.11: Impact of bulk treatment and ozone on THM formation potential

North Bay Aqueduct	Type of Treatment					
	Raw	Alum	MIEX	Raw+O_3	Alum+O_3	MIEX+O_3
THM Formation Potential, µg/L	247	196	144	151	117	68
Bromine Incorporation Factor	0.06	0.07	0.07	0.12	0.12	0.17
Cl_2 demand, mg/L	6.0	3.6	3.5	3.5	3.1	2.8
UV254, 1/cm	0.113	0.073	0.056	0.046	0.033	0.027
SUVA, L/mg-m	3.08	2.26	2.56	1.30	1.07	1.16
South Bay Aqueduct	**Type of Treatment**					
	Raw	Alum	MIEX	Raw+O_3	Alum+O_3	MIEX+O_3
THM Formation Potential, µg/L	199	167	98	138	96	61
Bromine Incorporation Factor	0.56	0.66	0.74	0.71	0.75	0.75
Cl_2 demand, mg/L	3.9	3.3	2.4	3.4	2.5	2.0
UV254, 1/cm	0.071	0.040	0.023	0.028	0.021	0.010
SUVA, L/mg-m	3.03	2.30	1.95	1.19	1.07	0.75
Lake Campbell	**Type of Treatment**					
	Raw	Alum	MIEX	Raw+O_3	Alum+O_3	MIEX+O_3
THM Formation Potential, µg/L	520	227	76	-	-	40
Bromine Incorporation Factor	0.02	0.03	0.04	-	-	0.04
Cl_2 demand, mg/L	11.0	5.6	2.9	-	-	2.5
UV254, 1/cm	0.256	0.117	0.033	-	-	0.016
SUVA, L/mg-m	2.94	2.40	1.18	-	-	0.67
Lake Campbell (Spiked)	**Type of Treatment**					
	Raw	Alum	MIEX	Raw+O_3	Alum+O_3	MIEX+O_3
THM Formation Potential, µg/L	-	375	156	-	239	83
Bromine Incorporation Factor	-	0.37	0.45	-	0.66	0.58
Cl_2 demand, mg/L	-	6.4	3.3	-	4.5	2.8
UV254, 1/cm	-	0.126	0.034	-	0.043	0.017
SUVA, L/mg-m	-	2.23	1.15	-	1.80	0.70

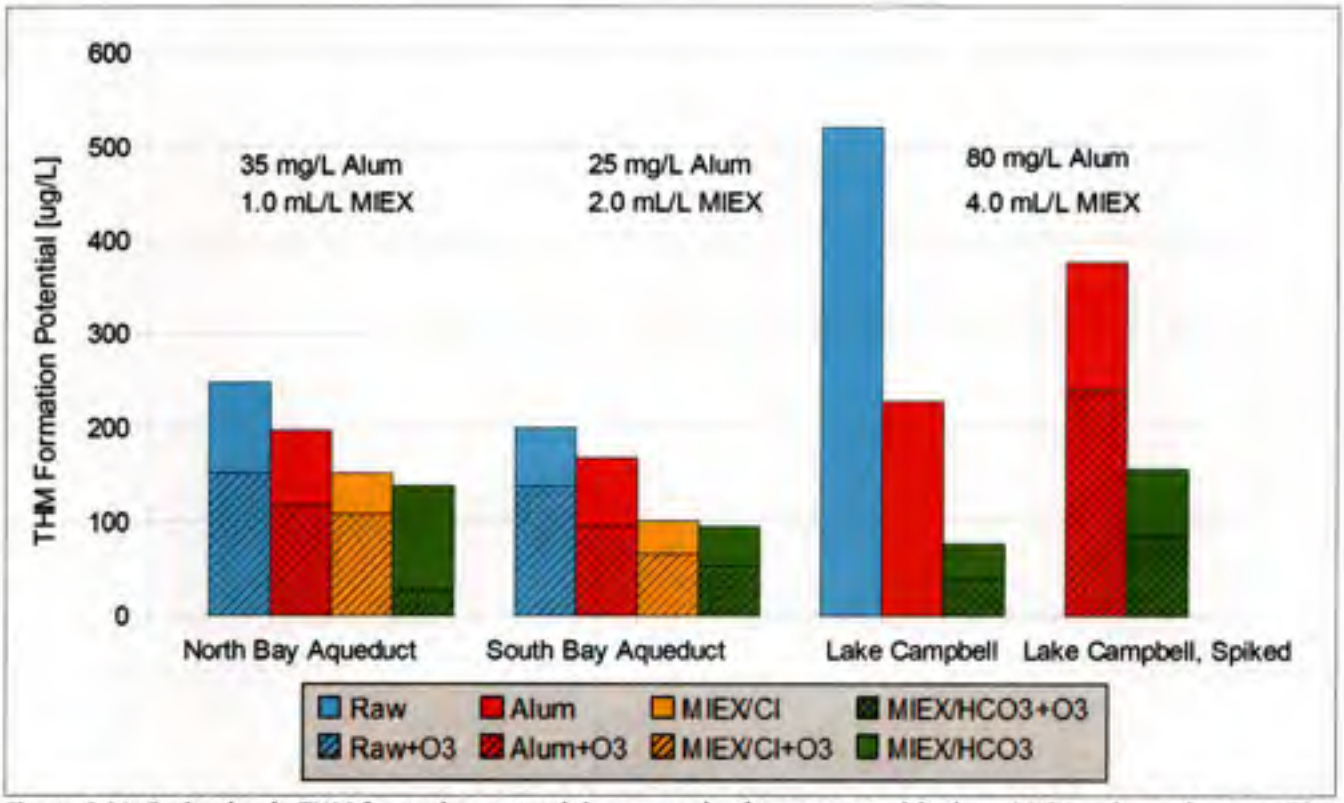

Figure 4.21: Reduction in THM formation potential as a result of treatment with alum, MIEX resin, and ozone. The shaded portion of each bar represents the THM formation potential after ozonation, while the total height of the bar represents THM formation potential before ozonation.

that ozone treatment generally reduced the THMFP by 35-45%, which comports with the observed decreases in UV absorbance after ozonation, shown in Table 4.11. By attacking aromatic structures, ozone rendered the organic carbon less reactive with chlorine and reduced the UV absorbance. This fact is illustrated explicitly in Figure 4.22, which shows the relationship between UV absorbance and THM formation potential (on a molar basis) for the high-bromide (SBA and spiked LC) and low-bromide (NBA and LC) waters studied. It can be seen that decreases in the UV absorbance are directly correlated with decreases in the THMFP for both the high- and low-bromide waters, regardless of the treatment used. This result is similar to findings by Archer and Singer (2006). The degree of bromine incorporation in the THMs, indicated by the BIF, increased as a result of treatment with alum, and increased to a greater degree as a result of treatment with MIEX resin. This can be attributed to the increased Br:DOC ratio following these treatments. Alum removes DOC but not bromide, and while

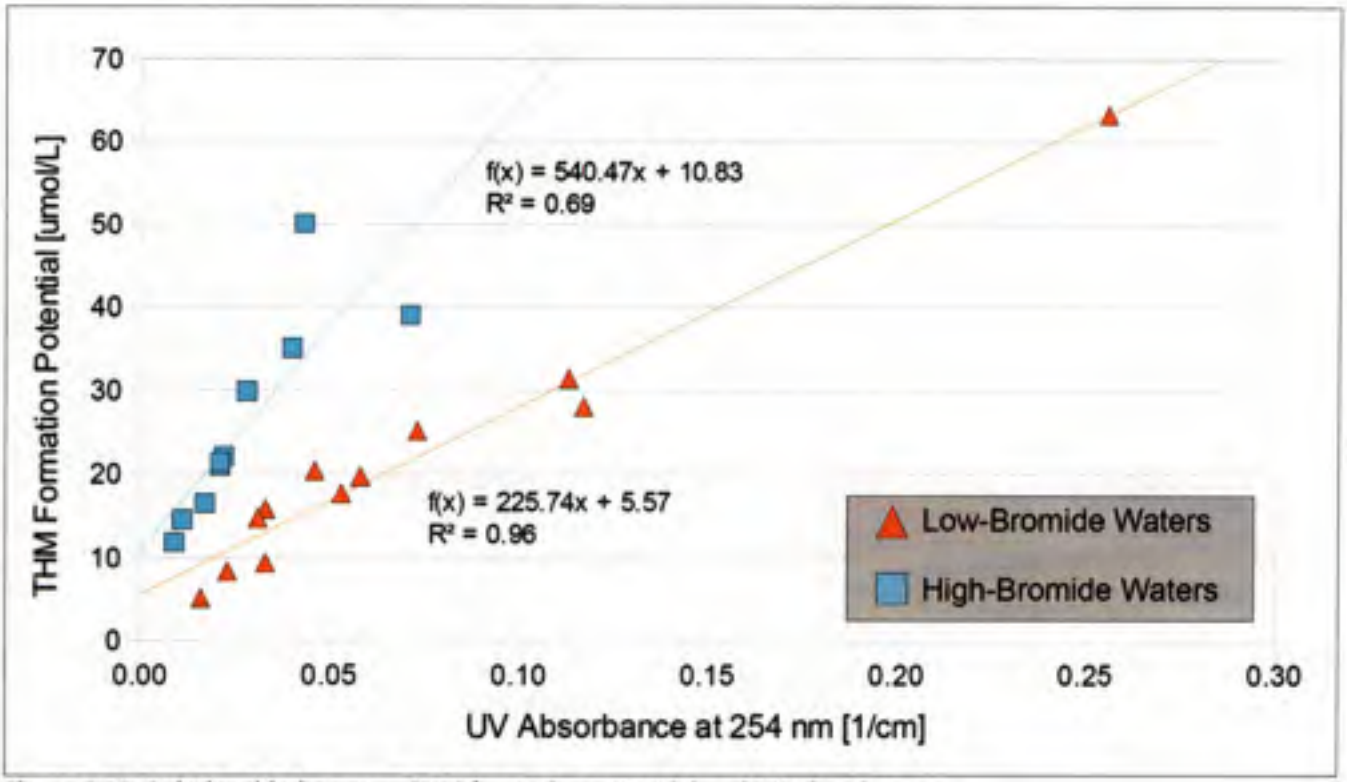

Figure 4.22: Relationship between THM formation potential and UV absorbance

MIEX does remove bromide, bromide removal is less than DOC removal, so the Br:DOC ratio is still increased as a consequence of treatment. The BIF increased further after ozonation. This fact is most likely a consequence of the transformation of the organic carbon brought about by ozone, which rendered the NOM more hydrophilic, and therefore more reactive with bromine (see Liang and Singer, 2003).

4.5.3 Ozone Demand and Bromate Formation

A summary of the effect of TOC removal on ozone demand for all waters studied is shown in Figure 4.23. For all alum-treated waters, higher ozone exposure is achieved at lower ozone doses as the TOC concentration in the water is decreased. The same trend is observed over the set of MIEX resin-treated waters. It is evident that for each source water, MIEX resin treatment removed TOC and reduced the ozone demand to a greater extent than alum coagulation, enabling higher levels of ozone exposure to be achieved at lower ozone doses. The ozone exposure (CT) achieved at various

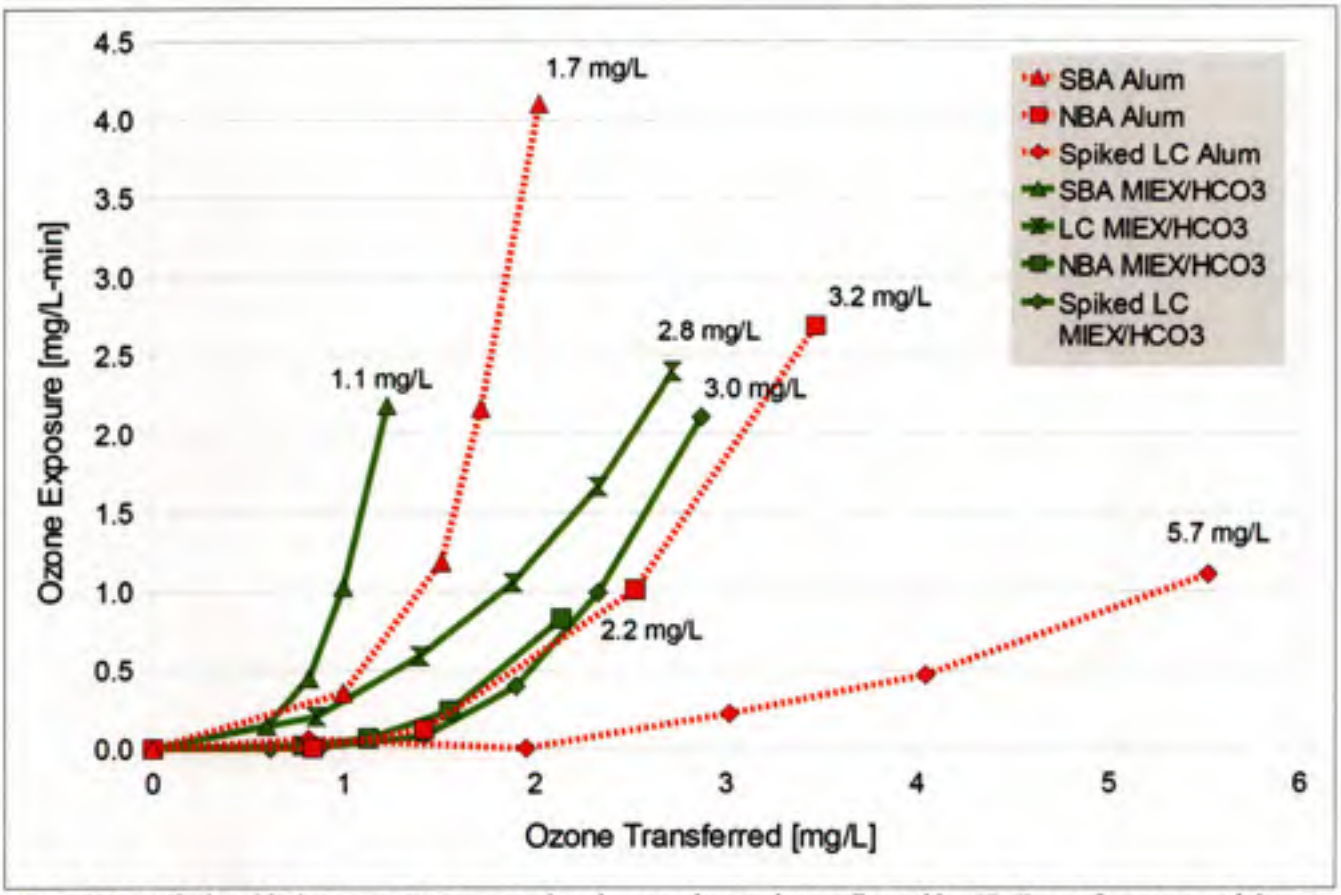

Figure 4.23: Relationship between TOC removal and ozone demand, as reflected by CT. Type of treatment (alum or MIEX resin) is indicated by color; source water is indicated by the shape of the marker. Numbers at the end of each curve represent the TOC concentration of the water.

transferred ozone doses is summarized in Table 4.12.

Table 4.12: Ozone exposure (CT, mg-min/L) achieved at various transferred ozone doses

Treatment	Source Water	TOC mg/L	CT at Transferred Ozone Dose: 1 mg/L O_3	2 mg/L O_3
Alum	NBA	3.2	0	0.5
	SBA	1.7	0.4	4
	Spiked LC	5.7	0	0
MIEX/HCO_3	NBA	2.2	0	0.6
	SBA	1.3	1	>>2
	Spiked LC	3	0	0.5

The relationship between bromate formation and ozone exposure is summarized in Figure 4.23 for all waters in which bromate was detected. The figure shows that for each water source, bromate

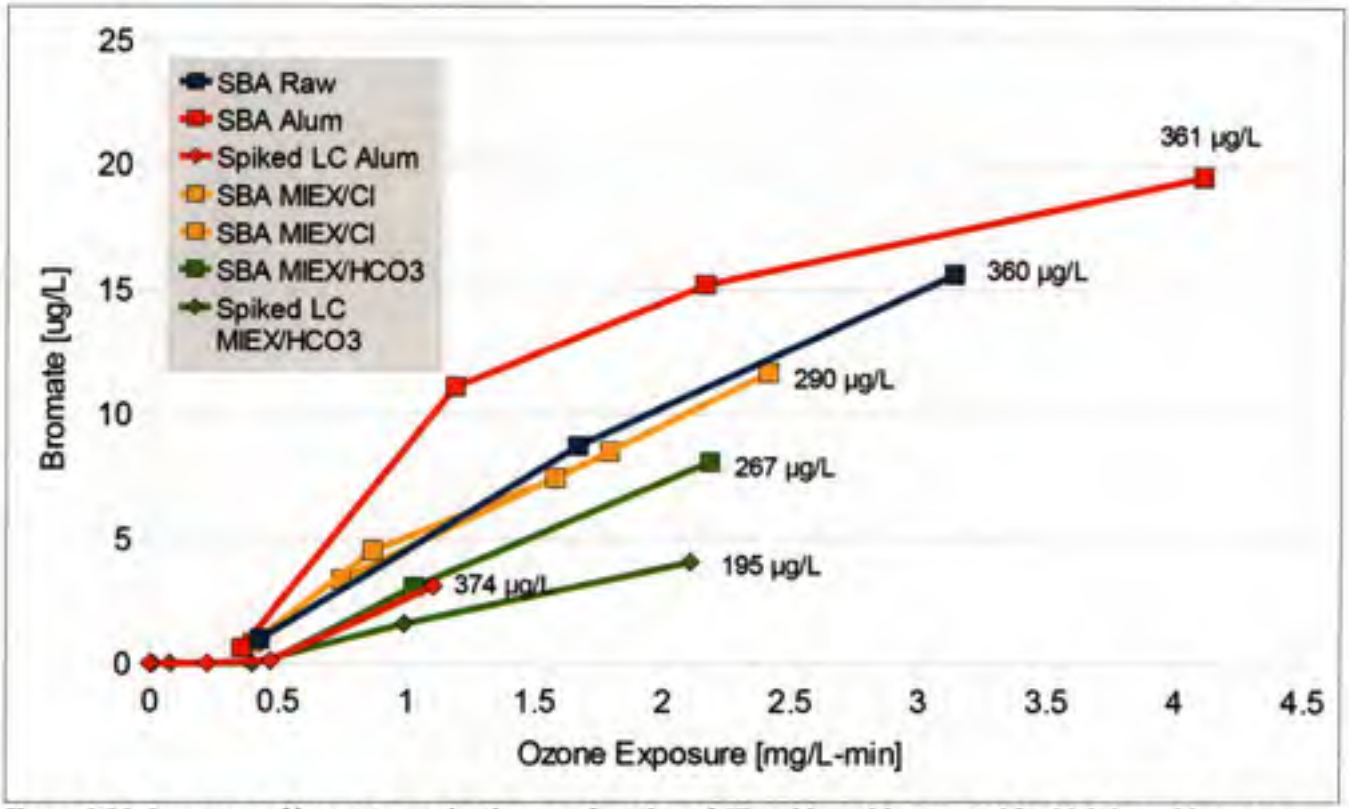

Figure 4.24: Summary of bromate production as a function of CT and bromide removal for high-bromide waters. Type of treatment is indicated by color; source water is indicated by the shape of the marker. Values at the end of each curve indicate the bromide concentration in the water.

formation is driven primarily by the level of bromide in the water. MIEX/HCO_3 treatment provided the most effective bromide removal for both South Bay Aqueduct and spiked Lake Campbell waters, and therefore these waters produced the lowest amount of bromate. For a given level of ozone exposure, somewhat less bromate was formed in the MIEX/HCO_3 treated waters than in either the raw or MIEX/Cl-treated waters, which performed similarly in this regard. In both SBA and spiked LC waters, alum-coagulated water formed more bromate than MIEX resin-treated water for a given level of CT. In the case of SBA (the only raw water for which bromate was detected), significantly more bromate was produced in the alum-coagulated water than in the raw water as well. The reason for this result is not entirely clear, but it may be attributable to an increased Br:DOC ratio which makes bromide more accessible to attack by ozone. Ozonation of the spiked LC water produced little bromate in comparison with the SBA water, suggesting that the elevated TOC concentration may have interfered with the

formation of bromate.

Table 4.13 summarizes these results in terms of the quantity of bromate produced at two different CT values. Note that a CT value of 1.0 corresponds to 0.5-log inactivation credit for *Cryptosporidium* at 20 °C (U.S. EPA, 2006). A comparison of the various treatments used on South Bay Aqueduct water reveals that MIEX/Cl treatment produces equivalent amounts of bromate as ozonation of the raw water, while MIEX HCO_3 treatment offers a modest reduction in bromate production. Alum coagulation, by contrast, appears to increase the bromate production.

Table 4.13: Comparison of bromate production (in µg/L) associated with various CT values in South Bay Aqueduct and spiked Lake Campbell waters.

CT Value	Treatment	Source Water	
mg-min/L		SBA	Spiked LC
1.0	Raw	4.5	-
	Alum	9	2.5
	MIEX/Cl	5	-
	MIEX/HCO3	3	1.5
2.0	Raw	10	-
	Alum	14.5	-
	MIEX/Cl	9.5	-
	MIEX/HCO3	7	4

4.6 IMPLICATIONS

The combination of MIEX resin and ozonation of Delta waters may be a viable means of simultaneously achieving control of chlorinated DBPs and bromate while meeting disinfection goals. Moreover, this process is capable of accommodating the wide seasonal variability experienced in the Delta. The four waters studied approximate the minimum and maximum TOC and bromide concentrations encountered at Delta pumping stations throughout the year (see Figures 2.2 and 2.3). In all cases, MIEX resin achieved superior TOC removal to alum coagulation, while aiding in the control of bromate formation upon subsequent ozonation. Furthermore, MIEX resin was the only treatment

capable of reducing the THMFP of Lake Campbell water (representing worst-case TOC) below regulatory limits.

CHAPTER 5: CONCLUSIONS

5.1 CONCLUSIONS

The use of MIEX resin prior to ozonation of drinking waters is an effective means of controlling bromate and halogenated DBP formation while achieving disinfection goals. This work indicates that in bromide-rich waters in which ozone disinfection is used, MIEX resin is a more appropriate treatment than alum, as it achieves superior TOC and THM precursor removal and decreases the production of bromate. The specific findings of this study are as follows:

- At doses reflective of those used in practice, MIEX resin treatment results in greater removal of TOC and UV-absorbing substances than alum coagulation. In the waters studied, MIEX removed 41-68% of raw water TOC, compared to 12-44% for alum. MIEX resin and alum reduced the SUVA of raw water, indicating preferential removal of UV-absorbing substances.
- MIEX resin can remove bromide as well as TOC. Bromide removal increased with increasing resin doses and ranged from 20-50% in the waters studied at resin doses of 1-4 mL/L. MIEX resin in the bicarbonate form removed slightly more bromide than resin regenerated in the chloride form. This finding is consistent with the competitive nature of ion exchange and the respective selectivities of anion exchange resins for different anions.
- Treatment with alum and MIEX resin significantly reduced the ozone demand, leading to higher CT values (ozone exposure) for a given ozone dose. MIEX reduced the ozone demand to an equal or greater degree than alum in all waters studied.
- MIEX resin or alum in combination with ozonation significantly reduced the THMFP of the raw waters studied. MIEX resin reduced THMFP to a greater extent than alum. MIEX removed 39-85% of THMFP compared to 16-56% removal by alum. Ozonation reduced THMFP by 35-45% in all cases. MIEX removed more TOC than alum, but because the resin

removed bromide in addition to TOC, however, the bromine incorporation factor of THMs was similar for MIEX and alum-treated waters.

- For a given level of disinfection (CT), the amount of bromate produced by ozonation of MIEX-treated waters was similar to or slightly less than that of raw water. This result is attributable to the increased Br:DOC ratio following MIEX resin treatment and to bromide removal by the MIEX resin.

5.2 RECOMMENDATIONS

This research has shown that MIEX resin can achieve superior removal of organic carbon and THM formation potential to alum at bench-scale without increasing the bromate production arising from ozonation. The ozonation experiments in this study were performed on a semi-batch basis, in which the same volume of water was held in contact with ozone for an extended period. These findings should be examined in a continuous-flow ozonation apparatus which more closely resembles the conditions encountered in practice.

In addition, this study employed only virgin MIEX resin, so potential effects of regeneration were not addressed. Because the ions released by the resin may themselves compete with bromide in the process water, a continuous-flow system may yield very different bromide removal results. Experiments conducted in a continuous-flow pilot-scale MIEX system are needed to further explore the long-term implications of regeneration for bromide removal.

Competition between naturally-occurring bromide and chloride as well as chloride or bicarbonate released from the resin was briefly investigated in this work. Future research should explore the competition among various other naturally-occurring anions, such as sulfate, and their impact on the removal of TOC and bromide. If the concentrations of all relevant anions are measured in each sample before and after MIEX treatment, charge balances could be used to quantify the degree of exchange for

each species. Such research should also explore the impact of increased chloride or bicarbonate concentrations in the process water that result from anion exchange. This information would aid in optimizing treatment conditions for bromide removal.

Ozone exposure values achieved in this study were generally lower than what would be expected in practice if *Cryptosporidium* inactivation were a treatment objective. Future studies should apply higher ozone doses to ensure that higher values of CT are reached. These higher values would make comparisons of bromate production in treated waters more robust. In addition, the dissolved ozone measurements and CT calculations in this experiment assumed that ozone decayed very rapidly and did not impart additional CT to the water after samples were collected. Future studies should examine the persistence of ozone in the treated waters and account for this additional increment of ozone exposure when calculating CT, particularly if higher ozone doses are used.

Finally, this work was conducted at room temperature (20 °C). Colder water temperatures may slow the kinetics of ion exchange, increase the half-life of ozone, impact the ozone exposure (CT) achieved, and alter the rate of bromate formation. The cumulative effect of these phenomena cannot be predicted from this work. An investigation of the impact of low temperatures on bromide removal and ozone performance would yield valuable information for full-scale operations in which water temperature cannot be controlled.

THIS PAGE LEFT BLANK INTENTIONALLY

REFERENCES

American Public Health Association, American Water Works Association, Water Environment Federation, and Water Pollution Control Federation. *Standard methods for the examination of water and wastewater [serial] : Including bottom sediments and sludges.* New York : American Public Health Association, c1960-, 1998.

Archer, Aaron and Philip C. Singer. Effect of SUVA and enhanced coagulation on removal of TOX precursors. *Journal of the American Water Works Association* 98 (8): 97-107.

AWWA Disinfection Systems Committee. 2008. Disinfection survey part 2 - alternatives, experiences, and future plans. *Journal of the American Water Works Association* 100 (11): 110-24.

Bader, H., and J. Hoigné. 1981. Determination of ozone in water by the indigo method. *Water Research* 15 (4): 449-56.

Berne, F., G. Chasson, and B. Legube. 2004. Effect of addition of ammonia on the bromate formation during ozonation. *Ozone: Science & Engineering* 26 (3): 267-76.

Bolto, Brian, David Dixon, Rob Eldridge, and Simon King. 2002. Removal of THM precursors by coagulation or ion exchange. *Water Research* 36 (20): 5066-73.

Bolto, Brian, David Dixon, Rob Eldridge, Simon King, and Kathryn Linge. 2002. Removal of natural organic matter by ion exchange. *Water Research* 36 (20): 5057-65.

Bose, Purnendu, and David A. Reckhow. 2007. The effect of ozonation on natural organic matter removal by alum coagulation. *Water Research* 41 (7): 1516-24.

Boyer, Treavor H., and Philip C. Singer. 2005. Bench-scale testing of a magnetic ion exchange resin for removal of disinfection by-product precursors. *Water Research* 39 (7): 1265-76.

Boyer, Treavor H., and Philip C. Singer. 2006. A pilot-scale evaluation of magnetic ion exchange treatment for removal of natural organic material and inorganic anions. *Water Research* 40 (15): 2865-76.

Boyer, Treavor H., and Philip C. Singer. 2008. Stoichiometry of removal of natural organic matter by ion exchange. *Environmental Science & Technology* 42 (2): 608-13.

Boyer, Treavor H., Philip C. Singer, Abigail Holmquist, Jim Morran, and Michael Bourke. 2009. Integrated analysis of NOM removal by ion exchange. *Journal of the American Water Works Association* 101 (1): 65.

Buehler, Rolf E., J. Staehelin, and J. Hoigne. 1984. Ozone decomposition in water studied by pulse radiolysis. 1. perhydroxyl (HO2)/hyperoxide (O2-) and HO3/O3- as intermediates. *The Journal of Physical Chemistry* 88 (12): 2560-4.

Buffle, Marc-Olivier, Sonja Galli, and Urs von Gunten. 2004. Enhanced bromate control during ozonation: The chlorine-ammonia process. *Environmental Science & Technology* 38 (19).

CALFED Water Quality Program. *Draft CALFED water quality program stage 1 final assessment.* 2007. http://calwater.ca.gov/content/Documents/Draft_Final.pdf (accessed June 29, 2009).

Christman, Russell F., Daniel L. Norwood, David S. Millington, J. D. Johnson, and Alan A. Stevens. 1983. Identity and yields of major halogenated products of aquatic fulvic acid chlorination. *Environmental Science & Technology* 17 (10): 625-8.

Cory, Rose M., Kristopher McNeill, James P. Cotner, Andre Amado, Jeremiah M. Purcell, and Alan G. Marshall. 2010. Singlet oxygen in the coupled photochemical and biochemical oxidation of dissolved organic matter. *Environmental Science & Technology*. In press, Accepted Manuscript.

Crittenden, John C., R. Rhodes Trussel, David W. Hand, Kerry J. Howe, and George Tchobanoglous. 2005. *Water treatment: Principles and design*, ed. Montgomery Watson Harza. 2nd ed. Hoboken, N.J.: John Wiley.

DeRose, Paul C., Edward A. Early, and Gary W. Kramer. 2007. Qualification of a fluorescence spectrometer for measuring true fluorescence spectra. *Review of Scientific Instruments* 78(033107): 1-12.

Drikas, Mary, Christopher W. K. Chow, and David Cook. 2003. The impact of recalcitrant organic character on disinfection stability, trihalomethane formation and bacterial regrowth: An evaluation of magnetic ion exchange resin (MIEX®) and alum coagulation. *Journal of Water Supply Research Technology - AQUA* 52 (7): 475.

Droste, Ronald L. 1997. *Theory and practice of water and wastewater treatment*. Hoboken, NJ: John Wiley & Sons.

Fearing, David A., Jenny Banks, Soizic Guyetand, Carmen Monfort Eroles, Bruce Jefferson, Derek Wilson, Peter Hillis, Andrew T. Campbell, and S. A. Simon A. Parsons. 2004. Combination of ferric and MIEX® for the treatment of a humic rich water. *Water Research* 38 (10): 2551-8.

Gurol, Mirat D., and Philip C. Singer. 1982. Kinetics of ozone decomposition: A dynamic approach. *Environmental Science & Technology* 16 (7): 377-83.

Haag, Werner R., and Juerg Hoigne. 1983. Ozonation of bromide-containing waters: Kinetics of formation of hypobromous acid and bromate. *Environmental Science & Technology* 17 (5): 261-7.

Hammes, Frederik, Elisabeth Salhi, Oliver Köster, Hans-Peter Kaiser, Thomas Egli, and Urs von Gunten. 2006. Mechanistic and kinetic evaluation of organic disinfection by-product and assimilable organic carbon (AOC) formation during the ozonation of drinking water. *Water Research* 40 (12): 2275-86.

Hoigné, J., and H. Bader. 1976. The role of hydroxyl radical reactions in ozonation processes in aqueous solutions. *Water Research* 10 (5): 377-86.

Hsu, Susan, and Philip C. Singer. Removal of bromide and natural organic matter by anion exchange. *Water Research*. In Press, Accepted Manuscript.

Hudson, Naomi, Andy Baker, and Darren Reynolds. 2007. Fluorescence analysis of dissolved organic matter in natural, waste and polluted waters - a review. *River Research and Applications* 23 (6): 631-49.

Humbert, Hugues, Hervé Gallard, Hervé Suty, and Jean-Philippe Croué. 2005. Performance of selected anion exchange resins for the treatment of a high DOC content surface water. *Water Research* 39 (9): 1699-708.

Humbert, Hugues, Hervé Gallard, Valérie Jacquemet, and Jean-Philippe Croué. 2007. Combination of coagulation and ion exchange for the reduction of UF fouling properties of a high DOC content surface water. *Water Research* 41 (17): 3803-11.

International Ozone Association. 1998. Revised Guideline Document III. Colorimetric Method for Manual Determination of Ozone Concentration in Water. *Ozone Science and Engineering* 20(6): 443.

Jacangelo, Joseph G., Nancy L. Patania, Kevin M. Reagan, E. Marco Aieta, Stuart W. Krasner, and Michael J. McGuire. 1989. Ozonation: Assessing its role in the formation and control of disinfection by-products. *Journal of the American Water Works Associations* 81 (8): 74.

Johnson, Clayton J., and Philip C. Singer. 2004. Impact of a magnetic ion exchange resin on ozone demand and bromate formation during drinking water treatment. *Water Research* 38 (17): 3738-50.

Krasner, Stuart W., Michael J. McGuire, Joseph G. Jacangelo, Nancy L. Patania, Kevin M. Reagan, and E. Marco Aieta. 1989. The occurrence of disinfection by-products in US drinking water. *Journal of the American Water Works Association* 81 (8): 41.

Krasner, Stuart W., William H. Glaze, Howard S. Weinberg, Phillippe A. Daniel, and Issam N. Najm. 1993. Formation and control of bromate during ozonation of waters containing bromide. *Journal of the American Water Works Association* 85 (1): 73-81.

Krasner, Stuart W., and Gary Amy. 1995. Jar-test evaluations of enhanced coagulation. *Journal of the American Water Works Association* 87 (10): 93.

Leenheer, Jerry A., and Jean-Philippe Croué. 2003. Characterizing aquatic dissolved organic matter. *Environmental Science & Technology* 37 (1): 18A-26A.

Leenher, Jerry A. 2009. Systematic approaches tocomprehensive analyses ofnatural organic matter. *Annals of Environmental Science* 3 : 1,1-130.

Liang, Lin, and Philip C. Singer. 2003. Factors influencing the formation and relative distribution of haloacetic acids and trihalomethanes in drinking water. *Environmental Science & Technology* 37 (13): 2920-8.

Magazinovic, Rodney S., Brenton C. Nicholson, Dennis E. Mulcahy, and David E. Davey. 2004. Bromide levels in natural waters: Its relationship to levels of both chloride and total dissolved solids and the implications for water treatment. *Chemosphere* 57 (4): 329-35.

McKnight, Diane M., Elizabeth W. Boyer, Paul K. Westerhoff, Peter T. Doran, Thomas Kulbe, and Dale T. Andersen. 2001. Spectrofluorometric characterization of dissolved organic matter for indication ofprecursor organic material and aromaticity. *Limnological Oceanography* 46 (1): 38-48.

Mercer, Kenneth, William Taplin P.E., Jim Borchardt P.E., Richard Lin, and David Okita P.E. 2004. Advanced pre-treatment with ion exchange technology for organic carbon removal. Paper presented at Proceedings of the AWWA Annual Conference and Exposition.

Mobed, Jarafshan J., Sherry L. Hemmingsen, Jennifer L. Autry, and Linda B. McGown. 1996. Fluorescence characterization of IHSS humic substances: Total luminescence spectra with absorbance correction. *Environmental Science & Technology* 30(10): 3061-3065.

Morran, J. Y., M. Drikas, D. Cook, and D. B. Bursill. 2004. Comparison of MIEX treatment and coagulation on NOM character. *Water Science and Technology: Water Supply* 4 (4): 129.

Najm, Issam N., and Stuart W. Krasner. 1995. Effects of bromide and NOM on by-product formation. *Journal of the American Water Works Association* 87 (1): 106-15.

Nemes, Attila, Istvan Fabian, and Rudi van Eldik. 2000. Kinetics and mechanism of the carbonate ion inhibited aqueous ozone decomposition. *The Journal of Physical Chemistry A* 104 (34): 7995-8000.

Obolensky, Alexa, and Philip C. Singer. 2005. Halogen substitution patterns among disinfection byproducts in the information collection rule database. *Environmental Science & Technology* 39 (8): 2719-30.

Pinkernell, Ulrich, and Urs von Gunten. 2001. Bromate minimization during ozonation: Mechanistic considerations. *Environmental Science & Technology* 35 (12).

Plewa, Michael J., Yahya Kargalioglu, Danielle Vankerk, Roger A. Minear, and Elizabeth D. Wagner. 2002. Mammalian cell cytotoxicity and genotoxicity analysis of drinking water disinfection by-products. *Environmental and Molecular Mutagenesis* 40 (2): 134-42.

Rice, Rip G., Michael Robson, G. Wade Miller, and Archibald G. Hill. 1981. Use of ozone in drinking water treatment. *Journal of the American Water Works Associations* 73 (1): 44-57.

Rice, Rip G. 1999. Ozone in the united states of america - state-of-the-art. *Ozone Science and Engineering* 21 (2): 99-118.

Richardson, Susan D., Alfred D. Thruston, Tashia V. Caughran, Paul H. Chen, Timothy W. Collette, Terrance L. Floyd, Kathleen M. Schenck, Benjamin W. Lykins, Guang-ri Sun, and George Majetich. 1999. Identification of new drinking water disinfection byproducts formed in the presence of bromide. *Environmental Science & Technology* 33 (19): 3378-83.

Richardson, Susan D., Alfred D. Thruston, Tashia V. Caughran, Paul H. Chen, Timothy W. Collette, Terrance L. Floyd, Kathleen M. Schenck, Benjamin W. Lykins, Guang-ri Sun, and George Majetich.. 1999. Identification of new ozone disinfection byproducts in drinking water. *Environmental Science & Technology* 33 (19): 3368-77.

Rook, J. J., A. A. Gras, der Heijden van, and J. de Wee. 1978. Bromide oxidation and organic substitution in water treatment. *Journal of Environmental Science and Health .Part A: Environmental Science and Engineering* 13 (2): 91-116.

Rubin, Mordecai B. 2001. History of ozone: The schonbein period, 1839 - 1868. *Bulletin for the History of Chemistry* 26 (1): 40.

Singer, Philip C., and Katya Bilyk. 2002. Enhanced coagulation using a magnetic ion exchange resin. *Water Research* 36 (16): 4009.

Staehelin, Johannes, and Juerg Hoigne. 1982. Decomposition of ozone in water: Rate of initiation by hydroxide ions and hydrogen peroxide. *Environmental Science & Technology* 16 (10): 676-81.

Staehelin, J., R. E. Buehler, and J. Hoigne. 1984. Ozone decomposition in water studied by pulse radiolysis. 2. hydroxyl and hydrogen tetroxide (HO4) as chain intermediates. *The Journal of Physical Chemistry* 88 (24): 5999-6004.

Stedmon, Colin L., and Rasmus Bro. 2008. Characterizing dissolved organic matter with parallelfactor analysis: a tutorial. *Limnology and Oceanography Methods* 6: 572-579.

Stumm, Werner, and James C. Morgan. 1996. *Aquatic chemistry: Chemical equilibria and rates in natural waters* . New York: Wiley.

Summers, Scott, Stuart M. Hooper, Hiba M. Shukairy, Gabriele Solarik, and Douglas Owen. 1996. Assessing DBP yield: Uniform formation conditions. *Journal of the American Water Works Association* 88 (6): 80.

Thurman, Earl M., and Ronald L. Malcolm. 1981. Preparative isolation of aquatic humic substances. *Environmental Science & Technology* 15 (4): 463-6.

U.S. EPA, National Exposure Laboratory, Office of Research and Development. *Determination of inorganic anions in drinking water by ion chromatography.* 1997.

U.S. EPA. *Toxicological review of bromate.* 2001. http://www.epa.gov/iris/toxreviews/1002-tr.pdf (accessed 6/2/2009).

U.S. EPA, Office of Water. *Occurrence assessment for the final stage 2 disinfectants and disinfection by-products rule.* 2005. http://www.epa.gov/safewater/disinfection/stage2/pdfs/assesment_stage2_occurance_main.pdf

U.S. EPA. *National primary drinking water regulations: Stage 1 disinfectants and disinfection byproducts rule; final rule.* 1998. http://www.epa.gov/ogwdw000/mdbp/dbpfr.html.

U.S. EPA. National primary drinking water regulations: Long-term 2 enhanced surface water treatment rule. 2006. http://www.epa.gov/fedrgstr/EPA-WATER/2006/January/Day-05/w04a.htm.

U.S. EPA. *National primary drinking water regulations: Stage 2 disinfectants and disinfection byproducts rule; final rule.* 2006. http://www.epa.gov/fedrgstr/EPA-WATER/2006/January/Day-04/w03.pdf.

Urfer, Daniel, Peter M. Huck, Stephen D. J. Booth, and Bradley M. Coffey. 1997. Biological filtration for BOM and particulate removal: A crtical review. *Journal of the American Water Works Association* 89 (12): 83-98.

von Gunten, Urs, and Juerg Hoigne. 1994. Bromate formation during ozonization of bromide-containing waters: Interaction of ozone and hydroxyl radical reactions. *Environmental Science & Technology* 28 (7).

von Gunten, Urs. 2003. Ozonation of drinking water: Part I. oxidation kinetics and product formation. *Water Research* 37 (7): 1443-67.

von Gunten, Urs. 2003. Ozonation of drinking water: Part II. disinfection and by-product formation in presence of bromide, iodide or chlorine. *Water Research* 37 (7): 1469-87.

Weinberg, Howard S., William H. Glaze, Stuart W. Krasner, and Michael J. Sclimenti. 1993. Formation and removal of aldehydes in plants that use ozonation. *Journal of the American Water Works Association* 85 (5): 72-85.

Wert, Eric C., Jessica C. Edwards-Brandt, Philip C. Singer, and George C. Budd. 2005. Evaluating magnetic ion exchange resin (MIEX)® pretreatment to increase ozone disinfection and reduce bromate formation. *Ozone: Science & Engineering* 27 (5): 371-9.

White, Mark C., Jeffrey D. Thompson, Gregory W. Harrington, and Philip C. Singer. 1997. Evaluating criteria for enhanced coagulation compliance. *Journal of the American Water Works Association* 89 (5): 64.

APPENDIX A: DETERMINATION OF BULK TREATMENT MIXING INTENSITY

The revolutions per minute used for bulk treatment in the 16-L vessel were calculated to provide an equivalent amount of mixing energy as the jar test configuration. The mixing energy is represented by the mean temporal velocity gradient, G:

$$G = \sqrt{\frac{P}{\mu V}}$$

where P is the power imparted to the mixing vessel, μ is the viscosity of the water, and V is the volume of the vessel. For rotating mixers, the power input is given by:

$$P = \rho N^3 D^5 \phi$$

where ρ is the fluid density, N is the rate of rotation (Hz), D is the diameter of the paddle blades, and φ is known as the power number, analogous to a drag coefficient. The power number is constant for fully turbulent flow (Re>10; Droste, 1997). The Reynolds number for a mixer is given by:

$$\Re = \frac{\rho N D^2}{\mu}$$

Jar Test Conditions

Coagulation jar tests were conducted in 500 mL jars with two-blade, 3" x 1" paddles at 35 rpm. Assuming a water temperature of at 20°C, the Reynolds number indicates fully turbulent flow (>10):

$$\Re = \frac{\rho N D^2}{\mu} = \frac{(998\,kg/m^3)(35\,min^{-1}/60\,s/min)[(3\,\text{in})(.0254\,m/\text{in})]^2}{.001002\,kg-s/m^2} = 3373$$

For these conditions and a diameter to width ratio of 3, the power number is equal to 1.70 (Droste, 1997). The power input is thus:

$$P = \rho N^3 D^5 \phi = (998\,kg/m^3)(35\,min^{-1}/60\,s/min)^3[(3\,\text{in})(.0254\,m/\text{in})]^5(1.70) = .000865\,W$$

and the velocity gradient is:

$$G=\sqrt{\frac{P}{\mu V}}=\sqrt{\frac{.000865\,W}{(.001002\,kg-s/m^2)(.0005\,m^3)}}=41.5\,s^{-1}$$

MIEX jar tests were conducted in the same equipment, but at 100 rpm. The velocity gradient for these conditions is found by analogous calculations to be 200.7 s^{-1}.

Bulk Treatment Conditions

The bulk treatment vessel consisted of a 16-L glass carboy and a removable mixer with an 8-inch x 1.25-inch rectangular, 2-blade paddle. The above three equations were used to determine the mixing speed necessary to achieve a velocity gradient of 41.5 s^{-1} for bulk coagulation:

$$G=41.5\,s^{-1}=\sqrt{\frac{P}{(.001002\,kg-s/m^2)(.016\,m^3)}}\rightarrow P=0.028\,W$$

$$P=0.028\,W=(998\,kg/m^3)(N/60\,s/min)^3[(8\,\text{in})(.0254\,m/\text{in})]^5(1.70)\rightarrow N=22\,min^{-1}$$

MIEX bulk treatment was performed on the same equipment. The mixing rate required to achieve a velocity gradient of 200.7 s^{-1} was found to be 62 rpm using the same approach. At both speeds, flow in the bulk treatment vessel is fully turbulent, so the power number of 1.70 used above is still valid.

Before experiments began, the paddles on the jar testing apparatus were inadvertently changed to 2-inch by 1-inch paddles. As this change went unnoticed, the bulk treatment mixing speeds were not adjusted. The velocity gradient for alum coagulation and MIEX resin treatment using 2-inch paddles was calculated to be 15 s^{-1} and 73 s^{-1}, compared to 41.5 s^{-1} and 200.7 s^{-1} with the 3-inch paddles (and bulk treatment). Consequently, bulk treatment imparted significantly more mixing energy to the samples than jar testing.

APPENDIX B: EXAMPLE TRANSFERRED OZONE CALCULATIONS

This appendix contains details of the calculations used to determine transferred ozone dose and ozone exposure (CT) from liquid- and gas-phase ozone measurements taken during ozonation experiments. The table below shows an example of these calculations in spreadsheet form; yellow cells indicate measurements, while white cells indicate calculated values. Each calculation is explained on the next page. References for the formulas used are provided in Section 3.2.3.

Calculation of Transferred Ozone Dose

4.0 mL/L MIEX, Bicarbonate Form, Spiked Water

Lake Campbell Water

Date: 01/26/10

MW of O_3	48000	mg / mol
Cell path length	5	cm
Molar Absorptivity of O_3	3000	L / cm / mUV600
Gas flow rate	0.93	L /min
Volume of Sample	9	L

	Pre-O3	Post-O3	
TOC	2.96	2.42	mg/L
UV254	0.034	0.017	1/cm
pH	8.31	8.29	
Temperature	20.8	-	°C

Time	Absorbance at 253.7 nm		Gas-Phase O_3 Conc.			O_3 Transferred	mg O_3 / mg TOC	Dissolved Ozone (Indigo)			Cumulative
	in	out	in	(interpolated)	out			Absorbance at 600 nm		Ozone conc	CT
min	-	-	mg/L		mg/L	mg/L		blank	sample	mg/L	mg-min/L
0	0.766		2.451	2.451		0.00	0.00	0.830	0.830	0.000	0
1		0.043	-	2.439	0.138	0.25	0.08			-	
2		0.215	-	2.427	0.688	0.45	0.15			-	
3		0.322	-	2.415	1.030	0.62	0.21			-	
5	0.747	0.390	2.390	2.390	1.248	0.88	0.30	0.830	0.823	0.004	0.01
10	0.740	0.439	2.368	2.368	1.405	1.42	0.48	0.830	0.785	0.024	0.08
15	0.746	0.469	2.387	2.387	1.501	1.90	0.64	0.830	0.634	0.104	0.40
20	0.728	0.486	2.330	2.330	1.555	2.33	0.79	0.830	0.578	0.133	0.99
27	0.743	0.519	2.378	2.378	1.661	2.87	0.97	0.830	0.479	0.186	2.11

Example of transferred ozone calculations

NOTE: Example calculations shown here are for t=15 minutes into the ozonation experiment

Gas-phase Ozone Concentration into and out of reactor:

$$[O_3]_{in} = \frac{(MW)(\text{Abs}_{in})}{b\epsilon} = \frac{48{,}000\, mg/mol * 0.746}{3{,}000\, L/cm-mol * 5\, cm} = 2.387\, mg\, O_3/L_{gas}$$

$$[O_3]_{out} = \frac{(MW)(\text{Abs}_{out})}{b\epsilon} = \frac{48{,}000\, mg/mol * 0.469}{3{,}000\, L/cm-mol * 5\, cm} = 1.501\, mg\, O_3/L_{gas}$$

Ozone Transferred

Ozone transfer is determined by the difference between influent and effluent concentrations. The value was calculated by averaging this difference for the current and previous time step (i.e. discrete integration using a midpoint sum). For some time intervals (e.g. at t=2 min in this example), the influent gas concentration was not measured because it was relatively stable in time. In these cases, linear interpolation was used to estimate the influent ozone concentration.

$$\text{Average}\,\Delta O_3 = \frac{(2.387\, mg\, O_3/L_{gas} - 1.501\, mg\, O_3/L_{gas}) + (2.368\, mg\, O_3/L_{gas} - 1.405\, mg\, O_3/L_{gas})}{2} = 0.925\, mg\, O_3/L_{gas}$$

$$\text{Incremental}[O_3]_{transferred} = \frac{\Delta O_3 Q t}{V} = \frac{0.925\, mg\, O_3/L_{gas} * 0.93\, L_{gas}/min * (15\, min - 10\, min)}{9\, L_{water}} = 0.48\, mg\, O_3/L_{water}$$

$$\text{Cumulative}[O_3]_{transferred} = 1.42 + 0.48 = 1.90\, mg\, O_3/L_{water}$$

Dissolved Ozone Concentration

$$[O_3]_{aq} = \frac{10(\Delta \text{Abs})}{f\, b\, V} = \frac{10 * (0.830 - 0.634)}{0.42 * 5 * 9} = 0.104\, mg\, O_3/L_{water}$$

Cumulative Ozone Exposure (CT)

Ozone exposure was calculated as the product of dissolved ozone and contact time for each time interval. The average of the two endpoint dissolved ozone concentrations was used for each increment.

$$\text{Incremental CT} = \frac{(0.104\ mg\ O_3/L_{water} + 0.024\ mg\ O_3/L_{water})}{2} * (15\ min - 10\ min) = 0.32\ mg - min/L$$

$$\text{Cumulative CT} = 0.08 + 0.32 = 0.4\ mg - min/L$$

THIS PAGE LEFT BLANK INTENTIONALLY

APPENDIX C: ILLUSTRATIVE ION CHROMATOGRAM AND CALIBRATION CURVES

Ion chromatograph calibration curves were constructed based on the integrated peak area of each ion of interest. Linear regression lines were fit to plots of standard concentrations vs. peak area and used to calculate the ion concentrations for unknown samples. A typical chromatogram of a water sample is shown below; example calibration curves appear on the next page.

Method File Name : C:\PeakNet\method.aci\DW_ANIONS_AS19_ISOCRATIC.MET
Date Time Collected : 10/29/2009 12:15:31 PM
System Operator :

Peak Information : All Peaks

Peak #	Component Name	Retention Time	Amount (ug/L)	Peak Area	Peak Height
1	Bromate	6.53	0.00	1182909	92901
2	Chloride	8.05	0.00	28917452290	990111857
3	Bromide	11.98	0.00	42544686	3144369

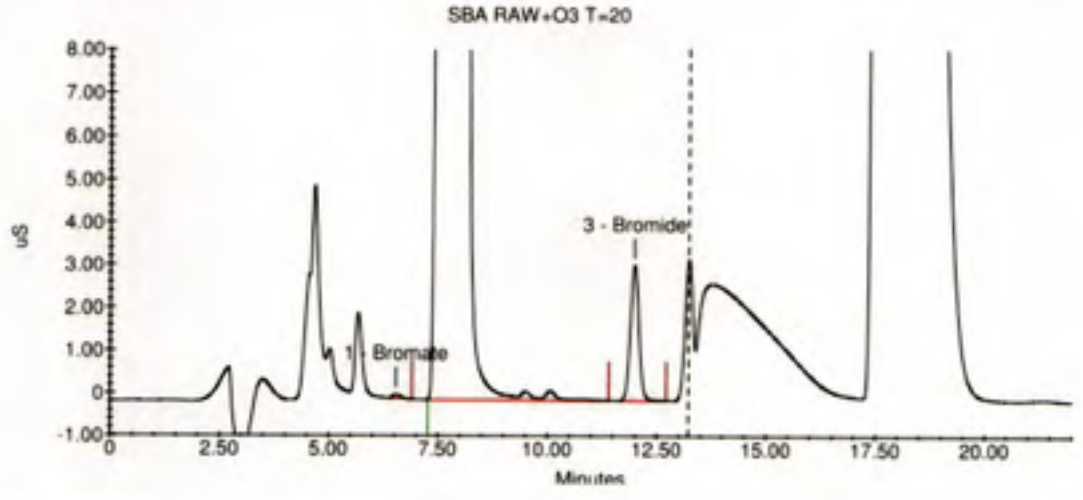

Typical sample chromatogram used for bromide and bromate analysis

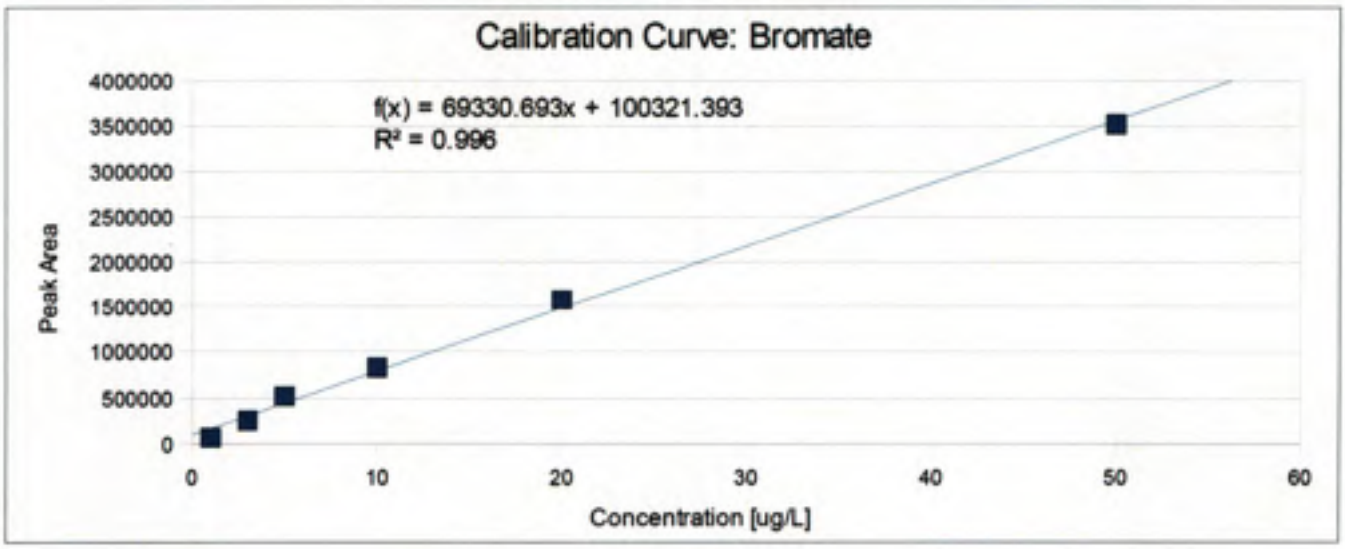
Calibration Curve: Bromate
f(x) = 69330.693x + 100321.393
R² = 0.996
Peak Area
4000000
3500000
3000000
2500000
2000000
1500000
1000000
500000
0
0
10
20
30
40
50
60
Concentration [ug/L]

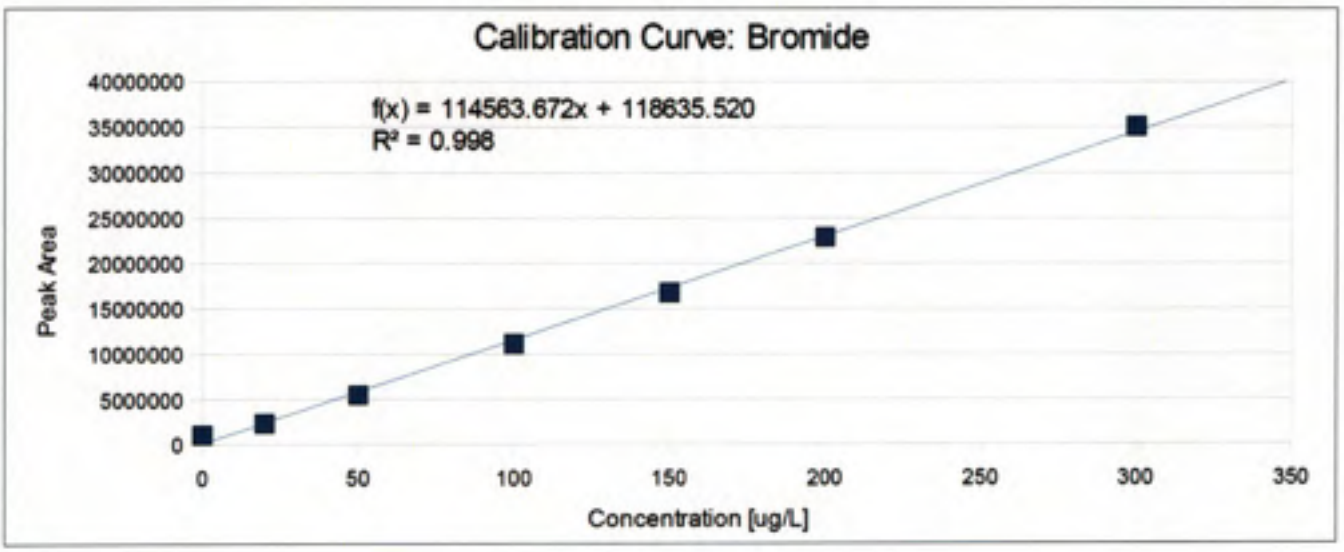
Calibration Curve: Bromide
f(x) = 114563.672x + 118635.520
R² = 0.998
Peak Area
40000000
35000000
30000000
25000000
20000000
15000000
10000000
5000000
0
0
50
100
150
200
250
300
350
Concentration [ug/L]

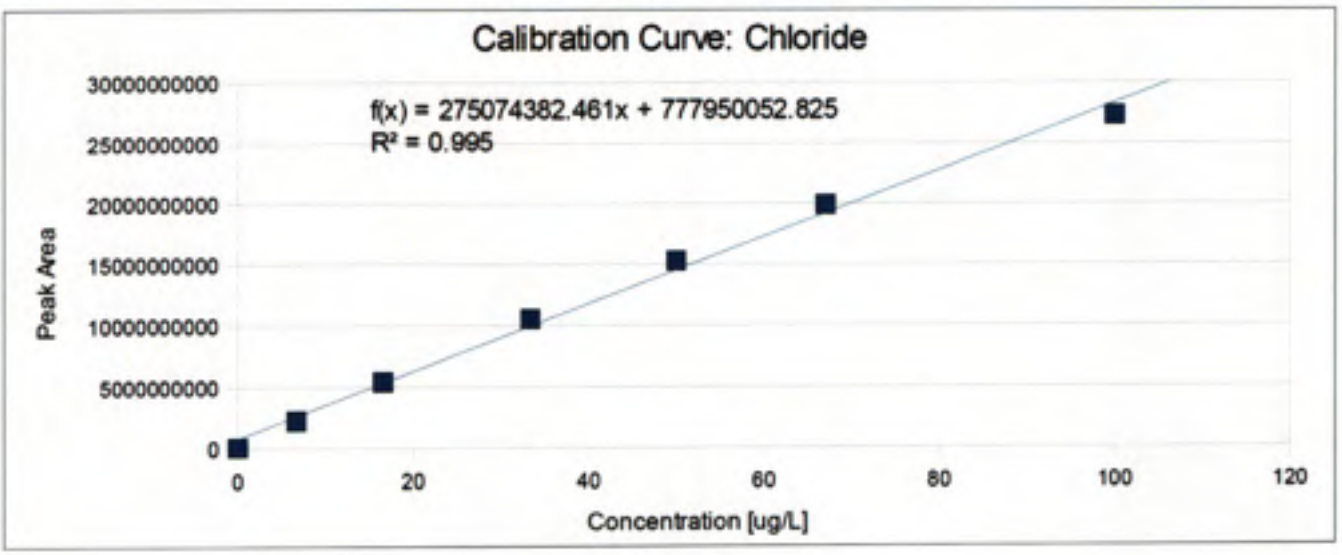
Calibration Curve: Chloride
f(x) = 275074382.461x + 777950052.825
R² = 0.995
Peak Area
30000000000
25000000000
20000000000
15000000000
10000000000
5000000000
0
0
20
40
60
80
100
120
Concentration [ug/L]

APPENDIX D: ILLUSTRATIVE GAS CHROMATOGRAMS AND CALIBRATION CURVES

THM concentrations were determined by integrating the five peaks (four THMs and the internal standard), as shown in the chromatograms below. Calibration curves (shown on the next page) were constructed using either a linear or power-fit regression of the calibration standards. The two trend lines were compared, and the one that gave the highest R^2 value was used in subsequent analysis of each compound. Calibration was based on relative peak area, unless relative peak height provided a better fit to the calibration data. In the SBA and Lake Campbell waters, a co-eluting peak distorted the internal standard peak area, so relative peak height was used for calibration.

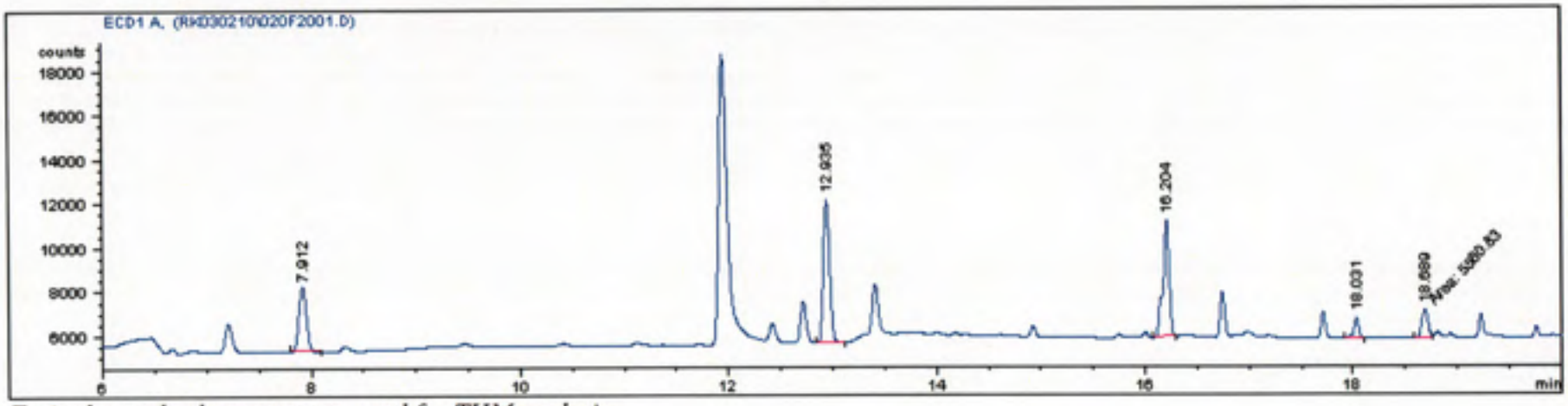

Typical sample chromatogram used for THM analysis

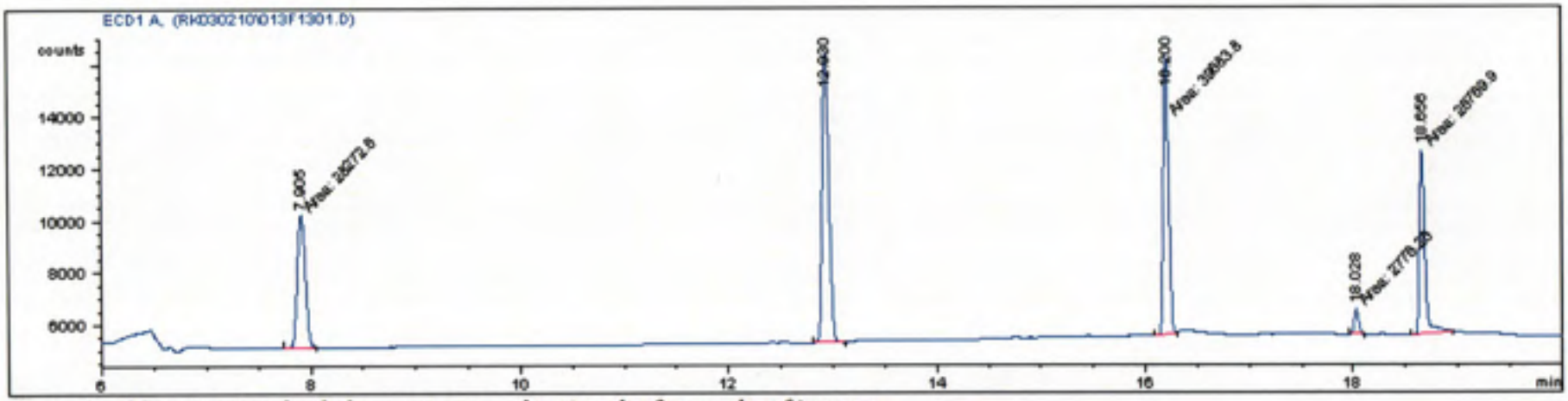

Typical calibration standard chromatogram, showing the five peaks of interest

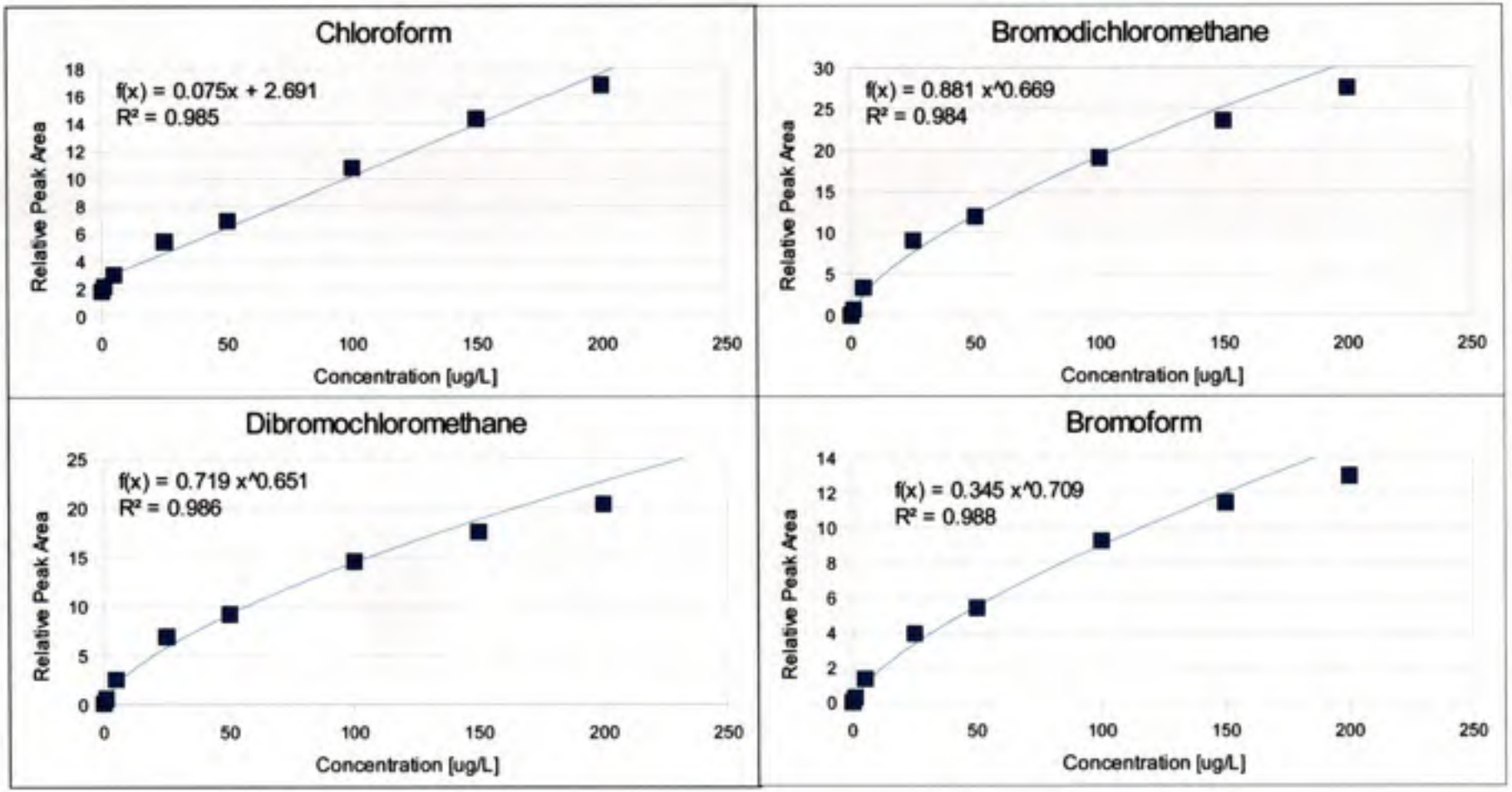

LINEAR CALIBRATION CURVES

Rel Area = mC+b	R-Squared	Slope	Intercept
Chloroform	0.985	0.075	2.691
Bromodichloromethane	0.950	0.135	2.899
Dibromochloromethane	0.941	0.100	2.341
Bromoform	0.952	0.065	1.240

POWER FIT CALIBRATION CURVES

Rel. Area =A[C]^b	R-Squared	A	b
Chloroform	0.960	1.798	0.391
Bromodichloromethane	0.984	0.881	0.669
Dibromochloromethane	0.986	0.719	0.651
Bromoform	0.988	0.345	0.709

THIS PAGE LEFT BLANK INTENTIONALLY

APPENDIX E: CALCULATION OF EQUILIBRIUM OZONE CONCENTRATION

As noted in the report, the driving force for the transfer of gas-phase ozone into the liquid phase is the difference between the dissolved ozone concentration and the saturation concentration of ozone in liquid. In these experiments, a typical influent ozone concentration was 1.85 mg O_3/L gas. At an assumed room temperature of 20°C:

$$P_{O3} = \left(\frac{1.85mg}{L_{gas}}\right)\left(\frac{1mol}{48{,}000mg}\right)\left(\frac{0.08205L_{gas} - atm}{K - mol}\right)(293K) = 0.000927 \text{ atm}$$

The equilibrium concentration of dissolved ozone can be found in accordance with Henry's Law. The "dimensionless" Henry's Law constant for O_3 at 20°C is equal to 3.74 (Stumm and Morgan, 1996).

$$C_{O3} = \frac{P_{O3}}{H_A} = \frac{(0.000927atm)}{(3.74)\left(\frac{0.08205L_{gas} - atm}{K - mol}\right)(293K)}\left(\frac{48{,}000mg}{mol}\right) = \mathbf{0.49\ mg\ O_3 / L_{H2O}}$$

THIS PAGE LEFT BLANK INTENTIONALLY

APPENDIX F: SUPPLEMENTARY TREATMENT RESULTS

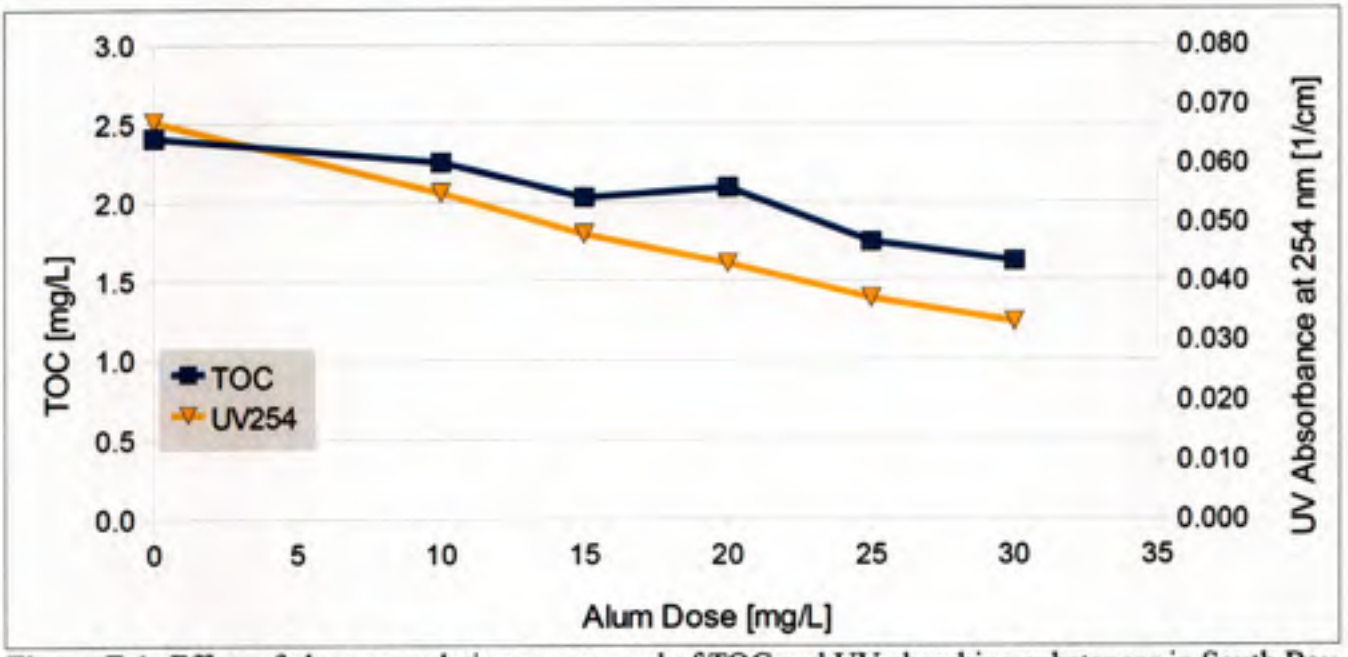

Figure F-1: Effect of alum coagulation on removal of TOC and UV-absorbing substances in South Bay Aqueduct water

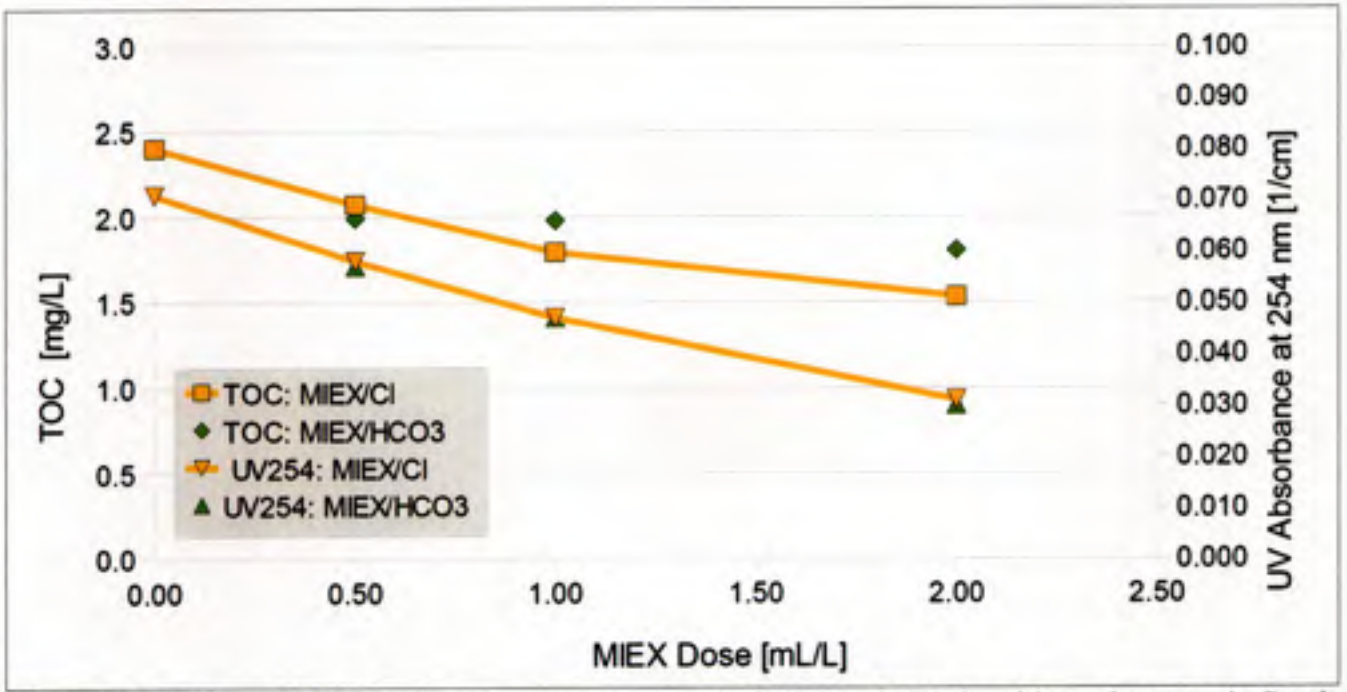

Figure F-2: Effect of MIEX resin treatment on removal of TOC and UV-absorbing substances in South Bay Aqueduct water. MIEX resin charged with both chloride and bicarbonate counterions was used in this jar test.

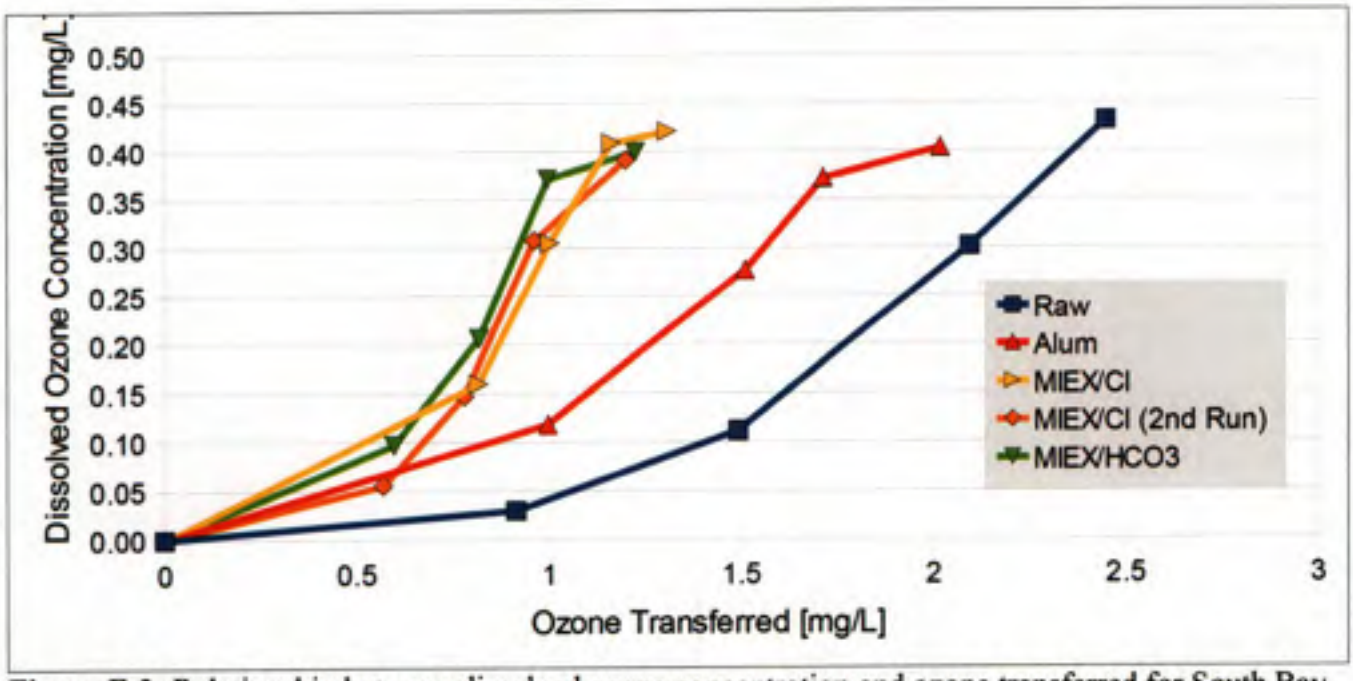

Figure F-3: Relationship between dissolved ozone concentration and ozone transferred for South Bay Aqueduct water.

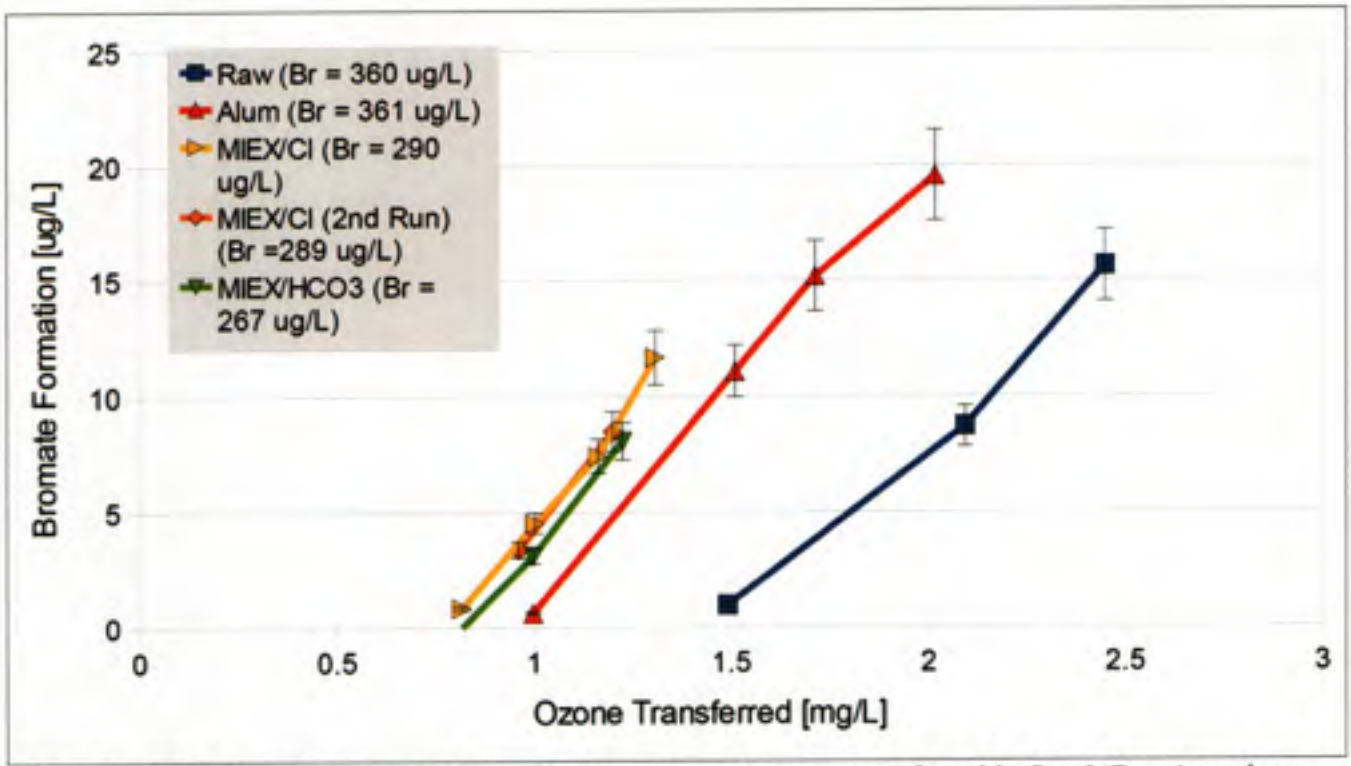

Figure F-4: Relationship between bromate formation and ozone transferred in South Bay Aqueduct water. Error bars represent 10% of the measured bromate concentration.

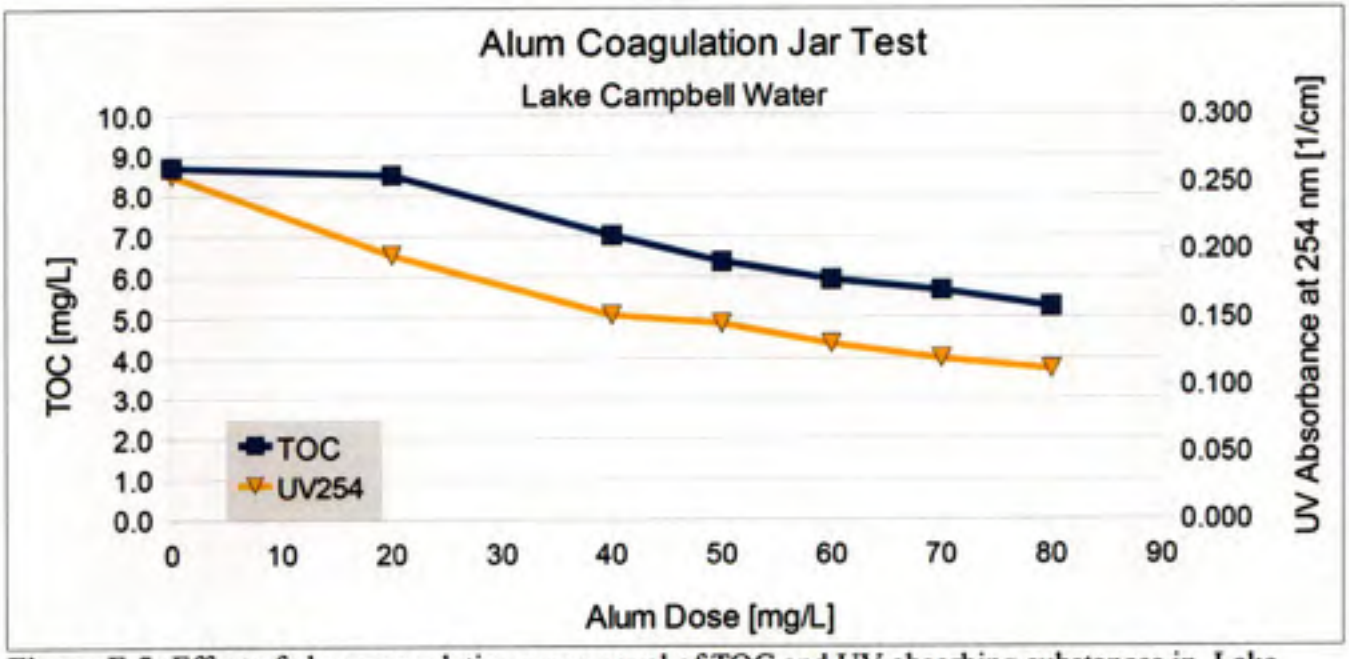

Figure F-5: Effect of alum coagulation on removal of TOC and UV-absorbing substances in Lake Campbell water

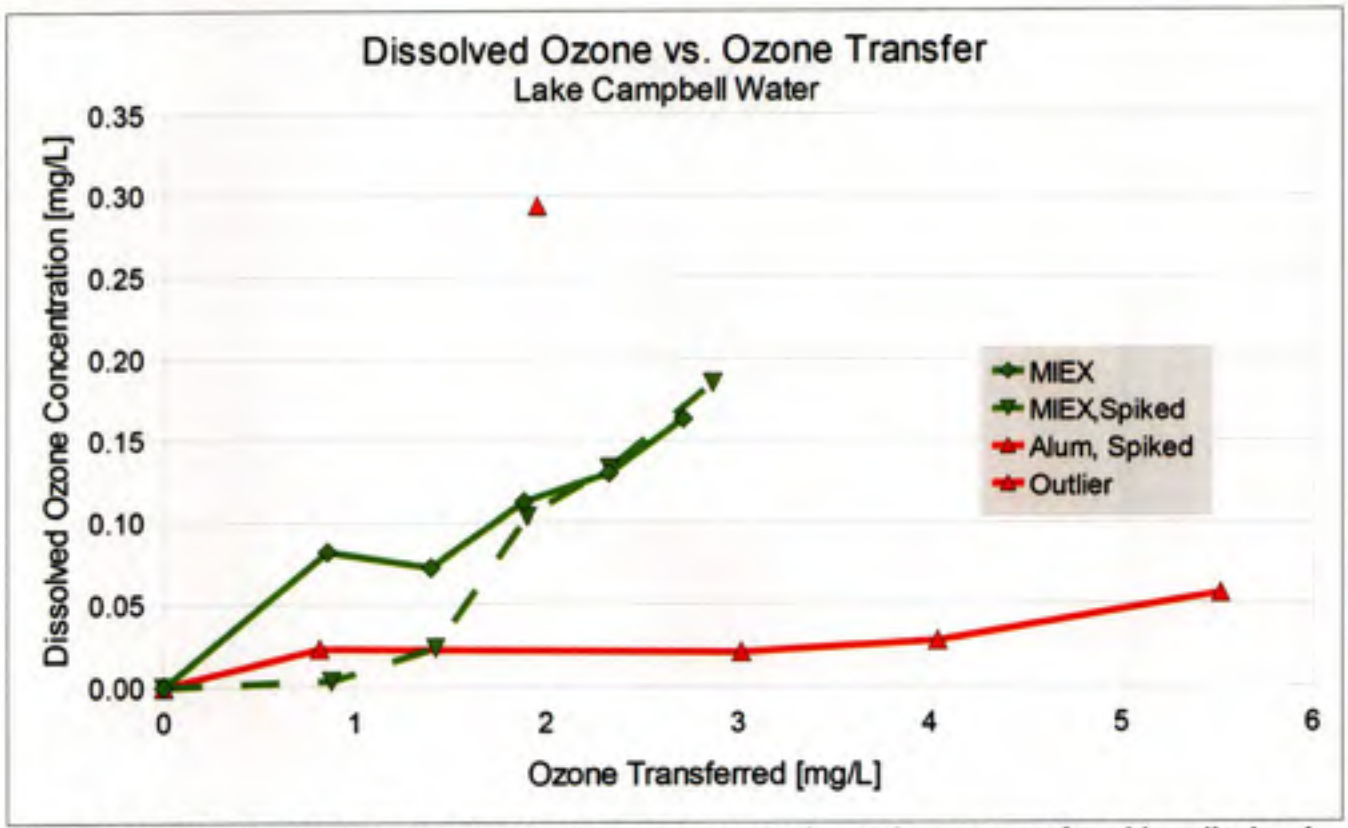

Figure F-6: Relationship between dissolved ozone concentration and ozone transferred in spiked and unspiked Lake Campbell water. The data point marked" outlier" was excluded from further analysis.

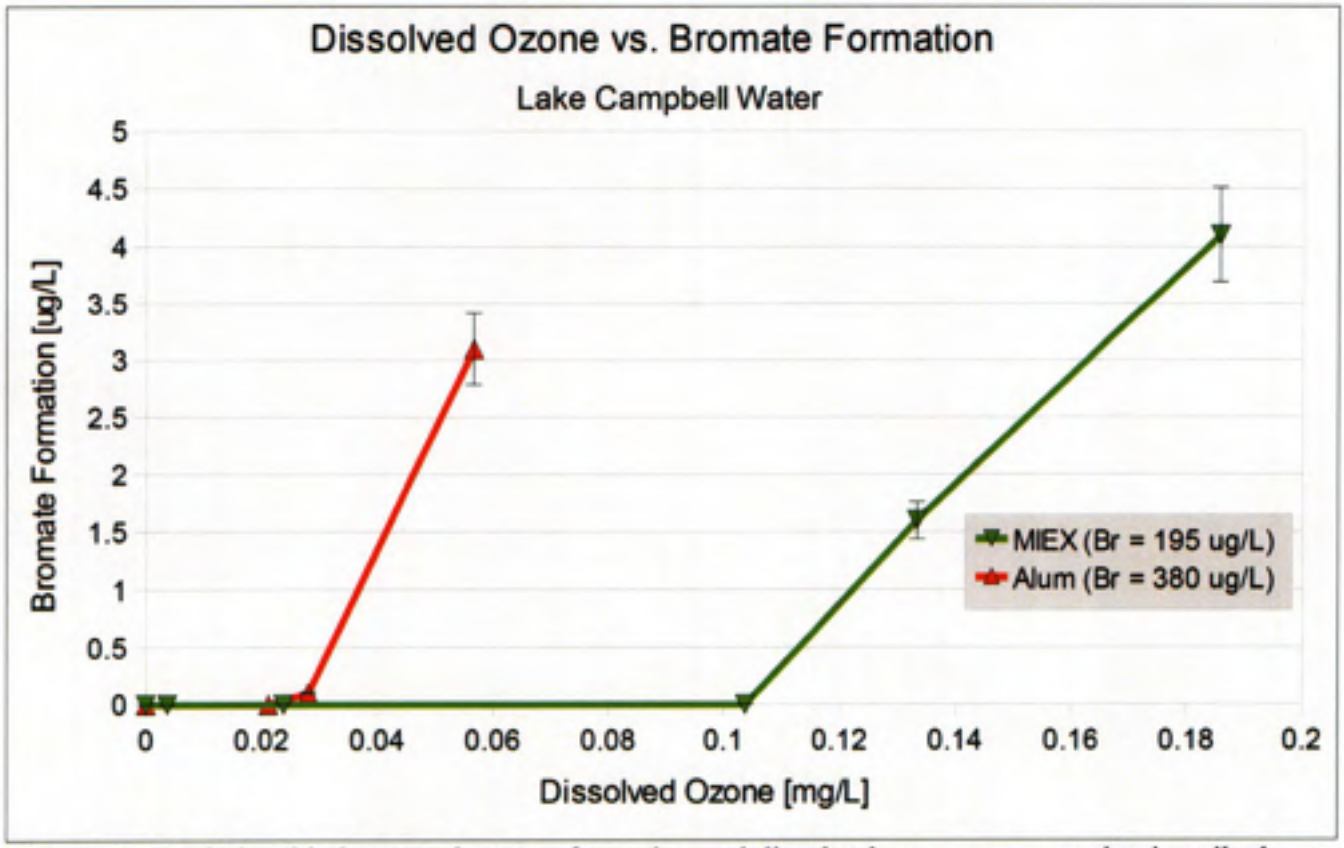

Figure F-7: Relationship between bromate formation and dissolved ozone concentration in spiked Lake Campbell water. Error bars represent 10% of the measured bromate concentration.

APPENDIX G: EXCITATION-EMISSION FLUORESCENCE SPECTRA

The excitation-emission fluorescence spectra (EEMs) for each water studied are shown below. The fluorescence intensity is indicated by the scale in Raman Units (see section 3.3.6). Numerical values of the intensity for three peaks of interest are tabulated below.

Peak "P" - excitation/emission = 280 nm / 330 nm
Peak "A" - excitation/emission = 240 nm / 450 nm
Peak "C" - excitation/emission = 300 nm / 400 nm

Table G-1: Change in fluorescence intensity at three peaks of interest

Sample	FI	Fluorescence Intensity			Change in Fluorescence Intensity		
North Bay Aqueduct		P	A	C	ΔP	ΔA	ΔC
Raw	1.39	0.11	0.95	0.35	-	-	-
Raw +O_3	1.38	0.02	0.21	0.07	-0.09	-0.73	-0.28
Alum	1.47	0.10	0.74	0.29	-0.01	-0.21	-0.06
Alum+O_3	1.45	0.03	0.13	0.05	-0.08	-0.82	-0.3
MIEX/Cl**	1.47	0.43	2.89	1.06	0.32	1.94	0.73
MIEX/Cl+O_3	1.36	0.02	0.15	0.05	-0.09	-0.8	-0.3
MIEX/HCO_3	1.46	0.06	0.42	0.17	-0.04	-0.53	-0.18
MIEX/HCO_3+O_3	1.33	0.02	0.14	0.05	-0.09	-0.81	-0.3
South Bay Aqueduct							
Raw	1.43	0.10	0.63	0.26	-	-	-
Raw +O_3	1.48	0.02	0.14	0.05	-0.08	-0.49	-0.21
Alum	1.56	0.08	0.41	0.18	-0.02	-0.22	-0.08
Alum+O_3	1.58	0.02	0.08	0.03	-0.09	-0.55	-0.23
MIEX/Cl	1.61	0.05	0.21	0.10	-0.05	-0.42	-0.16
MIEX/Cl+O_3	1.53	0.03	0.08	0.03	-0.08	-0.55	-0.23
MIEX/HCO_3	1.64	0.06	0.17	0.08	-0.05	-0.46	-0.18
MIEX/HCO_3+O_3	1.57	0.01	0.05	0.02	-0.09	-0.59	-0.24
Lake Campbell							
Raw	1.43	0.31	2.10	0.87	-	-	-
Alum	1.6	0.23	1.09	0.54	-0.08	-1.01	-0.33
Spiked Alum	1.58	0.22	1.14	0.55	-0.09	-0.96	-0.32
Spiked Alum+O_3	1.62	0.03	0.21	0.08	-0.28	-1.89	-0.79
MIEX/HCO_3	1.78	0.11	0.25	0.15	-0.19	-1.85	-0.72
MIEX/HCO_3+O_3	1.56	0.03	0.09	0.04	-0.28	-2.01	-0.83
Spiked MIEX/HCO_3	1.74	0.13	0.26	0.16	-0.18	-1.84	-0.71
Spiked MIEX/HCO_3+O_3	1.54	0.04	0.10	0.04	-0.27	-2	-0.83

** this sample was discarded due to contamination

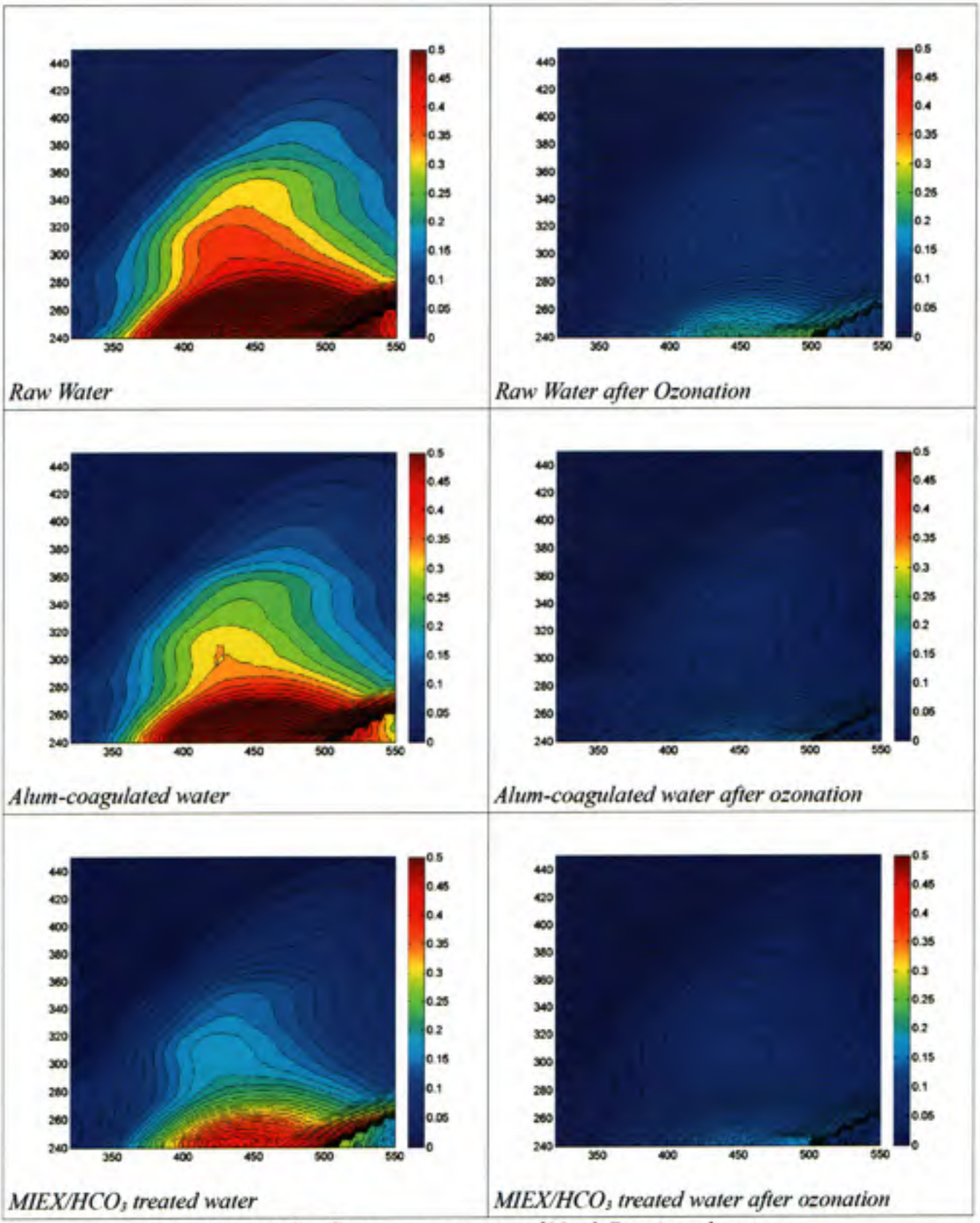

Figure G-1 – Excitation-emission fluorescence spectra of North Bay Aqueduct waters

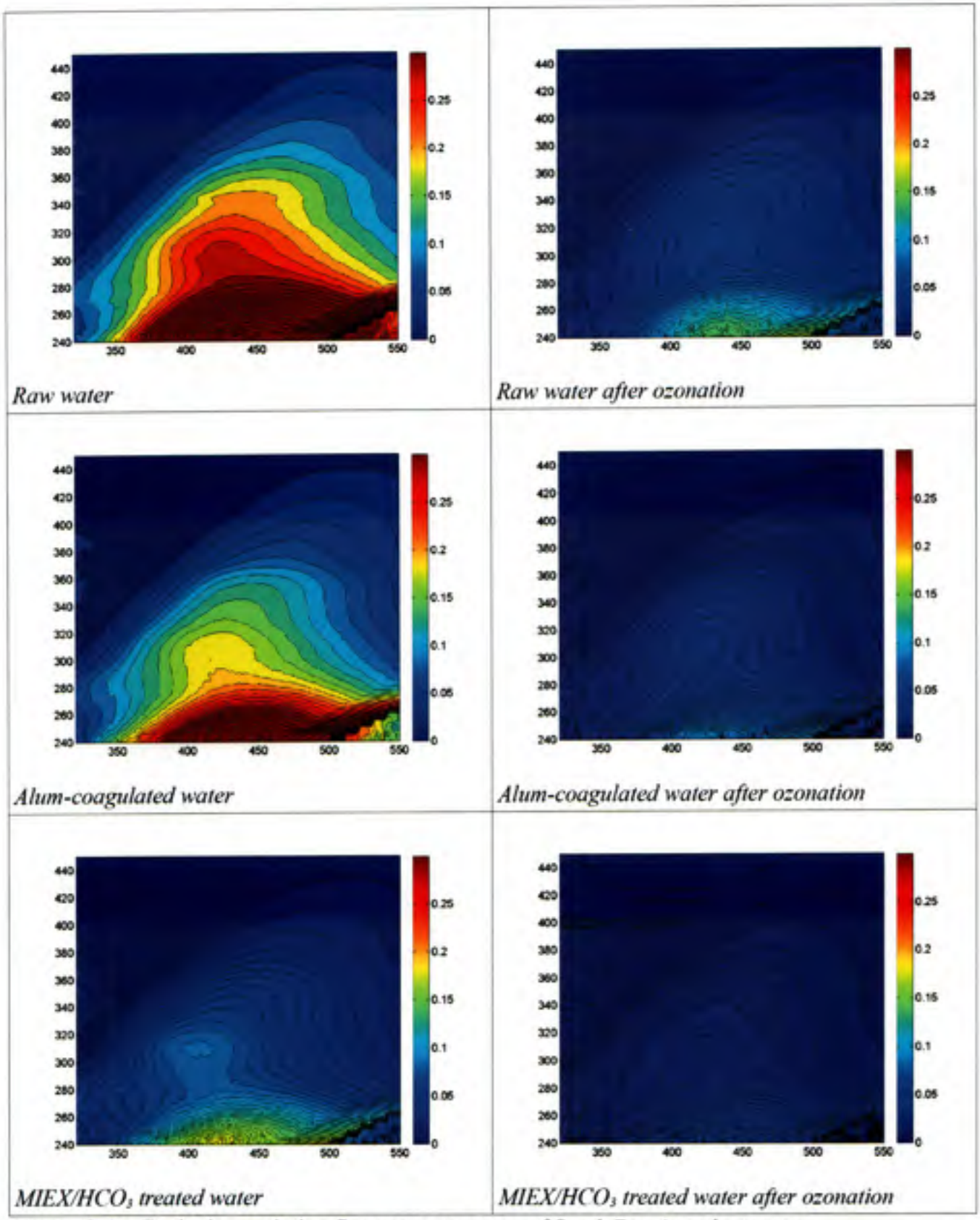

Figure G-2 – Excitation-emission fluorescence spectra of South Bay Aqueduct waters

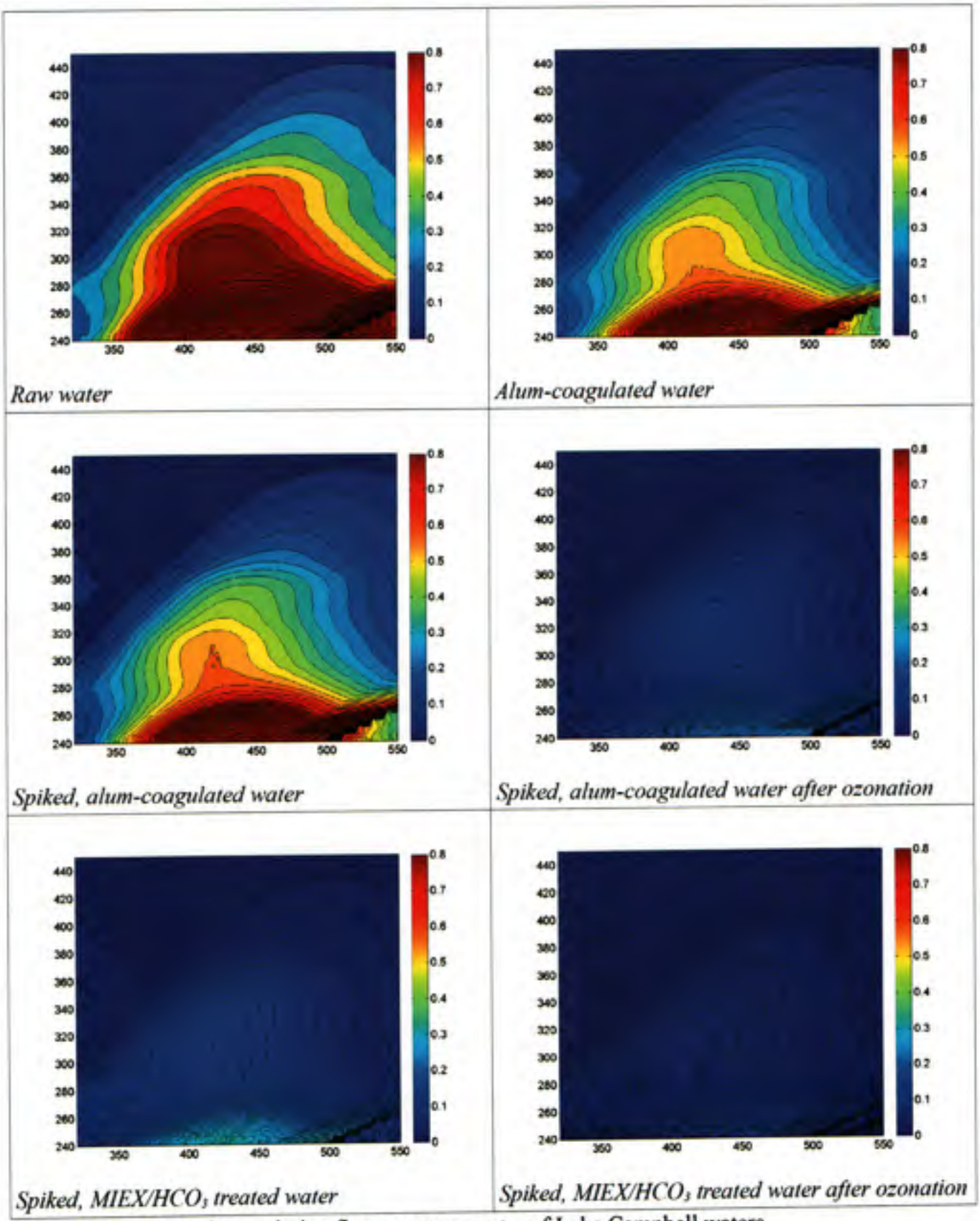

Figure G-3 – Excitation-emission fluorescence spectra of Lake Campbell waters